Intrinsic Properties of Poly(Ether-*B*-Amide) (Pebax®1074) for Gas Permeation and Pervaporation

by

Yiyi Shangguan

A thesis

presented to the University of Waterloo

in fulfillment of the

thesis requirement for the degree of

Master of Applied Science

in

Chemical Engineering

Waterloo, Ontario, Canada, 2011

Author’s Declaration

I hereby declare that I am the sole author of this thesis. This is a true copy of the thesis, including any required final revisions, as accepted by my examiners.

I understand that my thesis may be made electronically available to the public.

Abstract

Poly(ether-*b*-amide) (Pebax® grade 1074) is a waterproof breathable block copolymer containing soft poly(ethylene oxide) and rigid polyamide 12 segments. Its intrinsic gas permeabilities to nitrogen, oxygen, methane, helium, hydrogen, and carbon dioxide were tested under different feed pressures (0.3 – 2.5 MPa) and temperatures (20 – 80 °C). This helps to obtain a comprehensive understanding of the polymer, because prior work reported in the literature addressed only a few gases and used inconsistent membrane preparation and test methods. Relatively high polar (or quadrupolar)/nonpolar gas selectivity were observed. CO_2/N_2 selectivity was demonstrated to be as high as 105±0.4 in Pebax®1074, with CO_2 permeability coefficient of approximately 180±1 Barrer at room temperature. Additionally, the effects of solvent used in membrane preparation, heat treatment, membrane thickness, and polymer solution concentration on the membrane permeability were evaluated.

Pebax® is a highly breathable material, thus its application as breathable chemically-resistant protective clothing was studied. Dimethyl methylphosphonate (DMMP) – a sarin simulant – was selected as the challenge agent. The liquid pervaporation of pure water (simulating perspiration) and pure DMMP were measured for Pebax®1074, Pebax®2533, nitrile, latex, poly(vinyl chloride), low density polyethylene, silicone, and silicone-polycarbonate copolymer under pervaporation mode. Pebax®1074 was not only the most water permeable material but also the most selective of all the tested materials for water/DMMP – making it a very promising material for this application.

Acknowledgements

I wish to express my sincerest gratitude to my supervisor – Professor Xianshe Feng – for opening my eyes to the world of membrane technology, and the opportunity to learn and work together. This thesis would not have been possible without his unwavering patience and diligent guidance throughout my Masters studies. I would also like to thank my reviewers Professors Ali Elkamel and Neil McManus for taking the time out of their busy schedule to carefully critique my thesis.

I am grateful to my parents for believing in me, and for their constant support, endless encouragement and immeasurable love. This thesis is dedicated to them.

I also greatly appreciate the contributions of my colleagues and friends. To Dr. Gil J. Fracisco for helping me build my experimental setups. To Yijie Hu for his insightful discussions and quick wit. To Ying Zhang for her kind, understanding, and warm heart.

To Charlie Ulloa, my dearest friend, for his motivational energy, for many long nights and weekends spent together in the lab, and for his support through everything else that life throws our way.

To my fellow members in the Membrane Technology group for their challenging minds. To my friends at the university for making me feel like part of a family.

Research support from Natural Sciences and Engineering Research Council (NSERC) and Ontario Centre of Excellence (OCE) is gratefully acknowledged.

Table of Contents

List of Figures

List of Tables

CHAPTER 1

Introduction

In the past four decades, the U.S. market for membranes used in liquid and gas separation applications has grown to an estimated $1.7 billion in 2010 (Hanft, 2010). Membrane-based gas and liquid separations have emerged as competitive alternatives to conventional separation technologies such as absorption, pressure swing adsorption and distillation. Prominent advantages to membrane separation systems include: low installation and operating costs, operational and process versatility, and environmental friendliness (Bernardo *et al.*, 2009; Shao and Huang, 2007).

According to Koros and Flemming (1993), the success of a membrane process depends on advancements in three key areas: material selection, membrane formation, and modules and system configurations. Thus, the progress of membrane technology has been restricted by the availability of membrane materials with both permeabilites and selectivities that are competitive with prevailing separation methods. Consequently, there is a constant need to develop membrane materials tailored to specific separation applications. Membranes can be made from a plethora of

materials. A broad classification can be made into biological and synthetic membranes. Biological membranes are those surrounding each living cell, and differ entirely in functionality and structure from synthetic ones. Synthetic membrane materials may be further categorized as in Figure 1.1 (Mulder, 1991).

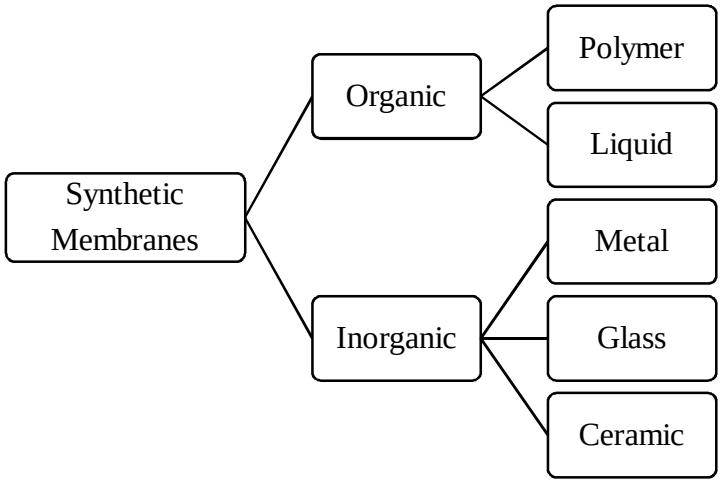

Figure 1.1 General synthetic membrane materials classification

Polymer membranes are not only versatile but can also form stable, thin, inexpensive structures that can be packaged into high-surface-area modules (Baker, 2004).

Currently, many polymeric membranes have proven to be successful in industrial separation applications. For instance, polyimide membranes have shown high stability and selectivity for hydrogen recovery in refineries (Bernardo *et al.*, 2009). Additionally, commercial polymeric membrane modules, such as MEDAL™, can operate at a high pressure (120 bar) and flow rates up to 330,000 Nm^3/h to achieve H_2 recovery of 98% at a purity as high as 99.9% (Bernardo *et al.*, 2009). This is a significant improvement in the separation performance compared to traditional pressure swing adsorption systems, which at typical flow rates of 50×10^6 std. ft^3/day

(58,993 Nm^3/h) yields 88% H_2 recovery at 99+% purity (Prasad *et al.*, 1994). Baker (2002), Bernardo *et al.* (2009) and Jonquiere *et al.* (2002) explored the current and future prospects of industrial membrane technologies in gas separation and pervaporation applications.

Poly(ether-*block*-amide) is a relatively recent line of thermoplastic elastomers introduced by Arkema Inc. The polymer consists of rigid polyamide (PA) and soft polyether (PE) blocks as shown in Figure 1.2. Numerous grades of the copolymers have been developed under the trade name of Pebax® by changing the weight fraction and the types of the PA and PE components.

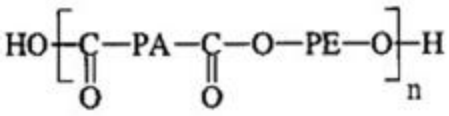

Figure 1.2 Structure of Pebax®

The copolymer boasts unique waterproof and breathable properties, which make it useful in a wide variety of applications including medical, textile, construction, and agriculture ("Pebax® Breathable Films", 2009). In particular, Pebax®1074 contains 55 wt% of poly(ethylene oxide) (PEO) and 45 wt% of polyamide 12 (PA 12) (Bonder *et al.*, 2000). This distinctive combination renders the polymer slightly hydrophilic; coupled with superior breathability, the moisture vapour transmission rate (MTVR) of this material is among the best available on the market (Nguyen *et al.*, 2001).

Only a handful of studies were conducted in the past regarding gas permeation properties of Pebax®1074. Additionally, different membrane preparation conditions have been employed by various researchers, and there are discrepancies in the permeability data reported in the literature.

Moreover, only a few gases were examined in these studies at select pressures and temperatures. A comprehensive understanding of gas permeation properties in the polymer is still lacking.

The high water vapour permeation fluxes of Pebax®1074 makes it a prime candidate for applications in textiles, because perspiration from the body can escape easily through the material. It was of particular interest to determine how the polymer would fare in protection against chemical warfare agents (CWA), because insufficient moisture transport through protective suits limits their usefulness.

Chemical warfare agents use poisons, which enter the body through inhalation, ingestion, and skin adsorption in the form of gas, liquid, or aerosols, to incapacitate, injure, or kill target subjects. It has been used since ancient Greek and Roman times, and was first deployed for mass destruction during World War I (Szinicz, 2005). The technology has since grown to have a large "footprint", where a relatively small amount of agent can cause catastrophic casualties. Therefore, it is often considered to be less expensive than conventional weapons. Nerve agents are a large sub-category of CWAs that use organophosphates to disrupt the acetylcholinesterase (AChE) process of the nervous system (Albuquerque, 1985). Sarin (GB) (a.k.a. isopropyl methylphosphonofluroidate) is an AChE inhibitor developed in 1937 from synthetic insecticides by Gerhard Schrader of IG Farben (Szincz, 2005). A lethal dose of 0.13 mg/kg causes inhibition of AChE, which leads to muscle paralysis through the entire body, resulting in bronchoconstriction and eventually asphyxiation (Albuquerque *et al.,* 1985). The most recent large-scale sarin attack took place on March 20, 1995 in a Tokyo subway system, where 12 people died and 5500 were injured (Mohtadi and Murshid, 2006). For this reason, sarin has since been the main focus of study. Considering the toxicity of sarin, dimethyl methylphosphate

(DMMP) – a nerve agent precursor – is widely used as a simulant in studies of its detection and filtration properties (Zheng *et al.*, 1999).

Protection against CWAs begins at the route of entry. To prevent inhalation of toxins, respirators and various filters were developed. During WWI, impermeable oilcloth was first used as protection against sulfur mustard (SM) – a vesicant (Szinicz, 2005). It, however, was inconvenient to use because it was heavy, unwieldy and uncomfortable to wear. Another solution was barrier creams, but unfortunately, SM is extremely penetrative, and continual application of the creams is impractical (Szinicz, 2005). A complete protection against SM and nerve agents can be achieved with impermeable suits that are impregnated with activated charcoal. Although presently such suits have evolved to be lighter and more comfortable, their uses are still limited by their inability to transport moisture. Breathability of protective suits is important in preventing heat strokes in warmer environments or during periods of increased physical exertion (Szinicz, 2005). Thus, developing an impermeable material that has a high moisture permeability is imperative. Therefore, this study also investigated the possible use of Pebax®1074 for protective wear by taking advantage of the breathability of the polymer to moisture transport.

1.1 Objectives

In order to have a meaningful comparison in the gas permeabilities of different gases through Pebax®1074, systematic membrane preparation and testing methods are required. This study attempts to address the lack of cohesiveness in the permeability data reported in the literature in order to have a better understanding of gas permeation properties of Pebax®1074.

Not only were the effects of temperature and pressure studied, key parameters during membrane preparation were also examined to determine whether the gas permeability would be affected by the membrane fabrication conditions. Additionally, a more extensive collection of gases was tested to give a more complete picture of the gas permeabilities of the polymer.

The uses of chemical protective garments are rather limited at present, because of inadequate moisture transport through the material. Pebax®1074 was shown to have a high moisture permeability, thereby making it a suitable candidate for application in this area. Its water and DMMP (a sarin simulant) permeability were tested and compared to those commonly used as chemical-resistant glove materials to determine its efficacy and performance in skin protection against nerve agents.

1.2 Thesis Outline

The goal of this thesis was to provide a better understanding of gas permeabilities of Pebax®1074 and to explore its possible use as chemical agent protectant. Figure 1.3 is a "lay out" of the research carried out in this study.

To provide a fundamental understanding of membrane permeation, an examination of polymers used and the mass transport mechanism is covered in Chapter 2. Especially, focus is placed on the two processes relevant to this study: gas separation and pervaporation. Their applications, transport model and factors affecting their performance were discussed. The chemical warfare agents and DMMP were addressed as well. Information on other polymers that were tested for purpose of comparison, including nitrile, latex, poly(vinyl chloride) (PVC), low

density polyethylene (LDPE), silicone rubber, and silicone-polycarbonate copolymer, was provided. Prior work on chemical protective clothing was also reviewed.

Chapter 3 presents the procedures for membrane preparation and the gas permeation tests. The gas permeability in Pebax® membranes was determined and the effects of feed pressure, temperature, membrane thickness and parameters involved in membrane preparation (e.g., solvent, polymer concentration) were evaluated.

Chapter 4 describes the water and DMMP pervaporation tests conducted to determine the feasibility of using Pebax®1074 as a chemical protective barrier. As a comparison, other polymer materials commonly used for chemical protection were also tested.

Lastly, Chapter 5 summarizes the conclusions drawn from this study as well as major contributions this work made to the research subject. Additionally, recommendations for further studies in the future were also provided.

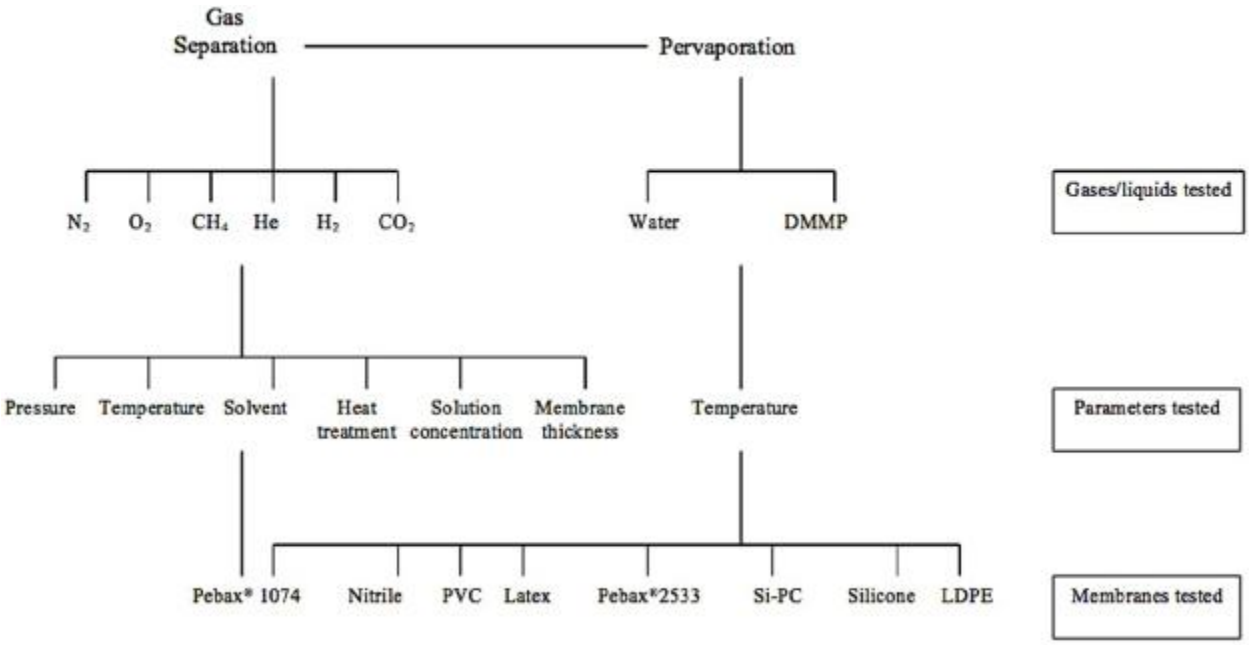

Figure 1.3 Schematic lay out of experimental work

CHAPTER 2

Literature Review

This thesis focuses on the permeability of Pebax®1074, a copolymer consisting of polyether and polyamide segments. This research was divided into two parts based on the separation processes: gas permeation (GS) and pervaporation (PV). The purpose of the gas permeation portion was to fill in the gaps in knowledge of the polymer's gas permeabilities with a better understanding of gas permeation in the polymer. The pervaporation section explores the ability of Pebax®1074 to protect against exposure of sarin using dimethyl methylphosphonate (DMMP) as a sarin simulant. Its performance was gauged against commonly available chemically-resistant glove materials.

Membrane technology is used in a wide range of applications, and new applications are continually being developed. Membranes are essential to everyday life – clothing, food packaging, and water purification, just to name a few. Several published books have provided an extensive description on the principles of membrane processes (Mulder, 1991; Nobel and Stern, 1995; Scott, 1998; Baker, 2004; Yampolskii *et al.*, 2006). The first volume of Journal of

Membrane Science was published in 1975, and has since been devoted to all aspects of membrane research and development. International conferences, such as International Congresses on Membranes and Membrane Processes (held every 3 years) and North American Membrane Society Meetings (held annually), share recent development and future directions in this field. Over the past 2 decades, the number of patents and other technical disclosures in this area has increased significantly providing extensive information on the development of the technology. Membrane technology has now evolved into the bases for large-scale commercially robust systems for separation and purification of gaseous and liquid mixtures.

2.1 An Overview of Membranes

Membranes are thin permselective barriers that moderate the permeability of chemical species in contact with it, as represented in Figure 2.1.

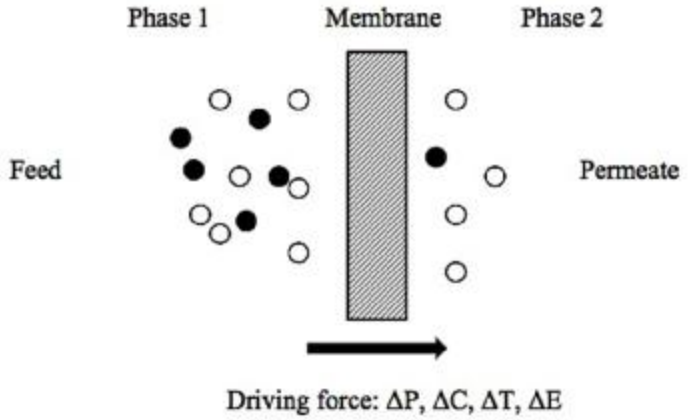

Figure 2.1 Selective permeation of penetrants through a membrane

The permeation may be driven by a pressure, concentration, temperature or electric potential gradient across the membrane. Sometimes there may be multiple driving forces, and the overall driving force may be represented by the chemical potential (μ). Separation is achieved when the membrane is able to transport one component more readily across than other components in the feed (Mulder, 1991).

Membranes can be made from organic (e.g. polymers, liquids) or inorganic (e.g., metals, ceramics, glasses) materials. In order to gain a more informative understanding of membranes, Pinnau and Freeman (2000) classified them based on their configuration, structure, fabrication method, separation regime and separation process, as shown in Figure 2.2.

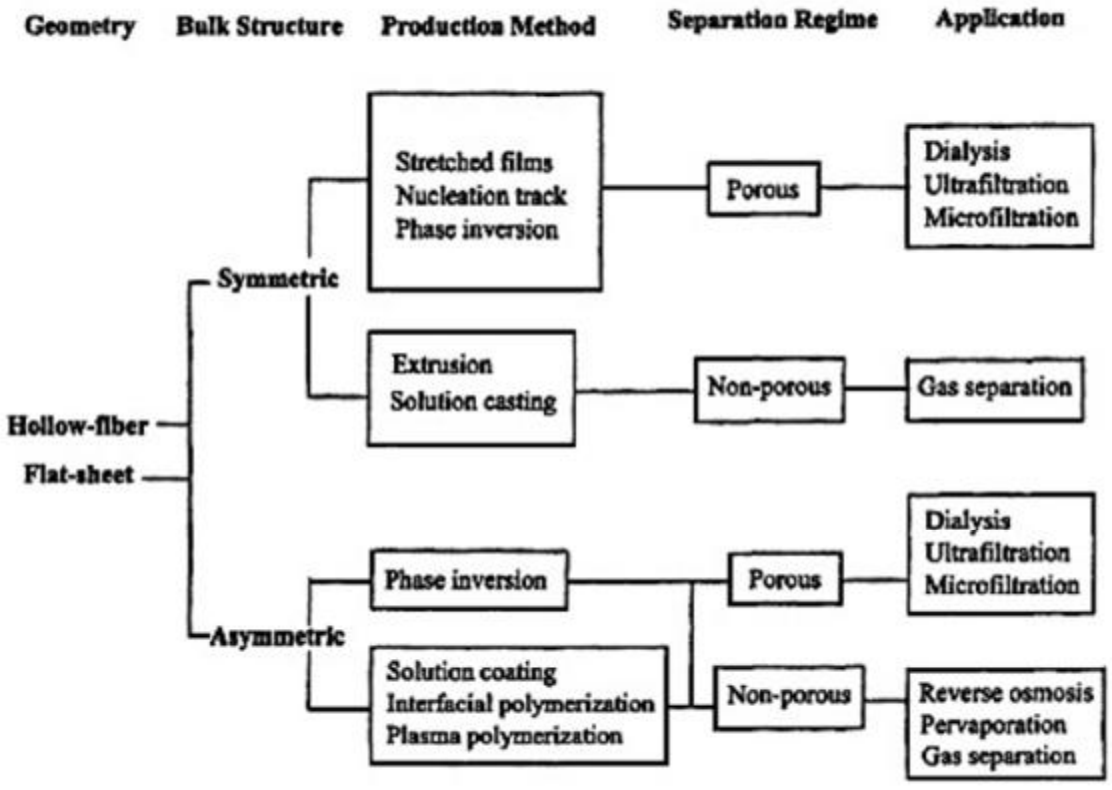

Figure 2.2 Classification of artificial membranes (Pinnau and Freeman, 2000)

Membranes either have a tubular (hollow-fibre) or flat-sheet geometry. Hollow-fibre membranes, packed into a tube-and-shell configuration, have a large surface area to volume ratio, resulting in a more compact module design. In fact, the first successful commercialization of gas separation membrane in 1980 was Monsanto's Prism Separator® in the form of polysulfone hollow-fibres (Ockwig and Nenoff, 2007). In contrast, flat-sheet membranes, packed in spiral-wound or plate-and-frame modules, are also commonly available in industry due to their simpler manufacturing and maintenance procedures (Abetz *et al.*, 2006). Membranes can be further categorized into symmetric (isotropic) or asymmetric (anisotropic) morphologies based on structures as illustrated in Figure 2.3 (Mulder, 1991). The thickness of a symmetric membrane can range from 10 – 200 μm (Mulder, 1991). Alternatively, Loeb and Sourirajan (Loeb, 1981) developed an asymmetric membrane, which is comprised of a 0.1 – 0.5 μm dense skin layer supported on a 50 – 150 μm porous substrate (Mulder, 1991). This structure combines both advantages of a high selectivity from a dense membrane and a high permeation rate from a thin membrane.

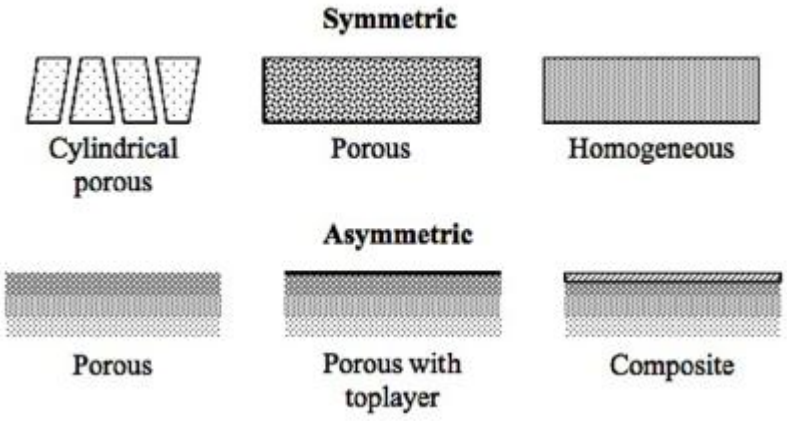

Figure 2.3 Cross section of membrane structures (Mulder, 19991)

Membrane preparation methods govern membrane morphology, and thus affect the membrane performance. Pinnau and Freeman (2000), Scott (1998), Mulder (1991), and Strathmann (1990) gave detailed descriptions of various processes of membrane preparation. The Pebax®1074 membranes used in this study were fabricated using the solution-casting method, which is straightforward and reproducible. However, one drawback of solution-cast membranes is their tendency to retain a trace amount of solvent thereby causing plasticization, as in the case of Hyflon AD® membranes (Jansen *et al.,* 2007). Generally, removal of the residual solvent can be achieved through evaporation without compromising the membrane integrity.

Lastly, membranes may be grouped based on their applications. The first generation of membrane processes such as microfiltration, ultrafiltration, nanofiltration, reverse osmosis, and electrodialysis, were well established from 1960 to 1980 (Mulder, 1991). The second-generation processes including gas separation, pervaporation, membrane distillation, and liquid membranes for gas separation, are the focus of current research. A simple yet reliable method of characterizing a nonporous membrane is to determine its permeability to gases and liquids experimentally. Gas permeation and pervaporation, which are relevant to the present study, are discussed in more details in the following sections.

2.1.1 Gas Separation

Gas separation membranes can be made of organic or inorganic materials. However, due to low gas solubility in inorganic materials and low gas diffusivity through liquid membranes, most gas separation membranes are made of polymers (Paul and Yampolskii, 1993). Polymers can also be tailored and optimized for specific applications. Almost all industrial gas separation

membranes are made of polymers (Bernardo *et al.*, 2009). Unfortunately, a gas separation membrane is far more sensitive to minor defects, such as pinholes, in the selective layer than other separation processes. For instance, during hydrogen/nitrogen separation, a pinhole that allows 1% un-separated gas mixture to pass through the membrane would reduce the overall membrane selectivity by half (Baker, 2004). Solutions to circumvent pinholes include lamination of multiple thin membrane layers (Salemme, 1977), and filling the holes with a caulking material (Henis and Tripodi, 1981). Consequently, the resistance-composite membrane was developed, and became the first industrial gas separation membrane under the trade name Prism®, where polysulfone hollow fibres were coated with silicone rubber to repair defects on the skin layer of polysulfone (Ockwig and Nenoff, 2007).

The main industrial applications of membrane gas separation and common membrane materials used are summarized in Table 2.1.

Table 2.1 Main industrial applications for membrane gas separation

Separation	Process	Membrane Materials
H_2/N_2	Ammonia purge gas	Polysulfone, polyaramide
H_2/CO	Syngas ratio adjustment	Polyimide
H_2/hydrocarbons	Hydrogen recovery in refineries	Cellulous acetate
O_2/N_2	Nitrogen generation, oxygen enriched air	Polyimide
CO_2/hydrocarbons (CH_4)	Natural gas sweetening, landfill gas upgrading	Nafion –Ethylenediamine (EDAH) [a]
H_2O/hydrocarbons (CH_4)	Natural gas dehydration	Cactus Membrane Air Dryer (Permea)
H_2S/hydrocarbons	Sour gas treating	Cellulous acetate
He/hydrocarbons	Helium separation	Polyimide
He/N_2	Helium recovery	Polyimide
Hydrocarbons/air	Hydrocarbon recovery, pollution control	Polydimethylsiloxane (PDMS) [b]
H_2O/air	Air dehumidification	Cactus Membrane Air Dryer (Permea)
Volatile organics/light gases	Polyolefin purge gas purification	Polydimethylsiloxane (PDMS)

[a] Ockwig and Nenoff (2007)
[b] Bodzek (2000)

A review of the main gas separation applications can be found in Bernardo *et al.* (2009), Koros and Mahajan (2000), Pinnau and Yampolskii (1994), and Koros and Fleming (1993).

2.1.2 Pervaporation

Pervaporation is a membrane process in which a liquid feed is vapourized through a nonporous permselective membrane, and the vapour permeate is collected through condensation, as shown in Figure 2.4. The permeate side is normally evacuated to 133 – 400 Pa (Huang and Shao, 2006), which serves as the driving force for mass transfer; thus the feed pressure is usually not crucial (Feng and Huang, 1997). Alternatively, a sweeping gas, such as helium, can be used to remove the permeate vapour from the permeate membrane surface. Often the membrane is swollen (or plasticized) on the feed side, leading to a gradient fading towards the permeate side

(Neel, 1995), especially at high temperatures. Solutions to reduce or control membrane swelling include using rigid backbone polymers to provide structural support (White *et al.*, 2006) and block copolymers with rigid segments for support and soft segments for permeation (Schucker, 1991).

The major advantage of pervaporation is its ability to separate azeotropic mixtures, such as water and pyridine (Neel, 1995), because the separation relies on the penetrant-polymer physiochemical interactions instead of the relative volatility of the feed components as in distillation (Feng and Huang, 1997). Additionally, energy required in pervaporation is equal to the heat of vaporization of the penetrant species plus energy used to maintain the low pressure on the permeate side. This drastically reduces the energy consumption in comparison to other energy-intensive processes (Huang and Shao, 2006).

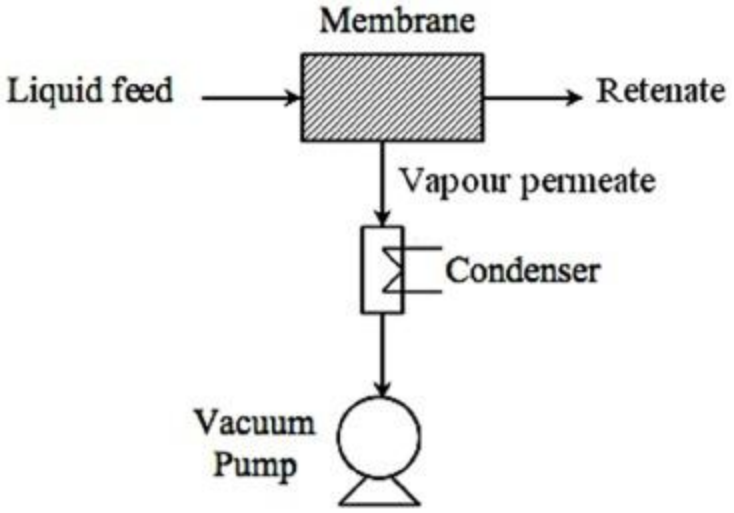

Figure 2.4 Schematic of pervaporation process

Pervaporation membranes can be fabricated from polymeric or zeolite materials. Bowen *et al.* (2004) published an extensive review of zeolite membranes for pervaporation. Table 2.2 lists the three viable industrial applications of pervaporation and their corresponding membrane materials. A number of review articles on the state-of-the-art of pervaporation can be found in Shao and Huang (2006), Jonquieres *et al*. (2002b), and Semenova *et al.* (1997). Approaches used to select PV membrane materials are described by Feng and Huang (1997).

Table 2.2 Main industrial applications for pervaporation (Baker, 2004)

Separation	**Process**	**Membrane Materials**
H_2O/organics (ethanol, isopropanol, glycol)	Dehydration of organics	Crosslinked poly(vinyl alcohol) (PVA) on polyacrylonitrile support
VOC (toluene, trichloroethylene, methylene chloride)/H_2O	VOC water separation	Silicone on polyimide support
Organic/organic	Organic/organic separation	PVA on cellulose acetate support for alcohol/ether separation Polyurethane-polyimide block copolymers for aroma/aliphatic separation

2.2 Mass Transport in Membranes

The mechanism of transport through membranes depends on whether the membranes are porous or nonporous. Figure 2.5 illustrates two mechanisms of the permeation process: the pore-flow model, and the solution-diffusion model based on Fick's Law (Baker, 2004). The key difference between the two models is that the pore-flow model considers any molecular-sized free-volume elements in the membrane as permanent pores, whereas the solution-diffusion model suggests thermally-induced motion of polymer chain segments cause random molecular-

sized pores to open and close, and the penetrant molecules undergo diffusive jumps from one open pore to another to get across the membrane (Hwang, 2011). Depending on the sizes of the penetrants, the pore-flow model may be classified into three sub-categories: convective flow, Knudsen diffusion, and molecular sieving (Baker, 2004). When the pores are large (0.1 – 10 μm), mass transport occurs through convective flow, and no separation is achieved. When the pore diameters are equal to or smaller than the mean free path of the penetrants, Knudsen diffusion dominates the mass transfer, and the selectivity is determined by the inverse square root ratio of the penetrant molecular weights (Graham's Law of diffusion) (Koros and Flemming, 1993). When the pores sizes are extremely small (5 – 20 Å), the separation is achieved based on solubility and diffusivity (Baker, 2004).

The pore-flow model was initially popular up till the mid-1940s because it was closer to physical experience (Wijmans and Baker, 1995). However, it became obsolete and unattractive for gas separation and pervaporation because the model broke down when the pore diameter fell below 5 Å (Wijmans and Baker, 2006). All current commercial membranes for gas separation and pervaporation are based on nonporous or dense polymer membranes – the separations of which are described by the solution-diffusion model.

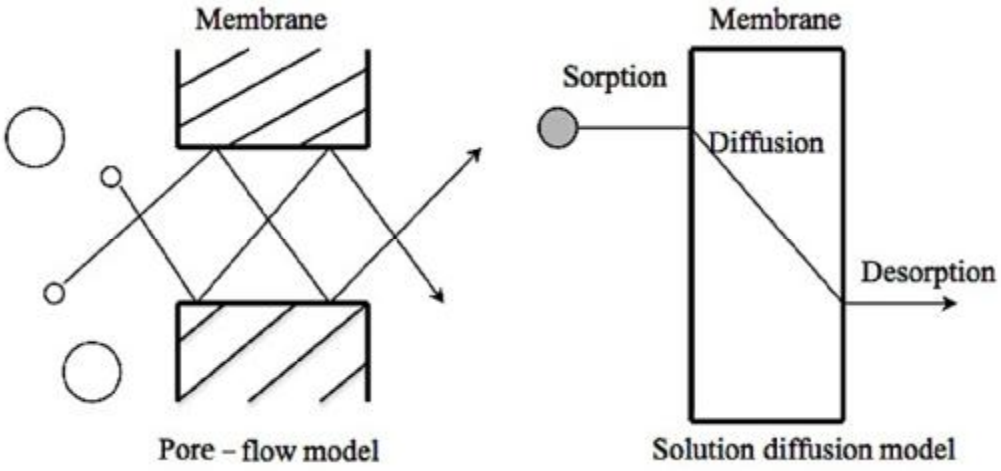

Figure 2.5 Two types of mass transport through membranes

The solution-diffusion model dictates the following three-step process:

1. Penetrant adsorption and dissolution at the polymer membrane feed interface,

2. Diffusion of penetrant through the polymer matrix, and

3. Desorption of penetrant into the other side of the membrane.

A couple of assumptions need to be made in order to define the solution-diffusion model. The first is that the fluids in contact with a membrane are at equilibrium with the membrane material at the interface (Wijmans and Baker, 2006). This means the chemical potential gradient across the membrane is continuous, and the rates of sorption and desorption are much faster than that of diffusion. The second assumption states that the pressure within a membrane is uniform, and the chemical potential gradient across the membrane can thus be represented as the penetrant concentration gradient (Wijmans and Baker, 2006). Figure 2.6 depicts the two assumptions.

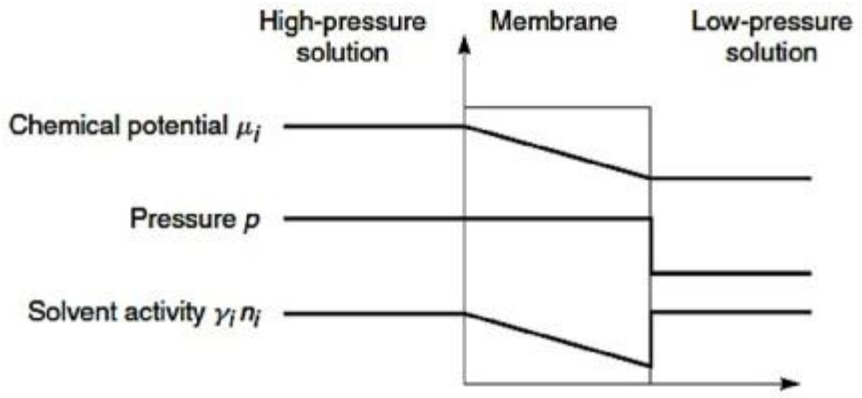

Figure 2.6 Driving force gradients for solution-diffusion model (Wijmans and Baker, 1995)

As shown in Figure 2.6, the pressure within a solution-diffusion membrane is constant at the highest value, indicating that it transmits pressure across the membrane similar to incompressible liquids. As a result, the chemical potential difference can be only represented by the concentration gradient alone.

Among the three steps, diffusion is the slowest, and thus the rate-limiting step (Jonquieres *et al.*, 2002a). The relationship between the permeation flux (*J*) and concentration gradient can be expressed as:

$$\mathrm{J} = -\mathrm{D}\frac{dC}{dx} \tag{2.1}$$

where *D* is diffusion coefficient of the penetrant in the membrane. The permeability coefficient is a quantitative measurement of a permeation process, and the derivation of the permeability coefficient can be found in Wijmans and Baker (1995).

The permeability coefficient, *P*, through a film of thickness, *l*, is defined as:

$$Permeability(P) = \frac{J}{\Delta p/l} = \frac{J}{(p_2 - p_1)/l} \tag{2.2}$$

where J is steady state flux, p_2 and p_1 are the feed and permeate pressures respectively. Barrer is a common unit for the permeability coefficient of a gas, named after Richard Barrer who developed the first scientific method for measuring gas permeation rate. Such permeability is an apparent one, because it may contain transport resistance of the potential boundary layers on the feed and permeate sides of the membrane (Metz *et al.*, 2005). A high flux is desired because it increases process productivity, and reduces the membrane area required at a given feed flow rate, thereby lowering the system capital cost. Alternatively, permeance, Q, is a measure of permeability without normalizing the membrane thickness, and is useful when determining the capability of the membrane to permeate.

$$Permeance(Q) = \frac{\mathrm{J}}{\Delta p} \tag{2.3}$$

The permeability coefficient is comprised of two components: diffusivity (D) and solubility (S) coefficients:

$$P = D \cdot S \tag{2.4}$$

The ideal selectivity, a_{AB}, quantifies the preference of a membrane for one species in the feed over another. A high selectivity is desired because it determines the purity of the product. (D_A/D_B) is considered the diffusivity selectivity and (S_A/S_B) is the solubility selectivity for components A and B in a feed mixture; the overall selectivity of the membrane is determined by the diffusivity and solubility selectivities jointly, as shown by Equation 2.5:

$$\alpha_{AB} = \frac{P_A}{P_B} = \left(\frac{D_A}{D_B}\right)\left(\frac{S_A}{S_B}\right) \tag{2.5}$$

where α_{AB} is the ideal selectivity of the membrane measured by the permeability ratio. Normally there exists a tradeoff between permeability and selectivity, where an increase in permeability is often coupled with a decrease in selectivity, and vice versa.

Not only are high flux and selectivity required for effective separation, other aspects (e.g., mechanical stability, tolerance to temperature variations, manufacturing reproducibility, low manufacturing cost and ability to be packaged into high surface area modules must also be considered for profitable industrial separation processes (Pinnau and Freeman, 2000).

Due to the swelling or plasticization of the membrane during pervaporation, the simple solution-diffusion model is often found inadequate, and a modification is needed. Plasticization occurs when a large amount of penetrant molecules dissolve into the polymer membrane matrix, forcing polymer chain segments to swell, which increases fractional free volume (FFV) and segmental motion, resulting in a reduced diffusivity selectivity and an increased permeability (Ghosal and Freeman, 1994). The plasticizants are considered to be fixed carriers for mass transport in the membrane matrix (Yoshikawa, 1984). Hence, the diffusion coefficient is influenced by plasticizant concentrations. Many modified solution-diffusion models have been proposed to improve the description of mass transport in plasticized membranes, including the "six-coefficients" model (Brun, 1985), a simplified Brun's model (Huang ***et al.***, 2002), and total solvent volume fraction model (Schaetzel ***et al.***, 2004). However, for the purposes of this study, the conventional solution-diffusion model was sufficient because the membrane was not substantially swollen by the penetrants.

2.3 Polymers

Polymers can be divided into two groups: glassy and rubbery, based on the glass transition temperature (T_g). Polymers above their glass transition temperatures are rubbery and those below are glassy. Some glassy and rubbery polymers used for making membranes are listed in Table 2.3.

Table 2.3 Common glassy and rubbery polymers used for membranes

Glass polymers	Rubbery polymers
Cellulose acetate	Polydimethylsiloxane (PDMS)
Polyperfluorodioxole	Ethylene oxide/propylene oxide – amide copolymer
Polycarbonate	
Polyimide	
Poly(phenylene oxide)	
Polysulfone	
Polyvinyl alcohol	

Typically, rubbery polymers contain a large amount of free volume owing to gaps created by the highly mobile polymer chain segments (Ghosal and Freeman, 1994). Free volume is the portion of volume in a polymer not occupied by the electronic clouds of the polymer, which affects penetrant diffusivity (Bernardo *et al.*, 2009). The distribution of free volume elements is also an important factor in mass transport. Due to the large free volume fraction in a rubbery polymer, its permeability is high and selectivity depends heavily on the solubility of the penetrants. On the other hand, glassy polymers are rigid, which results in a lower free volume fraction. The rigid polymers provide a high mechanical stability, and the separation is dependent on the difference in penetrant sizes. Various sizes of free volume elements can be "frozen-in" through cooling or rapid removal of the solvent (Bernardo *et al.*, 2009). Unlike rubbery

polymers, glassy polymers require an extended period of time to reach an equilibrium state, which process is also known as aging. The aging process has an effect on the mass transport of the membrane (Pfromm, 2006). Bernardo *et al.* (2009) and Stern (1994) analyzed rubbery and glassy polymer materials used in industrial membranes.

Most polymers are semi-crystalline, that is, they have both amorphous and crystalline regions. Crystalline fractions are considered impermeable and increase tortuosity of penetrant paths (Ghosal and Freeman, 1994). Thus, diffusional transport occurs mainly in the amorphous region. As a result, the degree of crystallinity, size and distribution of crystalline regions, extent of unsaturation, degree of crosslinking, and nature of substituents affects segmental mobility of the polymer chains and are important to permeation rates through the membrane (Geroge and Thomas, 2001; Mulder, 1991).

Pebax® is a group of thermoplastic elastomers combining flexible polyether (PE) blocks and rigid linear polyamide blocks (PA6, PA11, PA12 or mixed PA6/PA12) (Bondar *et. al.*, 1999). Diffusion occurs predominately in the PE phase, whereas the PA phase provides the necessary mechanical support for the membrane. The first generation of Pebax® polymers were poly(tetramethylene oxide) (PTMO) based. However, with the development of the second generation of Pebax®, the use of poly(ethylene oxide) (PEO) as the soft phase was introduced (Jonquieres *et al.*, 2002a). The hydrophilicity of the PEO blocks significantly improves the water vapour transmission rate (VTR) in Pebax®.

Conventional water vapour transmission rate measurement techniques, such as ASTM E96, do not generally lead to consistent values. Moreover, discrepancies are often reported for systems under different operating conditions – making comparisons of published data very

difficult (Nguyen *et al.*, 2001). This can be attributed to mass and heat transfer resistances in the external phases adjacent to the membrane (Nguyen *et al.*, 2001). Consequently, Nguyen and coworkers (2001) proposed the use of pervaporation process to measure water VTR for membranes of high breathability, because pervaporation can minimize mass and heat resistances in the boundary layer, thereby providing well-determined operating conditions. For this reason, the permeation of water and DMMP in this study was measured under pervaporation mode.

Due to outstanding physical cross-linking, film-forming ability, structural versatility, and water transmission rate of Pebax® polymers, they have been found suitable for dehydration processes, recovery of aniline and phenol from dilute solutions as well as recovery of aromas and flavours (Jonquieres *et al.*, 2002a). It has been patented as ingredient materials in OSMOFILM® (Jonquiere et al., 2002a), catheters (Wilson, 2011), golf balls (Iwami, 2011), and textiles (Nakai, 2011).

2.3.1 Pebax®1074

Pebax®1074 has a unique composition of 55 wt% PEO and 45 wt% PA12 (Bondar *et al.*, 1999). The exact title for the Pebax®1074 grade used in this work is MV 1074 SA 01. The SA 01 designation indicates it is free of additives and intended for medical applications ("Pebax® Breathable Films", 2002). A selection of its properties is listed in Table 2.4. More information on this polymer may be found online at CAMPUS® international plastics registry.

Table 2.4 Physical properties of Pebax®1074

Property	Value
Density (g/cm^3) [b]	1.09
T_g (°C) [b]	-55
X_c, Crystallinity in PA Block (wt%) [b]	40
T_m (PE) (°C) [b]	11
T_m (PA) (°C) [b]	156
Melting Point (°C) [a]	158
Moisture Absorption at Equilibrium (%)[a]	1.4
Hardness, Shore D [a]	40
Tensile Test, Stress at break (MPa) [a]	30

[a] *Pebax® MV 1074 SA 01* (2009)
[b] Bondar *et al.* (1999)

The glass transition temperature (T_g) of Pebax®1074 is –55 °C. It is a combination of two distinct glass transition temperatures: T_g (PEO) of –67 °C (*Polymer Handbook*, 1999) and T_g (PA12) of 41 °C (Andrews and Grulke, 1999), which indicates it is a microphase-separated polymer (Rezac *et al.*, 1997). However the combined sorption isotherm only displayed a linear Henry's law relationship typical of rubbery polymers, and not the dual-mode type for glassy polymers. Thus, it behaves as a rubbery polymer overall at room temperature. Its contact angle was measured to be approximately 70°, which agrees with its hydrophilic characteristic.

The available gas permeation data in Pebax®1074 reported in the literature are compiled in Table 2.5.

Table 2.5 Available gas permeability data for Pebax®1074 in published work

Test Conditions		Permeability (Barrer)				Selectivity		Source
T (°C)	P (MPa)	N_2	He	H_2	CO_2	CO_2/N_2	CO_2/H_2	
35	Up to 1.5	2.33		12.24	120	51.4	9.8	Bondar *et al.* (2000)
30	0.22	2.2						Potreck *et al.* (2009)
25	0.3	0.58			25	43.8		Marcq *et al.* (2005)
30	0.25	2.45	8.3		122	49.8		Sijbesma *et al.* (2008)

It is evident that the permeability of carbon dioxide (CO_2) gas is much higher than the other gases listed. This is attributed to the interaction between the quadrupole moment in CO_2 and polar polyether backbone in Pebax®1074 (Ghosal and Freeman, 1994). Additionally, not only were the studies conducted at different testing conditions, but also the membranes used were fabricated using different procedures, see Appendix A. Therefore, it is difficult to compare the permeability results. In order to compare permeabilities for different tests, systematic experiments were thus carried out in this study, which included a few more gases (e.g. CH_4 and O_2) for a few other potential applications.

Permeation of water through Pebax®1074 and other Pebax® grades were tested by Nguyen and colleagues (2001) using the pervaporation technique. The results are shown in Table 2.6.

Table 2.6 MVTR values of different Pebax® films[a]

Pebax grade	**Flux (kg m^{-2} day^{-1})**
1074	85
3000	67.0
1041	28.8
3533	5.9

[a] At identical operating conditions (38 °C, 25 μm)

Pebax®1074 appears to have superior MVTR compared to other Pebax® grades, which makes it suitable for textile applications. Additionally, Pebax® membranes have performed exceptionally well in separating hydro-organic mixtures (Jonquieres *et al.*, 2001). Hence, the separation performance of water and dimethyl methylphosphonate (DMMP) using Pebax®1074 was explored in this study to determine the feasibility of using this polymer in chemically protective textiles.

2.4 Factors Affecting Gas Permeation

Gas permeation is measured quantitatively using permeability coefficient. Permeability is comprised of two factors: solubility and diffusivity. Various factors affect the solubility and diffusivity of a membrane, including the operating conditions (temperature, pressure, composition), properties of the penetrants (size, condensability), polymer morphology (crystallinity, orientation, etc.), and penetrant-polymer interaction. Some of the factors are discussed below.

2.4.1 Penetrants

The permeability of a penetrant in a membrane is influenced by the condensability and the size/shape of the penetrant. Its condensability affects the penetrant solubility. In contrast, the penetrant size and shape influence its diffusivity. While the normal boiling point and critical temperature measure the condensability, the critical volume and kinetic diameter measure the penetrant size (and to some extent, the shape). These parameters are listed in Table 2.7 for gases tested in this study.

Table 2.7 Size and condensability factors for tested gases

	Size		Condensability	
	Critical Volume (cm^3/mol)[a]	Kinetic diameter, d_k (Å)[b]	Normal Boiling Point (K)[a]	Critical Temperature (K)[a]
N_2	89.8	3.64	77.4	126.2
O_2	73.37	3.46	90.17	154.58
CH_4	98.6	3.82	111.66	190.56
He	57.30	2.6	4.30	5.19
H_2	64.2	2.89	20.27	32.98
CO_2	94.07	3.30	194.7	304.12

[a] Poling *et al.* (2001)
[b] Breck (1974)

Overall, gas solubility increases with increasing gas condensability, as illustrated in Figure 2.7.

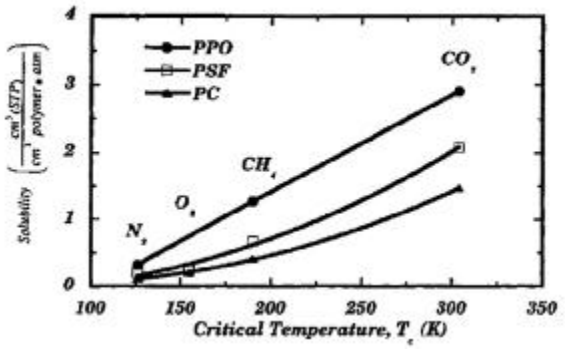

Figure 2.7 Effect of penetrant condensability on solubility for poly(phenylene oxide (PPO), polysulfone (PSF), and polycarbonate (PC) (Ghosal and Freeman, 1994)

The solubility is also sensitive to polar interactions between the polymer and the penetrant. Gas molecules, such as CO_2, with a quadruple moment are more soluble in polar polymers (Bondar *et al.*, 2000). In particular, the polar polyether oxygens in Pebax® backbone interact favourably with quadrupolar CO_2, resulting in a high solubility selectivity (Bernardo *et al.*, 2009). In addition, the degree of polarity of the polymer backbone also affects the permeability. Bondar et al. (2000) found that exchanging less polar backbone elements (PTMO/PA12) with

more polar elements (PEO/PA6) resulted in an increase in polymer cohesive energy density, which led to a decrease in diffusivity of nonpolar penetrants and an increase in permselectivity.

In general, diffusion coefficients increase with decreasing penetrant size, as shown in Figure 2.8 (Ghosal and Freeman, 1994). The kinetic diameter is defined as the smallest diameter zeolite window that can allow the molecule to enter its cavity (Breck, 1974). Rubbery polymers have weak size-sieving abilities compared to glassy polymers due to increased polymer chain segment motion (Bondar *et al.*, 2000).

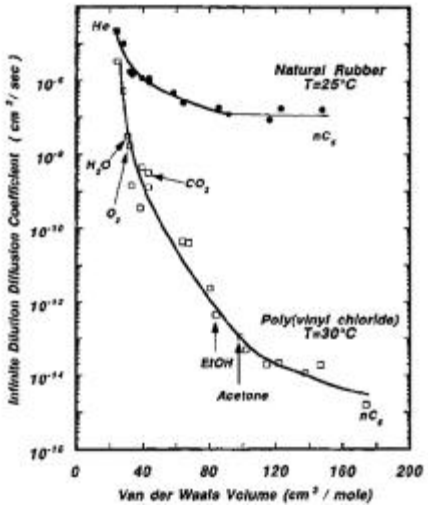

Figure 2.8 Effect of penetrant size on diffusivity of natural rubber and PVC (Ghosal and Freeman, 1994)

The diffusivity of linear or oblong gas molecules, such as CO_2, is higher than that of spherical molecules of equivalent molecular volume (Ghosal and Freeman, 1994). Berens and Hopfenberg (1982) showed that oblong molecules executed diffusive jumps parallel to their long axis, making them effectively smaller than symmetrical penetrants.

2.4.2 Feed Gas Pressure

The effect of feed pressure is attributed to competing hydrostatic pressure and plasticization effects (Bondar et al., 2000). High pressures tend to cause compaction in the polymer, thereby reducing its free volume and rate of diffusion (Reinsch *et al.*, 2000). However, plasticization increases permeability due to increasing penetrant solubility. Therefore, low sorbing gases, such as N_2, O_2, He, and H_2, affect permeability through hydrostatic pressure effects, whereas CO_2 influence permeability through plasticization effects.

There are typically four different permeability isotherm patterns found in rubbery and glassy polymers. In general, the permeability of low sorbing penetrants has a linear (slope near zero) relationship with pressure, whereas highly soluble gases are observed to have increasing permeability with increasing pressure in rubbery and glassy polymers (Ghosal and Freeman, 1994).

Lastly, there have been cases where polymer membranes have a "memory" or hysteresis of previous permeations (Chen, 2002). Chen (2002) observed that a second permeation test with propane gas through Pebax®2533 at identical pressures as the first run resulted in a significantly lower permeability. The exact reason for polymer hysteresis is still unclear, however it is evident that temperature and pressure changes may alter polymer structures permanently.

2.4.3 Temperature

The effects of temperature on the permeability, diffusivity, and solubility may be described by the Arrhenius relationship (Fried, 2006).

$$D = D_0 \cdot e^{\frac{-E_d}{RT}}$$
$$S = S_0 \cdot e^{\frac{-\Delta H_s}{RT}}$$
$$P = P_0 \cdot e^{\frac{-E_p}{RT}}$$
$$E_p = E_d + \Delta H_s \quad (2.6)$$

where E_d and E_p are the activation energies of diffusion and permeation, respectively, and ΔH_s is the enthalpy change of sorption. The activation energy for permeation E_p can be evaluated from the *ln P* vs. *1/T* plot.

An increase in temperature generally causes an increase in diffusion coefficients assuming the polymer does not undergo morphological changes, such as crystallization, over the temperature range investigated (Ghosal and Freemnan, 1994). This results in a decrease in diffusivity selectivity, because a higher temperature can elevate the diffusivity of larger less-permeable penetrants more than smaller more-permeable species (Ghosal and Freemnan, 1994). Meanwhile, the dissolution of a penetrant molecule into the polymer matrix is viewed as a two-step thermodynamic process: first is the penetrant "condensation", and then the creation of a molecular gap to accommodate the penetrant in the polymer matrix (Ghosal and Freeman, 1994). Hence, the heat of sorption may be expressed as:

$$\Delta H_s = \Delta H_{condensation} + \Delta H_{mixing} \quad (2.7)$$

For small non-condensable penetrants, the effect of $\Delta H_{condensation}$ is very small and ΔH_s depends on ΔH_{mixing}, resulting in an overall increased solubility with increasing temperature. However, for condensable penetrants, the ΔH_s depends heavily on $\Delta H_{condensation}$, resulting in an overall decrease in solubility with increasing temperature (Ghosal and Freeman, 1994).

Since $P = D\ddot{Y}S$, the activation energy of permeation is a summation of activation energy of diffusion and enthalpy change of sorption. In general, the permeability increases with an increase

in temperature, indicating that diffusivity is a stronger function of temperature than solubility (i.e. $E_d > |\Delta H_s|$). These effects were reflected in experiments conducted by Costello and Koros (1994) on a series of polycarbonate membranes. However, the activation energy may be of negative value as in the case of ethanol/water permeation through polyion membranes, because E_d is generally positive while ΔH_s is negative for exothermic sorption processes. Therefore, when negative ΔH_s dominates over E_d, a negative E_p occurs (Feng and Huang, 1996). Values of E_d, ΔH_s, and E_p for certain penetrant-polymer systems may be found in the *Polymer Handbook* (Pauly, 1999).

2.4.4 Polymer Solvents

The solvent used during membrane preparation may also affect membrane morphology, in particular the formation of pores. This is especially important for immersion precipitation technique used to form asymmetric membranes, where solvent and non-solvent interactions greatly affect the ultimate structure of the membrane. Although a simple method of precipitation by solvent evaporation was used to form homogeneous films for the purposes of this study, the solvent still plays a significant role in membrane morphology. During this process, a polymer is dissolved in a solvent, and the polymer solution is cast on a suitable support (e.g., glass plates or porous substrates). Phase separation is achieved when the solvent is evaporated to form a dense homogenous membrane.

According to Han and Nam (2002), the solvent in a polymer solution affects its thermodynamic and rheological properties. The thermodynamics aspect may be quantified using the polymer-solvent interaction parameter, χ, developed by Flory and Huggins (Schuld and Wolf,

1999). This parameter calculates the entropy of mixing (i.e., miscibility) and is dependent on temperature, polymer concentration in the solution, and the molecular weight of the polymer. Values of polymer-solvent interaction parameter for polymer-solvent pairs can be found in the *Polymer Handbook* (Schuld and Wolf, 1999). When this parameter increases, the mutual affinity and miscibility of the polymer-solvent decrease (Mulder, 1991). Elevated entropy of mixing enhances demixing and accelerates phase separation (Han and Nam, 2002). Thermodynamic mixing data are not available for all mixtures, and should therefore be measured or derived from group contribution theories (Mulder, 1991). On the other hand, an increase in polymer solution viscosity causes kinetic hindrance for phase separation (Han and Nam, 2002).

Additionally, the temperature and time for both solution mixing and solvent evaporation affects the distribution and dimensions of pores in a membrane. Intuitively, high temperatures and long periods of time for polymer dissolution would improve uniformity of the mixture and homogeneity of the resulting membrane. High drying temperatures suppress crystallization and allow liquid-liquid demixing to occur (Yeow *et al.*, 2004). It also increases solvent outflux and membrane shrinkage, resulting in the formation of macrovoids in the polymer matrix (Yeow *et al.*, 2004). A long drying period ensures complete removal of the solvent, thus preventing plasticization.

Kim *et al.* (2001) performed qualitative analysis of various solvents of their dissolution power on a collection of Pebax®(2533, 3533, 4033, and 1657) materials. A 3:1 mixture of propanol and butanol was found to be most powerful, whereas methanol and ethanol did not dissolve the polymers at all. These Pebax® polymers were found to be partially soluble in N-methyl-2-pyrrolidinone (NMP) and N,N-dimethylacetamide (DMAc). Similarly, for a given

solvent, the polymer concentration in the solution may also affect the permeability of the membrane prepared from the polymer solution.

2.4.5 Membrane Heat-Treatment

Heat-treatment may cause polymer segments to rearrange or crosslink and polymer chains to pack more closely, thereby reducing membrane free volume (Ghosal and Freeman, 1994). It is controlled by temperature and time. Zhao *et al.* (2006) found that increasing heat-treatment time resulted in a decrease in gas permeance and an increase in the gas selectivities at high pressures. This is because the membrane was densified during the treatment, thereby providing stronger size-sieving abilities. Similarly, an increase in the treatment temperature resulted in a reduced gas diffusivity in the membrane. However, this was only effective up to an upper-boundary temperature, and a further increase in temperature would cause the polymer to degrade, leading to an increase in diffusivity and a decrease in selectivity (Zhao *et al.*, 2006). Heat-treatment is often successful in stabilizing membrane performance and improving selectivity.

2.5 Dimethyl Methylphosphonate

Organophosphorous compounds were originally intended for insecticide applications. However, when Gerhard Schrader developed tabun (GA) and sarin (GB) in the late 1930s, he discovered these compounds were more toxic to mammals than insects, which led to their application as chemical warfare agents (Delfino, 2009). The phosphorus in these compounds is extremely versatile due to their multiple oxidation states, which allows them to have high nucleophilicity to electrophiles, to readily form bonds with oxygen, sulfur, nitrogen and

halogens, and to stabilize adjacent anions (Delfino *et al.*, 2009). These compounds were categorized as nerve gases, which possess distinct stereoisomers that react with acetylcholinesterase (AChE) in the human body at different rates (Albuquerque, 1985). AChE is an enzyme responsible for degradation of acetylcholine neurotransmitter, which is critical to proper muscular function (Delfin *et al.,* 2009). The pathways that nerve gases take to interfere with AChE have been described by Delfino *et al.* (2009).

Dimethyl methylphosphonate (DMMP) is an organophosphorous compound with chemical formula $C_3H_9O_3P$. It is a colourless liquid at room temperature, and highly water-soluble (614 g/L) (Lu *et al.,* 2008). Some of its physical properties are listed in Table 2.8 along with properties of sarin. Its current primary commercial use is in flame-retardants (Hoang and Kim, 2008). It was used as a precursor in the production of sarin (Zheng *et al.,* 1999). The chemical routes of sarin synthesis were reviewed by Barney (2010), Black and Harrison (1996), and Reesor *et al.* (1960). DMMP is an alternative reactant in the traditional di-di reaction method, where the addition of an alcohol to an equimolar mixture of methylphosphonic dichloride and methylphosphonic difluoride results in highly exothermic esterification and fluorination reactions to produce sarin (Black and Harrison, 1996; Reesor, 1960). This technique is suitable for the laboratory or commercial production of sarin due to its high yield and purity (Black and Harrison, 1996).

DMMP has been widely used as a sarin simulant for training exercises, calibration of detectors, and development of protective clothing, because of similarities in their chemical structures, most importantly the O=P and O–P bonds (shown in Figure 2.9), as well as its low toxicity and cost (Zheng *et al.,* 2010).

Table 2.8 Properties of dimethyl methylphosphonate and sarin

Property	DMMP[a]	Sarin[b]
Molecular weight (g/mol)	124.08	140.1
Boiling point (°C)	181	158
Vapour pressure (mmHg) @ 20 °C	< 0.1	2.1
Liquid density (g/cm^3) @ 25 °C	1.145	1.10

[a] Dimethyl Methylphosphonate (2011)
[b] Delfino *et al.*, 2009

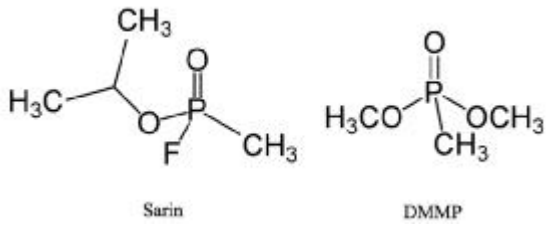

Figure 2.9 Chemical structures of sarin and DMMP

The vapour pressure or volatility of a chemical warfare agent is a critical physical property for chemical warfare defense research. It may be calculated using the Antoine Equation, (see Appendix B), which requires three constants unique to each chemical compound. The vapour pressure for DMMP was first calculated for temperature range -15 to 20 °C using ASTM E1194-87 (Tevault *et al.*, 1999). More recently, Butrow *et al.* (2009) combined gas saturation and differential scanning calorimetry to expand the temperature range of vapour pressure data to -15 °C to 180 °C. The resulting Antoine parameters from these experiments are compared in Table 2.9. Since the tests conducted in this study were carried out well above 20 °C, the parameters calculated by Butrow *et al.* (2009) were used.

Table 2.9 Comparison of DMMP Antoine parameters

Antoine Parameters	**Tevault *et al.* (1999)**	**Butrow *et al.* (2009)**
A	21.52	22.319
B	4000.35	4340.0
C	-60.519	-51.7

Permeation studies of DMMP through various materials have been conducted using either the cup method in ASTM E96 or vapour permeation cell apparatus. Almquist and Hwang (1999) conducted pervaporation tests using nitrogen sweep gas on a series of organophosphonates, including DMMP, through polydimethylsiloxane (PDMS) or silicone rubber. They found a permeation value of 56800 × 10^9 cm^3(STP).cm/(cm^2.s.cmHg) at 25 °C for DMMP, which was one of the lowest permeating organophosphonates tested. Additionally, the following general trends of organic vapour permeation in rubbery polymers were concluded: the diffusivities decrease with increasing molecular size, the solubilities increase with decreasing volatility, the permeabilities increase with decreasing volatility, and solubility is the dominant parameter in the permeability of organophosphorus compounds in silicone rubber at 25 °C (Almquist and Hwang, 1999).

Rivin *et al.* (2004) studied permeability of polyelectrolyte membranes (Nafion 117 and 112) used in electrochemical and protective fabrics applications. They discovered that the DMMP-water interaction in mixtures strongly affected membrane permeability, which could not be predicted from pure component permeability measurements (Rivin *et al.*, 2004). They used immersion sorption method to determine the solubility, and vapour permeation cell apparatus to determine permeability. The presence of DMMP was found to reduce water flux due to association of water with DMMP at the fluoroether interface, and decrease in fraction of free

water in the aqueous solution (Rivin *et al.*, 2004). The presence of water increased DMMP flux in co-current flow, because the DMMP transport was enhanced through water-solvated ionic pathways and solution in the more mobile aqueous phase (Rivin *et al.*, 2004). In the case of protective fabrics, counter-current flow is of interest, because pure water and DMMP are separated on opposite sides of the membrane. The increased DMMP flux associated with water is hampered by opposing concentration gradients in counter-current flow (Rivin *et al.*, 2004). A solution of 0.1:0.4 DMMP:water activity in counter-current flow resulted in water flux of 790 g/(m^2.day) and a DMMP flux of 599 g/(m^2.day) (Rivin *et al.*, 2004). The addition of Ca^{2+} or Fe^{3+} ion substitution of Nafion significantly reduced the DMMP flux, which was attributed to charge shielding effect on microphase segregation (Rivin *et al.*, 2004).

Napadensky and Elabd (2004) measured the water and DMMP vapour transmission rates through a variety of commercial and experimental materials using the ASTM E96 method. The most promising material, Material C (so named due to proprietary reasons) showed a water VTR of 2203 g/(m^2.day) [1.09×10^2 g/(mmHg.m.day)], DMMP VTR of 78.6 g/(m^2.day) [2.13×10^3 g/(mmHg.m.day)], and selectivity of 5.12. In 2006, Napadensky and Elabd developed n-methylolated nylon-6/chitosan blend membranes of various compositions and tested their permeability to water and DMMP. They found a composition of 2:1 n-methylol nylon-6 to chitosan had the largest water/DMMP selectivity of 15.3 with water vapour transmission rate (VPR) of 1543 g/(m^2.day) at 35 °C. According to Napadensky and Elabd (2006), a water VPR of 19 g/(m^2.day) is considered comfortably breathable and nerve gas levels of less than 13 g/(m^2.day) is required by the U.S. Army to be safe. They also thermally treated the membranes

by heat pressing at 100 °C for approximately 30 – 60 mins, which resulted in lower VPRs but higher selectivity.

In 2008, Lu and colleagues developed a breathable nanoporous cross-linked lyotropic liquid crystal (LLC)-butyl rubber (BR) composite membrane with a type I bicontinuoous cubic (Q_1) morphology to study penetration of DMMP using a vapour permeation cell apparatus. They found the Q_1 nanostructure was highly effective in providing breathability and chemical resistance, with thickness-normalized water vapour flux of 5900 g.μm/(m^2.day) and water/DMMP molar selectivity of 1600 at 25 °C. Due to the high water-solubility of DMMP, they found that the separation in the aqueous LLC nanopore system was not achieved through the solution-diffusion mechanism, but through a size-exclusion mechanism by its 0.57 nm pores. The size of DMMP was calculated to be 0.57 nm, and when it is dissolved in water, it forms mono- and di-hydrates with diameters 0.61 and 0.68 nm, respectively (Lu *et al.*, 2008).

More recently, Levine *et al.* (2010) studied the effect of addition of a fluoroethylene vinyl ether polyol (Lumiflon FE-4400) emulsion to waterborne military polyurethane topcoats on water and DMMP vapour solubility, diffusivity, and permeability using the solution-immersion and ASTM E96 methods. Their logic was that fluoropolymers would increase the hydrophobicity of a coating, thereby increasing its resistance to water and DMMP penetration, softening, and degradation. At 35 °C, DMMP was found to be 7 times more soluble in these polyurethane films than water (Levine *et al.*, 2010). Additionally, the sorption of DMMP dropped significantly in samples with 10 wt% or more Lumiflon content, which was attributed to the change in morphology of these films from uniform to having distinct aggregates (Levine *et al.*, 2010). The permeability of water (0.036 g/(h.m) at 10 wt% Lumiflon) and DMMP (0.061 g/(h.m) at 10 wt%

Lumiflon) vapour did not have strong correlation with Lumiflon content. This is surprising in view of their large differences in vapour pressures and sizes (Levine *et al.*, 2010). The diffusivity of DMMP was calculated to be 5 times lower than that of water.

More recently, Jung *et al.* (2010) filled highly selective poly(2-acrylamido-2-methyl-1-propanesulfonic acid) (PAMPS) with nonwoven fabrics to provide mechanical support, which showed a water VPR of 4000 – 6000 g/(m^2.day) at 35 °C. Its water/DMMP selectivity is approximately 40, which was higher than that of Nafion 112, which has a selectivity of 17.2.

2.6 Protective Materials

The U.S. Environmental Protection Agency (EPA) defines four levels of protection for chemically and biologically resistant clothing: from Level A being complete protection for skin, respiratory, and eye to Level D being not protective at all (Daugherty *et al.*, 1992). Additionally, the American Society for Testing and Materials (ASTM) has a committee targeted to develop test methods (F1001 and F739), terminology, classifications and performance specifications for occupational protective clothing (Yarborough, 2005). A history of chemical warfare agents and performance of some protective fabrics are reviewed by Szinicz (2005) and Daughtery *et al.* (1992).

A chemical can seep through a protective suit material via three processes: degradation of the material, penetration through imperfections in the suit, and permeation at the molecular level through the material (Daugherty *et al.*, 1992). In the past, the more commonly used material for chemical protection was butyl rubber, which worked on the principle of complete penetrant

blockage (Napadensky and Elabd, 2004). It was an effective barrier against chemical agents. However, its lack of breathability significantly reduced its usefulness. Lu *et al.* (2008) reported butyl rubber gloves manufactured by Brunswick had a thickness-normalized water vapour flux of 0.3×10^2 g.μm/(m^2.day), DMMP flux of 70×10^1 g.μm/(m^2.day), with a corresponding water/DMMP selectivity of 0.3×10^2 at 25 °C. A different approach of protection was introduced with the Military Oriented Protective Posture (MOPP) suit and the Joint Service Lightweight Integrated Suit Technology (JSLIST), where such fillers as activated carbon were used to capture toxic penetrants (Napadensky and Elabd, 2004). These materials are more breathable but not as protective as butyl rubber. Thus a new approach of using semi-permeable membranes is attractive because it would allow the passage of perspiration but block harmful penetrants, which would provide the necessary protection and minimize risks involved with heat fatigue and exhaustion (Napadensky and Elabd, 2004).

The permeation and breakthrough time data of nerve gases, including sarin (GB), in many commercial protective clothing and glove materials were compiled by Daughtery *et al.* (1992) and Lindsay (2001). The breakthrough time is defined as time it takes for the average permeation value to reach a defined threshold (ASTM F739). In this case the breakthrough threshold concentration was designated 9512 ng/(cm^2) (Lindsay, 2001). Lindsay (2001) found that latex and PVC had the shortest sarin breakthrough times, while butyl, neoprene, Sol-Vex (nitrile) and Viton (fluoropolymer) had breakthrough times greater than 1440 minutes.

The water and DMMP vapour permeability of Pebax®1074 were measured in this study using a pervaporation apparatus and compared to those of four commercially available chemical resistant gloves: acrylonitrile butadiene rubber copolymer (nitrile), polyvinyl chloride (PVC),

latex, and low-density polyethylene (LDPE), as well as three other materials that have a good permeability: Pebax®2533, silicone (PDMS), and silicone-polycarbonate (Si-PC) copolymer. The structures of these polymers are illustrated in Figure 2.10. The structure of silicone polycarbonate copolymer was obtained from Rich *et al.* (1990). Their chemical resistances and water VTR are compiled in Table 2.10. Each material may differ greatly with one another depending on its manufacturer, and due to proprietary restrictions the exact composition and properties of these materials are unknown. Pebax®2533 has 80 wt% poly(tetramethylene oxide) (PTMO) soft phase and 20 wt% rigid PA12 phase (Bondar *et al.*, 1999).

From data in Table 2.10, low-density polyethylene appears to have the lowest water VTR and silicone polycarbonate copolymer has the highest water VTR. Aungsupravate et al. (2008) claimed that the latex water VTR reported for their butadiene-methacrylic acid latex films are an order of magnitude higher than those in regular latex gloves.

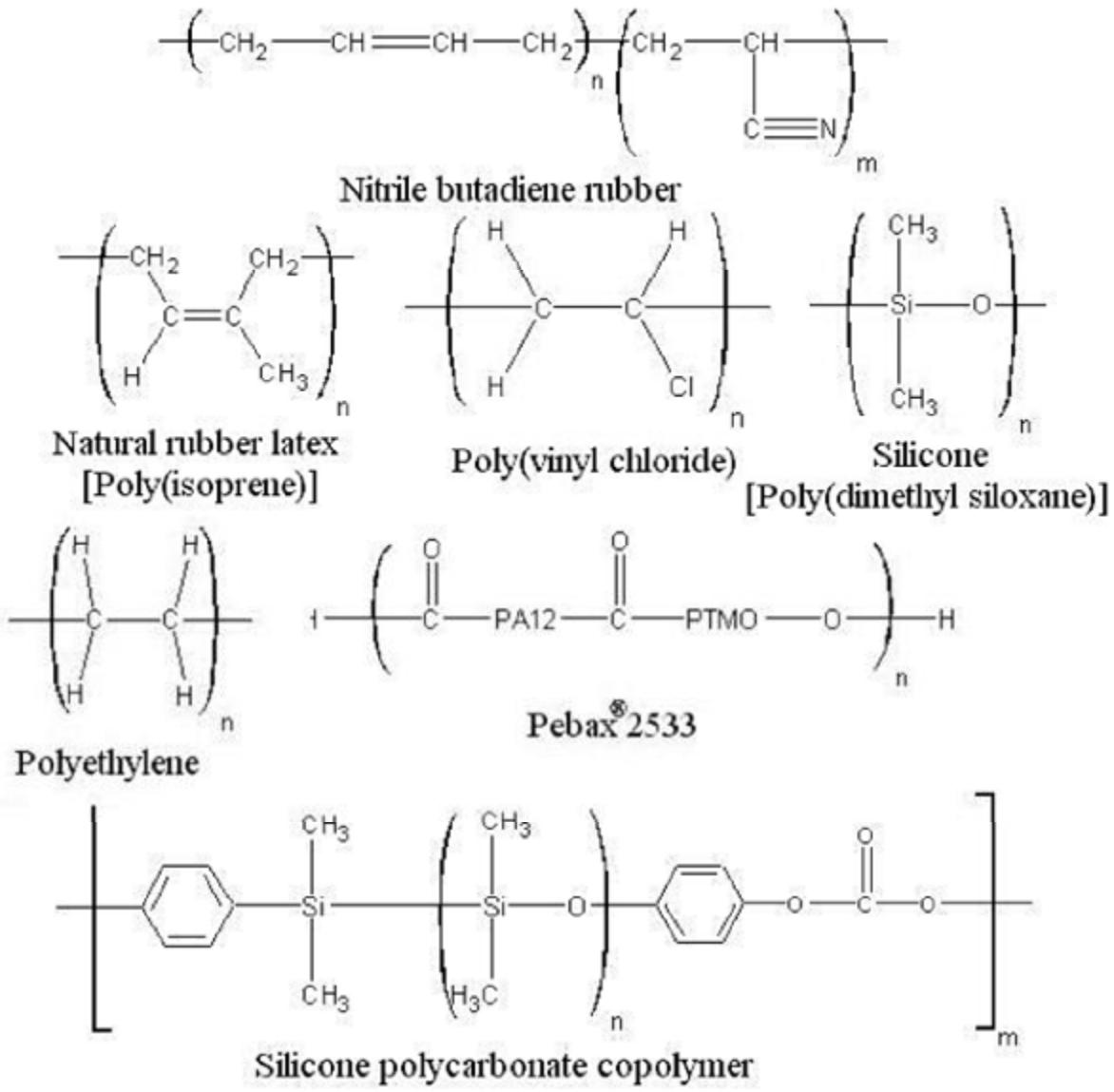

Figure 2.10 Chemical structures of test polymer materials

Table 2.10 Chemical resistance and water VTR

Polymer	**Chemical Resistance** [a]	**T_g** (°C) [b]	**Water VTR** [c] g.mm/(m^2.day) in temperature range
Nitrile	Hydrocarbon derivatives, aliphatic solvents, caustics NOT: aromatic solvents, ketones, esters, chlorinated solvents	Acrylonitrile: 82 – 125 Butadiene: -15	0.35 – 3.0 (24 °C – 40°C)
PVC	Strong acids and bases, salts, aqueous solutions, alcohols, glycol ethers NOT: aliphatic, aromatic and chlorinated solvents, aldehydes, ketones, nitro-compounds	61 – 135	1.18 (40 °C)
Latex	Weak acids and bases, alcohols, ketones, and aqueous solutions NOT: oil, grease, organics	-73	45 (24.5 °C)[e]
LDPE	Hydrogen peroxide, iodine, sodium hydroxide, sodium hypochloride, weak acids	-125	0.23 – 0.46 (20 °C – 40 °C)
Pebax®2533	NA	-77[d]	NA
Silicone	NA	-123	1.7 – 3.1 (37 °C)
Si-PC	NA	PC: 147	PC: 1.5 – 4.33 (23 °C – 40 °C)

[a] "Chemical Resistance Guide: Permeation & Degradation Data" (2003)
[b] *Polymer Handbook* (1999)
[c] Massey (2003)
[d] Bondar *et al.* (1999)
[e] Aungsupravate *et al.* (2008)

CHAPTER 3

Gas Permeation

3.1 Introduction

Gas separation is an important industrial process for many applications. Traditional gas separation processes, including cryogenic distillation, absorption, and pressure swing adsorption, consume large amounts of energy and are costly to build and operate. However, membrane gas separation processes are a competitive alternative to these well-established techniques due to their reduced capital cost, lower energy consumption, lower installation costs, versatility and simplicity in operation (George and Thomas, 2001).

The objective of this part of the study was to determine the intrinsic gas permeation properties of Pebax®1074. Additionally, there is not much existing research on Pebax®1074, and the permeability data could not be compared readily due to differences in membrane preparation and testing procedures. Hence, a wider selection of gases was tested systematically for comparisons. Lastly, a few parameters involved in membrane preparation and testing were studied to determine their effects on gas permeation.

Gas permeation through membranes follows the solution-diffusion mechanism, described in Section 2.2. A penetrant first absorbs through the feed surface of a membrane, then diffusion occurs through the membrane matrix, and eventually the penetrant desorbs from the permeate surface of the membrane. The solution-diffusion mechanism was described in detail by Wijmans and Baker (2006), and gas transport through polymers was reviewed in detail by George and Thomas (2001). The membrane separates a feed mixture when it transports one component – the faster permeating species – more readily across than other components. The permeability coefficient reflects quantitatively the ability of the membrane material to permeate the permeating species. The ideal selectivity provides a convenient measurement of relative ability of various polymer materials to separate gas mixtures. A sample calculation of these quantities is described in Appendix B. The membrane permeability and selectivity are affected by numerous factors related to the penetrant and polymer properties, membrane fabrication, and testing conditions. Transport studies are of considerable importance when designing membrane separation systems. A few factors critical to membrane transport and design were tested and discussed in further detail in Section 3.4.

3.2 Experimental

3.2.1 Materials

Sample of Pebax® MV 1074 SA 01 was supplied by Arkema Inc. (Philadelphia, PA) in the form of melt processed pellets (2-3 mm in diameter). Reagent grade 1-methyl-2-pyrrolidinone (NMP) (99%), 1-butanol (99.8%), isopropyl alcohol (IPA), and dimethylacetyamide (DMAc)

(99%) from Sigma Aldrich (Oakville, ON) were used separately as solvents for preparing membrane casting solutions. Nitrogen (N_2), oxygen (O_2), methane (CH_4), helium (He), hydrogen (H_2), and carbon dioxide (CO_2) pure gases were provided by Praxair Canada Inc. (Mississauga, ON). All materials were used without any further purification.

3.2.2 Membrane Preparation

The membrane preparation process involved three major steps: formulating the polymer solution, casting the solution, and drying the cast solution to produce the final membrane. This procedure is often referred to as the solution-casting method (Ulrich, 2005).

Pebax®1074 pellets were first dissolved homogeneously in a suitable solvent with vigorous stirring. A qualitative screening experiment was first conducted on the solubility of Pebax®1074 in four solvents: NMP, 1-butanol, isopropyl alcohol and N,N'-dimethylacetamide. NMP and 1-butanol were found to completely dissolve the polymer. For NMP, the solution was placed in a paraffin oil bath at 95 °C and dissolved with vigorous stirring for 36 hours. For 1-butanol, the solution was heated and agitated at 75 °C for 72 hours to ensure a homogeneous solution was produced. All polymeric solutions were then kept in the oil bath at their respective temperatures for 12 hours to degas any bubbles formed during the agitation.

Flat films of Pebax®1074 were prepared by casting the polymer solution on a heated glass plate (80 °C). Two casting methods were employed. For 15 wt.% solutions, the casting was performed using a casting knife in the form of a glass rod with wires at both ends to control the membrane thickness. The polymer solution was poured near one edge of the glass plate, and the

elevated glass rod was run across the plate on top of the solution to spread the solution evenly. The 6 wt.% solutions were less viscous than the 15 wt% solutions. Thus when cast using the former method, the solution quickly spread and flowed off of the glass plate – making the thickness of the membrane difficult to control. In order to prevent the spreading of the polymer solution, a dam was created by sticking electrical tape to four sides of the glass plate, thereby creating a trough for the polymer solution to sit in. The solution was poured near one edge of the glass plate, within the tape boundaries, and a bare glass rod was used to spread the solution onto the remaining space on the glass plate. In this case, the number of layers of tape on the glass plate controlled the membrane thickness. In both methods, the exact thickness of the membrane was controlled by the thickness of polymer solution cast on glass. The membrane thicknesses reported are averages of measurements taken from the center and four quadrants of a membrane after it has been produced.

The membrane was then formed by evaporation of the solvent in an oven at 80 °C for 48 hours. Then it was removed from the plate by immersing it in deionized water bath for 5 minutes, and almost immediately the membrane detached itself from the glass plate. The membrane was then dried again in the oven at 50 °C for 24 hours. The thicknesses of these free standing films ranged from 20 to 100 μm. The membranes were stored in a desiccator at room temperature until use.

3.2.3 Gas Permeability Experiments

Permeation experiments were performed using the dense films prepared. Pure-gas permeability coefficient was measured at pressures 0.3 to 2.5 MPa and temperatures 20 to 80 °C using a constant-volume variable-pressure method, except for CH_4, He, and H_2 gases, which were only measured up to 1.6 MPa because the maximum output gas pressure achieved by regulators on these gas cylinders was 1.6 MPa. A diagram of the membrane cell, acquired from Millipore (Billerica, MA), is shown in Figure 3.1.

A piece of membrane and Whatman® grade 1 qualitative filter paper was cut and placed between the O-rings and a porous metal plate (support screen), as shown in Figure 3.1. The filter paper did not provide resistance to permeation and acted only as a support underneath the membrane. The effective area of the membrane in the gas permeation cell was 21.22 cm^2.

The experimental setup consisted of the membrane cell, an upstream gas source, and downstream bubble flow meter, as shown in Figure 3.2. The bubble flow meter was a Mohr pipette filled with a couple of drops of Swagelok Snoop leak detector fluid. The membrane cell was immersed in a water bath (Haake-Fisons Instruments Inc.) to control and maintain its temperature. The permeation rate was measured using the bubble flow meter. New membrane samples were conditioned with low-pressure (0.2 MPa) nitrogen gas for 2 hours prior to carrying out the measurements. The retenate valve was bled prior to each run to purge the feed gas remaining in the membrane cell.

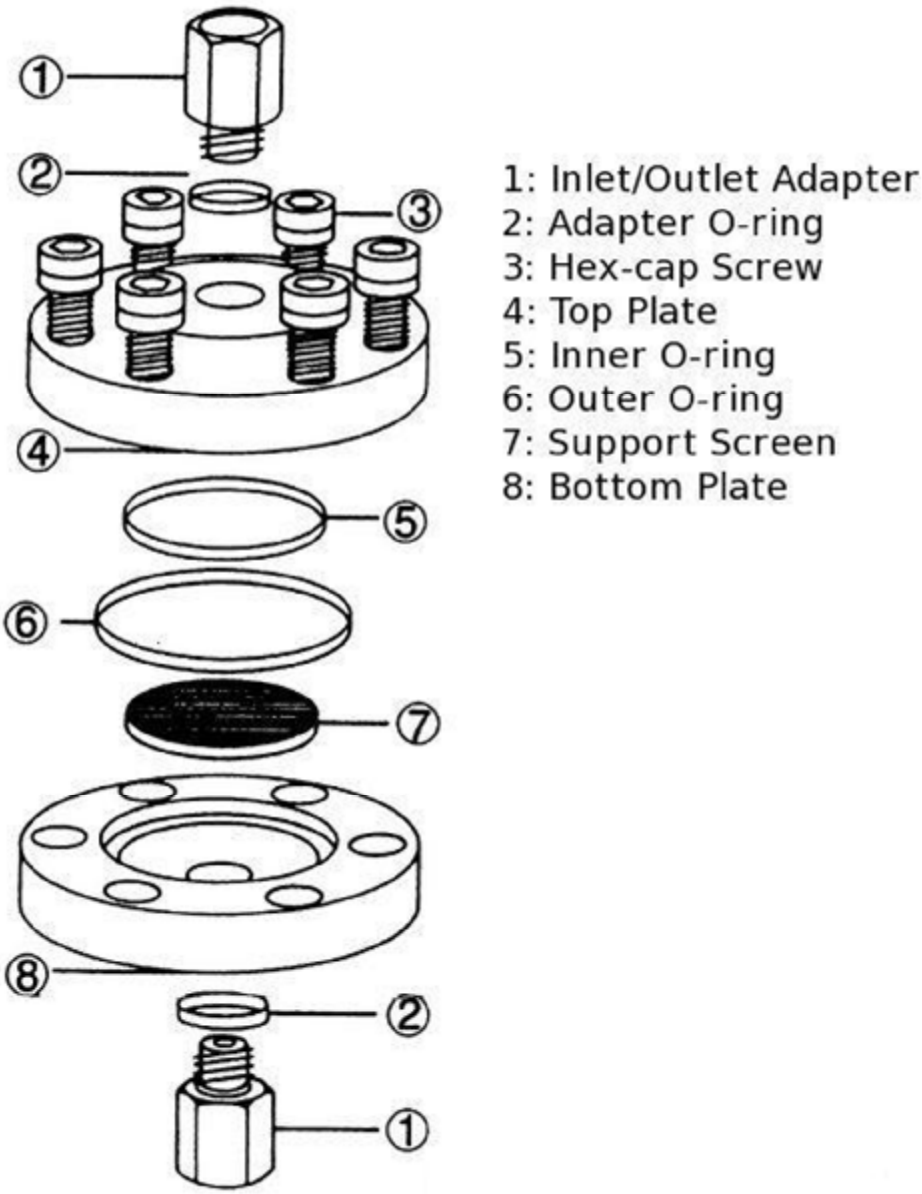

Figure 3.1 Schematic diagram of a gas permeation cell

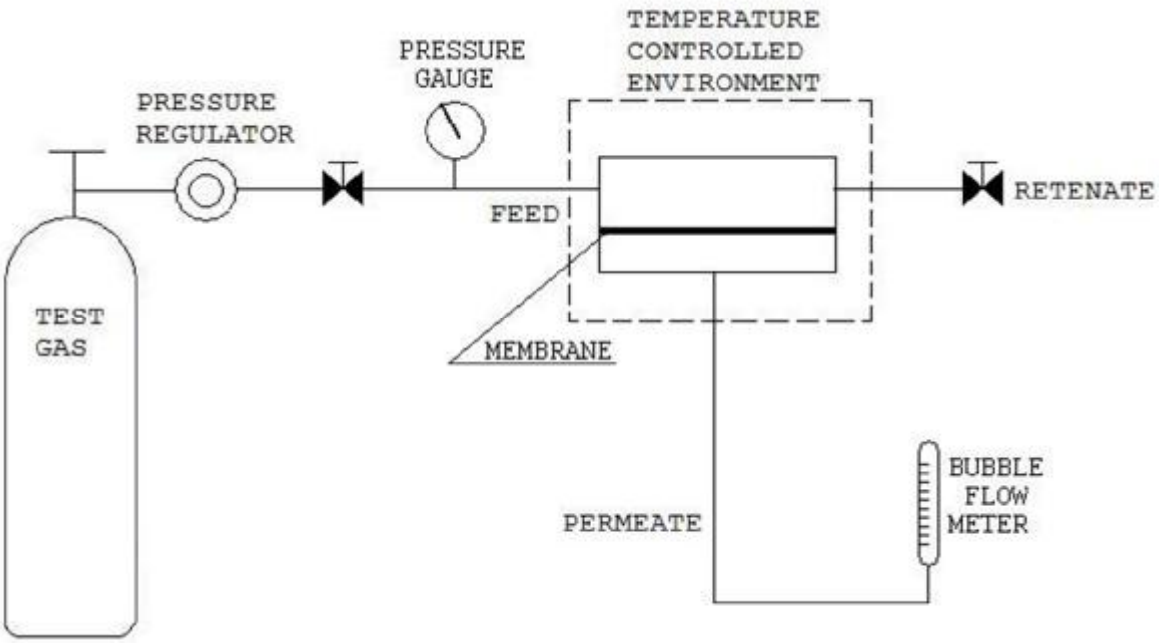

Figure 3.2 Schematic of gas permeation setup

3.3 Results and Discussion

3.3.1 Effect of Feed Gas Pressure

Gas separation processes operate at a wide range of feed pressures; therefore, it is very important to quantify the effect of feed pressure on the transport properties of polymers. Pure gas permeation tests were conducted with N_2, O_2, He, CH_4, H_2 and CO_2 at room temperature (approximately 23 °C) with increasing feed pressure from 0.3 MPa to 2.5 MPa. Permeation flux was determined as a function of pressure. At least three permeability measurements were made at each pressure to verify repeatability. The membrane used for this part of the work was cast from a 15 wt.% polymer solution in NMP.

As expected, the flux increases with an increase in the feed pressure as shown in Figure 3.3. However, the flux in fact is not proportional to feed gas pressure. As a result, the permeability coefficients are not independent of feed pressure, as shown in Figure 3.4. This behaviour is typical of pressure dependence permeability of rubbery or glassy polymer described by Ghosal and Freeman (1994). Feed pressure influences penetrant permeability through combined effects of hydrostatic pressure and plasticization.

The permeability coefficients of non-condensable gases (N_2, O_2, He, CH_4, H_2) were observed to decrease with increasing feed pressure. This is attributed to dominating hydrostatic pressure effects in non-condensable penetrants. Hydrostatic pressure mostly affects the rubbery component of the copolymer. As the pressure increases, the free volume within the polymer matrix decreases; thereby, reducing the diffusivity of a gas. This is also known as compression or compaction of the polymer matrix. Furthermore, Metz *et al.* (2005) suggested that the decrease in permeability might also result from increased resistance at the feed boundary layer with higher pressures.

On the other hand, plasticization occurs when the concentration of penetrant molecules dissolved into the polymer matrix is sufficiently high, causing the polymer chain segments to separate. This not only increases free volume of the polymer matrix, but also tend to increase the segmental motion of the polymer chains, resulting in more opportunities for penetrants to execute diffusive jumps. Consequently, the penetrant diffusion coefficient increases, which in turn increases its permeation rate. The observed increase in CO_2 permeability with feed pressure may be attributed to the plasticization effect. Among all the gases tested, CO_2 is the most condensable penetrant as evidenced by its high normal boiling point and critical temperature

(Table 2.7). It can thus dissolve into the polar polymer matrix more easily, due to its quadrupolar moment. Hence, the plasticization effects dominate CO_2 transport through the membrane. The plasticization effects of CO_2 in glassy polymers have been studied in detail, by Ismail and Lorna (2002).

Figure 3.4 shows CO_2 is the most permeable gas in Pebax®1074 among all the gases tested. The gas permeability follows the order of: $N_2<O_2<$ He $<CH_4<H_2<CO_2$. This is attributed to the joint effects of penetrant size, shape and condensability. The critical volume or kinetic diameter of a gas is an indication of the penetrant size, whereas the normal boiling point or critical temperature reflects the penetrant condensability. The penetrant size mainly affects diffusive transport, while penetrant condensability dictates its solubility in the membrane matrix. As shown in Table 2.7, He and H_2 are smaller in size than CO_2; thus, they have significantly higher diffusion coefficients than CO_2 does. The diffusivity tends to increase with decreasing penetrant size. Additionally, CO_2 is more condensable than any other gas tested, suggesting its high solubility in the membrane matrix. The penetrant solubility typically increases with an increase in the penetrant condensability (Bondar *et al.,* 2000). The polar ether linkages in Pebax® block copolymers have an affinity to dissolve CO_2 due to its quadrupole moment.

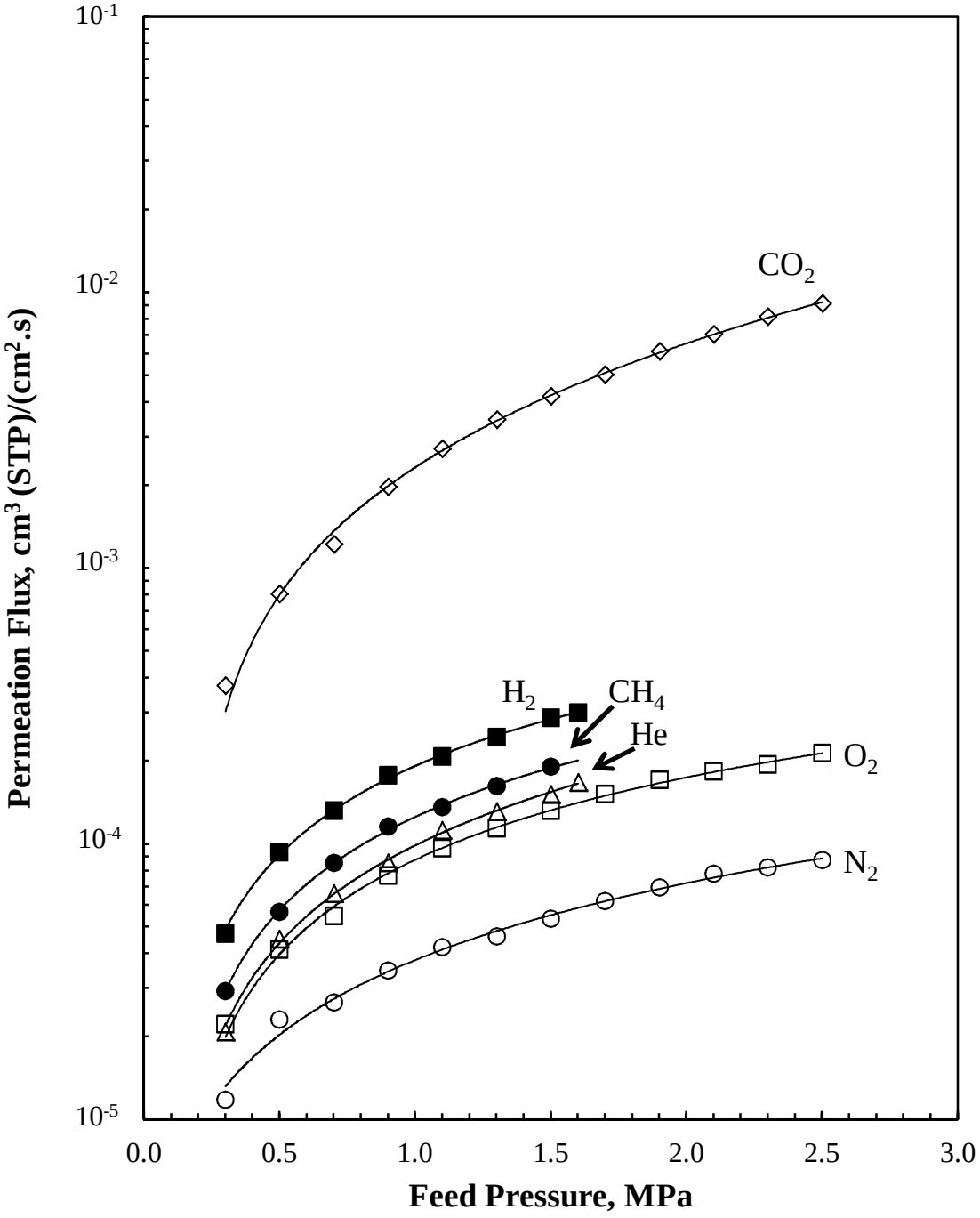

Figure 3.3 Effect of feed pressure on gas permeation flux

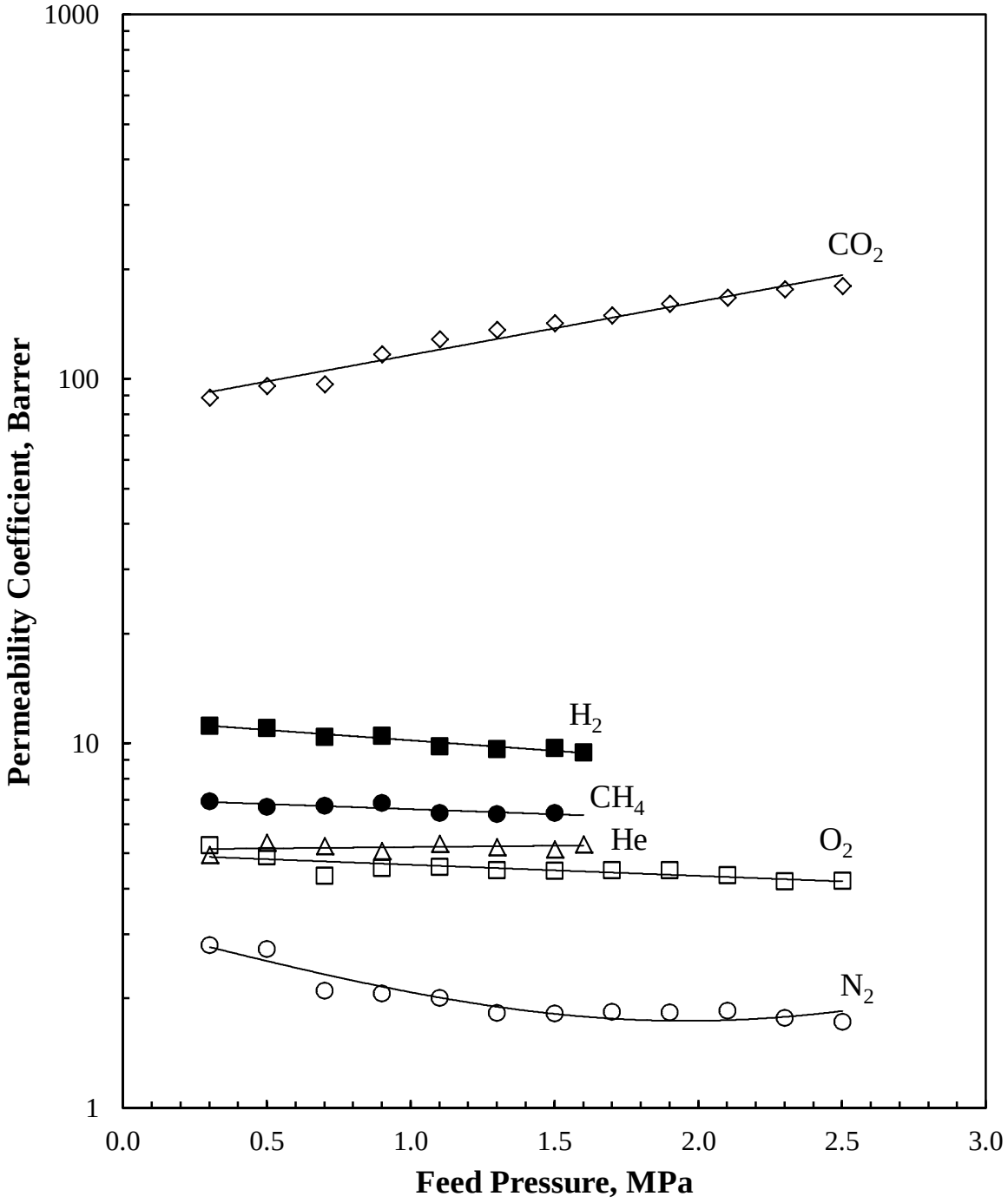

Figure 3.4 Effect of feed pressure on gas permeability coefficients

Figure 3.5 shows an increase in ideal selectivity with an increase in the feed gas pressure. The applications for each gas-pair selectivity are shown in Table 2.1. A few important selectivities were examined in detail for this study, including CO_2/N_2 for green house gas, CO_2/CH_4 for natural and landfill gas, CO_2/H_2 and H_2/N_2 for hydrogen processing, He/N_2 for breathing gas, and O_2/N_2 for oxygen enrichment. Separation of penetrant molecules is based on the selective permeability of the membrane, and is thus also controlled by the sizes and condensabilities of the penetrant molecules. For polar/non-polar gas pairs, such as CO_2/N_2 and CO_2/CH_4, the increase in permeability of CO_2 is far more significant than the decrease in N_2 or CH_4 permeability, resulting in an overall increase in CO_2/N_2 and CO_2/CH_4 selectivity with an increase in the feed pressure. The CO_2/N_2 selectivity is the highest, because CO_2 is not only more soluble in Pebax® but also smaller in size than N_2. As a result, both diffusivity and solubility selectivity are in favour of CO_2 permeation.

Furthermore, Pebax® polymers have a weak ability to "sieve" penetrants based on size. When such a weak size-sieving ability is coupled with high solubility selectivity, Pebax® polymers are ideal for the removal of CO_2 from other gases. In contrast, the selectivity of non-polar/non-polar gas pairs also increase with increasing feed pressure, because the diffusive transport dominates the non-polar penetrants. With an increase in the feed pressure, the membrane is compacted and the diffusivity selectivity increases, resulting in an overall increase in selectivity.

The gas permeation data obtained appear to be comparable to those in literature (Table 2.5) except for data reported by Marcq *et al.* (2005). They were the only group who extruded the

polymer pellets to obtain membranes; this may explain their large deviation in the permeability from other research groups.

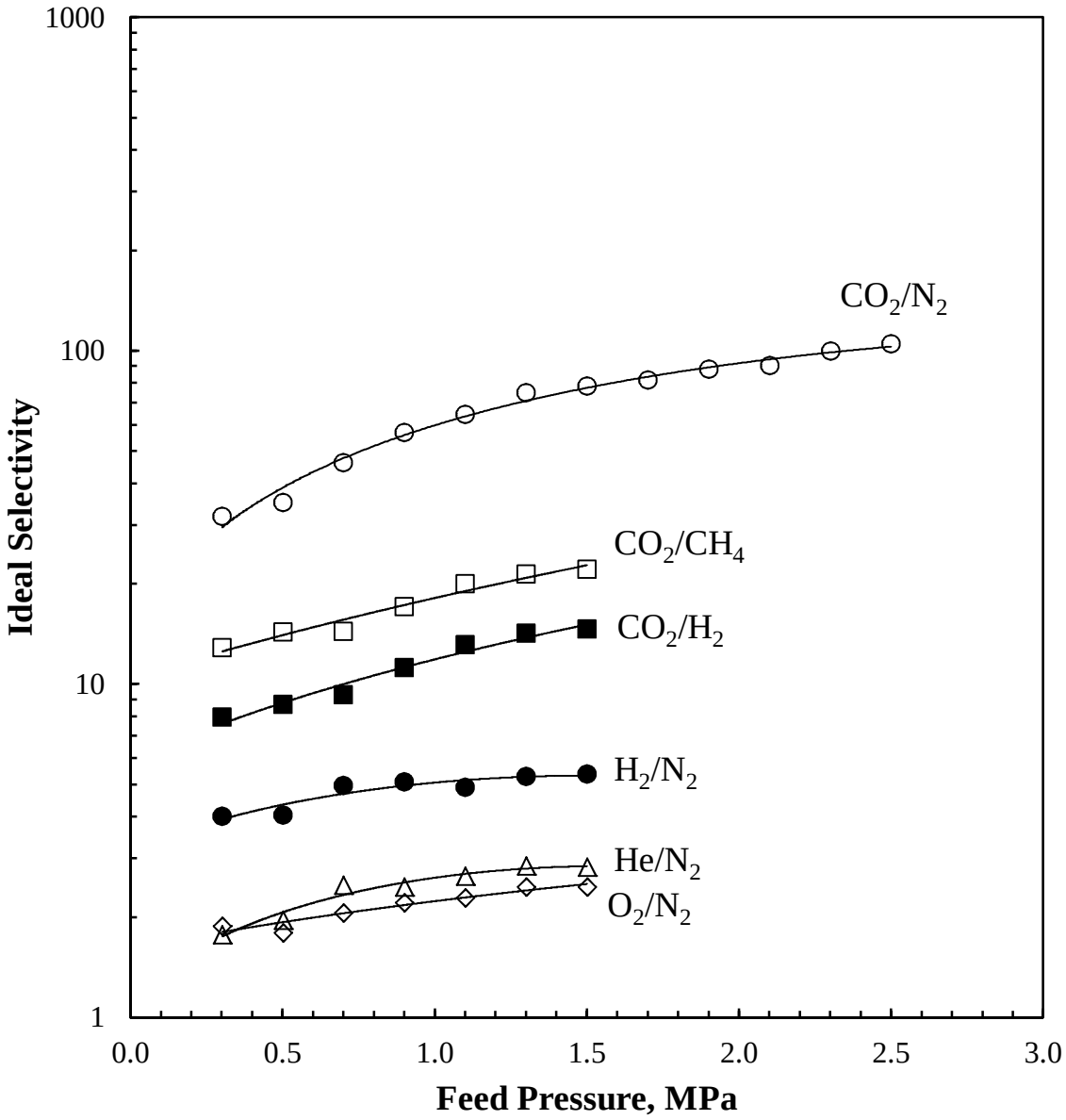

Figure 3.5 Ideal gas selectivity of selected gas pairs

As mentioned before, Pebax®2533 membranes have been observed to have a "memory" of previous permeations. Chen (2002) noticed a significant decrease in the permeability of propane gas through Pebax®2533 when the same permeation test was repeated on the same membrane sample. However, as seen in Figure 3.6, Pebax®1074 did not display similar behaviour. The gas permeations were first carried out with increasing feed pressure, and then the permeations were measured in decreasing feed pressure to study the reproducibility of the permeability data. The figure clearly shows agreement in permeability between the two sets of test conditions, and there is no hysteresis or "memory" effect observed. Pebax®2533 has 80 wt% soft poly(tetramethylene oxide) and 20 wt% rigid polyamide 12, whereas Pebax®1074 has 55 wt% soft poly(ethylene oxide) and 45 wt% rigid PA12. The large portion of rigid PA12 segments in Pebax®1074 matrix provides good structural support, and the solubility of CO_2 in Pebax® polymer is substantially lower than propane. This may cause the membrane chain conformation to respond with external pressure changes quickly.

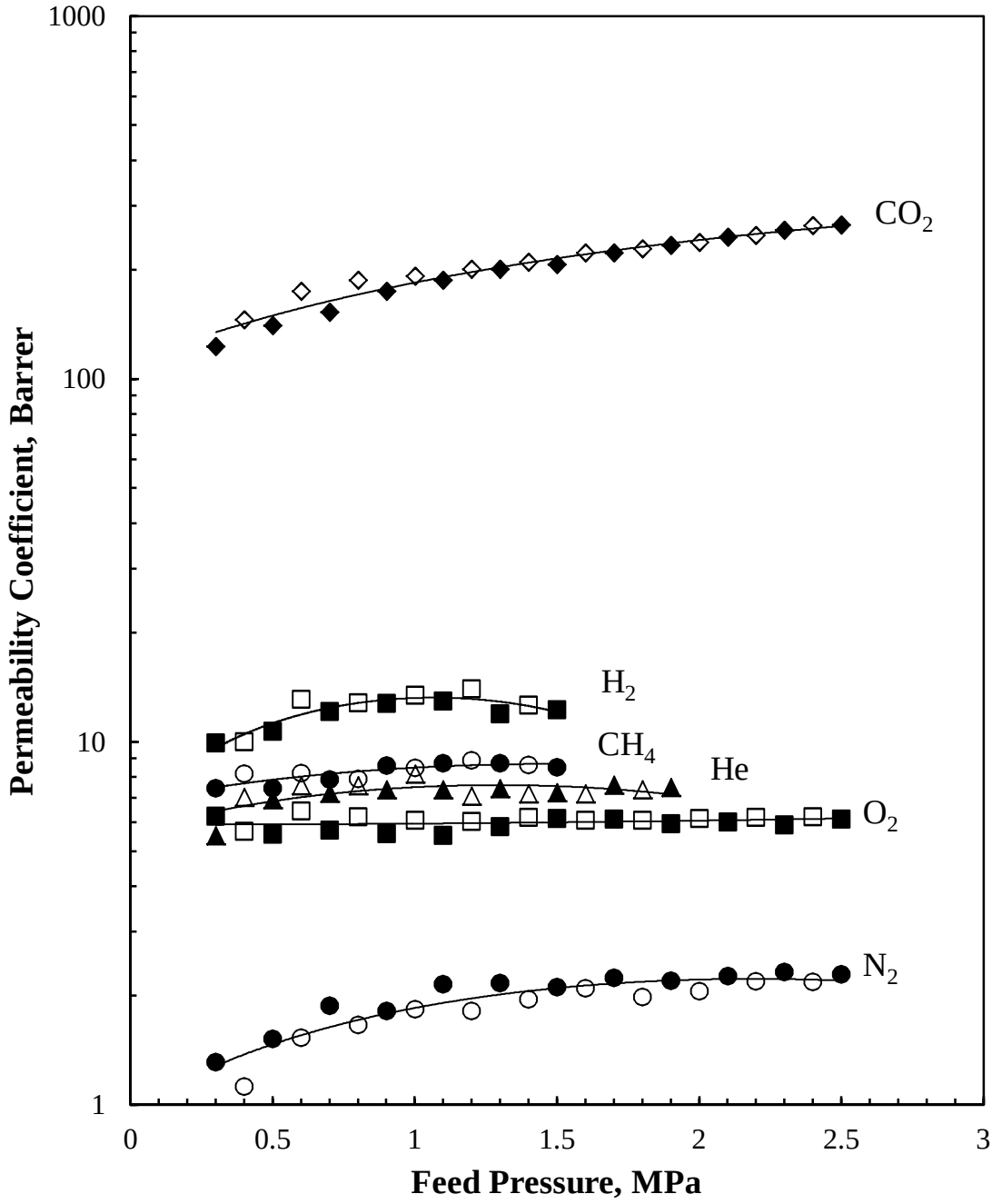

Figure 3.6 "Memory" of Pebax®1074 membranes
Note: open markers indicate increasing feed pressure and closed markers indicate decreasing feed pressure

3.3.2 Effect of Operating Temperature

Gas permeability through a polymer matrix is often a strong function of temperature. To analyze the effects of temperature on gas permeation through Pebax®1074, the membrane cell was immersed in a temperature-controlled water bath, and the temperature was varied in the range of 20 – 80 °C. During these tests, the permeation flux was determined at different pressures for a given temperature.

The effect of temperature on permeability can be expressed using the Arrhenius relationship. This agrees with the experimental data, as shown in Figure 3.7 for gas permeations at a feed pressure of 0.7 MPa. In general, the permeability is observed to increase with increasing temperature. This is because gas diffusion coefficients generally increase with increasing temperature, with the premise that the polymer does not change morphologically due to the temperature variation (Ghosal and Freeman, 1994). At higher temperatures, polymer chains gain increased segmental motion, resulting in more diffusive jumps conducted by the penetrant molecules. Contrarily, the solubility of CO_2 decreases with increasing temperature. However solubility of non-condensable penetrants often exhibit reverse solubility behavior, where the solubility increases with increasing temperature (Sato *et al.*, 1996). The sorption of penetrants into a membrane is comprised of two thermodynamic processes: first the "condensation" of the penetrant molecule, then the integration of the molecule into the polymer matrix. For non-condensable gases, their interaction with the polymer is weak, and the enthalpy change of the integration step dominates; therefore, the solubility increases with an increase in temperature. Meanwhile, the "condensation" step governs the solubility of CO_2, resulting in a decrease in its solubility as temperature increases. Additionally, due to the increased gas solubility, the polymer

matrix tends to swell, thereby increasing the penetrant diffusivity. Overall, the diffusivity is a stronger function of temperature than solubility. Thus, a higher gas permeability is observed at higher temperatures.

Figure 3.8 demonstrates the decrease in gas selectivity with an increase in temperature, especially for CO_2/N_2 gas pair. At higher temperatures, the increased segmental motion in the polymer chains reduces its ability to distinguish between penetrant sizes. Thus the diffusivity selectivity and overall permselectivity decrease. Generally speaking, the temperature affects more-permeable gases more significantly than less-permeable ones (Ghosal and Freeman, 1994). CO_2 is more condensable than N_2, and its temperature-effect on dissolution is expected to be more significant. Hence, an increase in temperature elevates N_2 permeability more significantly than that of CO_2, resulting in a decrease in the CO_2/N_2 selectivity.

The activation energy for permeation, which can be evaluated from the slopes in Figure 3.7 is shown in Figure 3.9. The calculation of the activation energy can be found in Appendix B. The activation energy represents the overall energy needed for penetrants to permeate through the membrane matrix. As shown in Equation 2.6, it is the summation of heat of sorption and the activation energy of diffusion. Du *et al.* (2006) compiled apparent activation energy for permeation of CO_2, O_2, N_2, CH_4, and H_2 in poly(N,N-dimethylaminoethyl methacrylate)/ polysulfone composite (PDMAEMA/PSF), cellulose, 6FDA-durene polyimide, and poly(lactic acid) membranes. The trend observed here are similar to those in their study. CO_2 tends to have a lower activation energy, whereas N_2 has the highest activation energy because of its lower condensability and larger size.

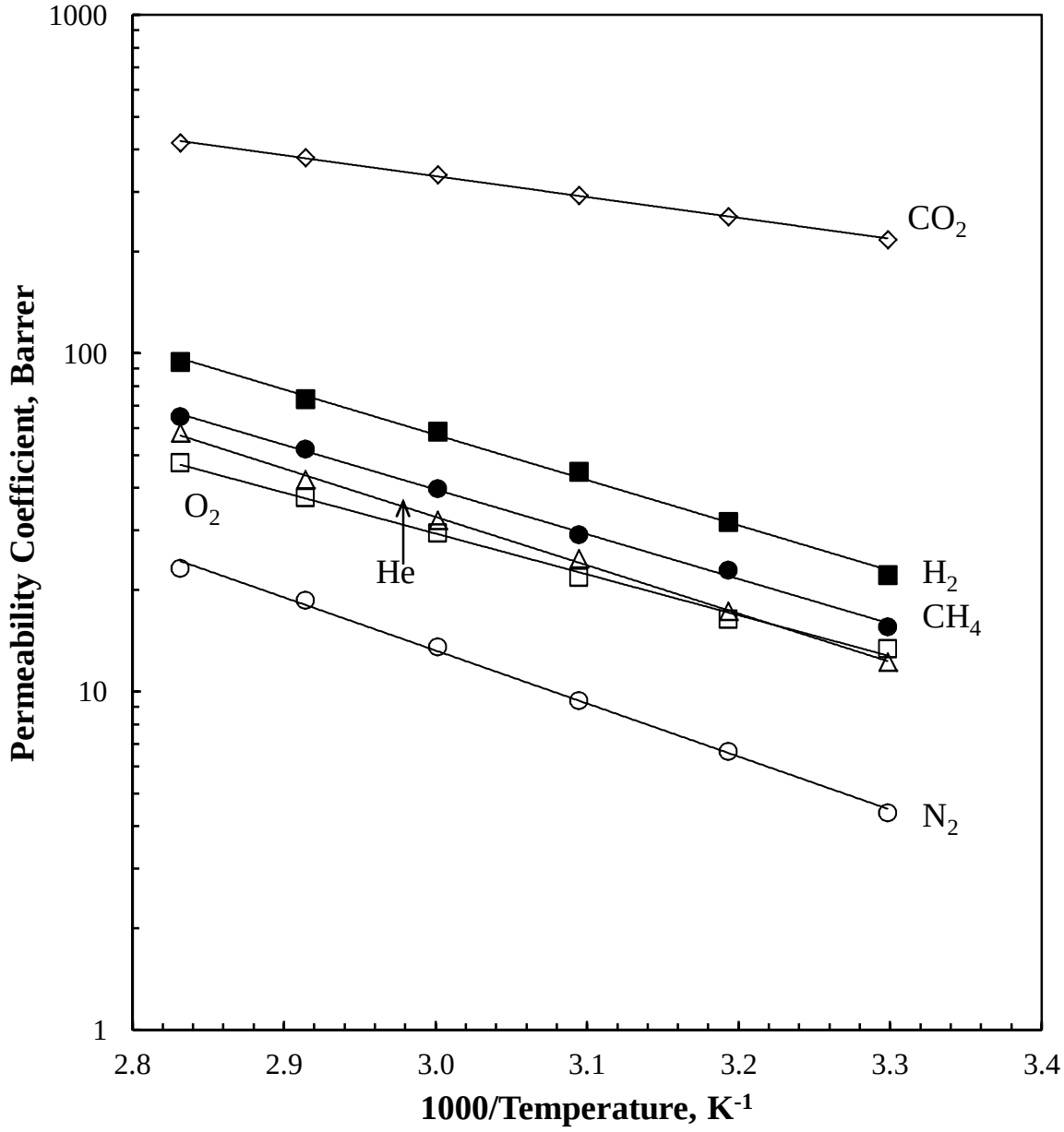

Figure 3.7 Effect of temperature on gas permeability at 0.7 MPa

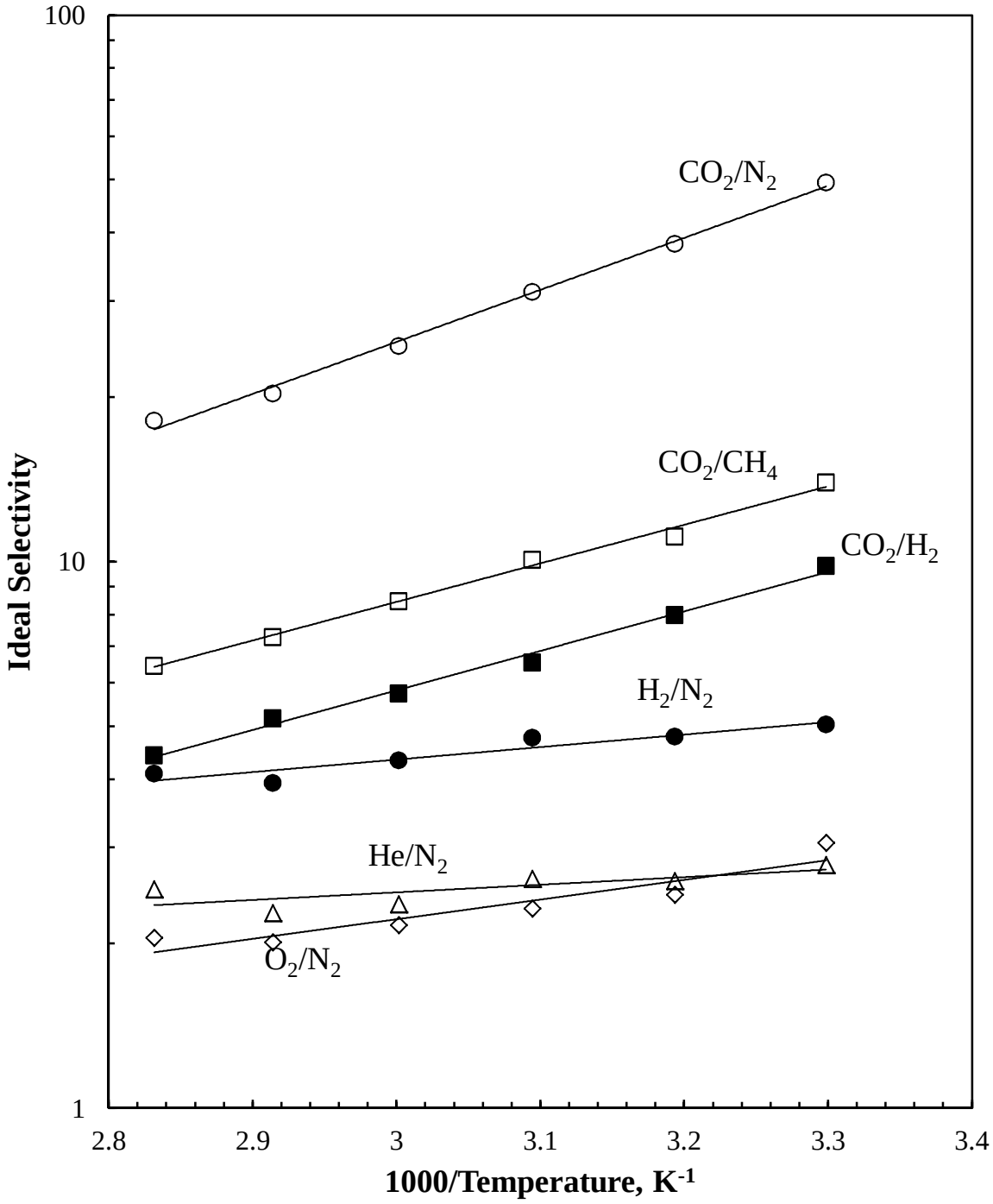

Figure 3.8 Effect of temperature on ideal selectivity

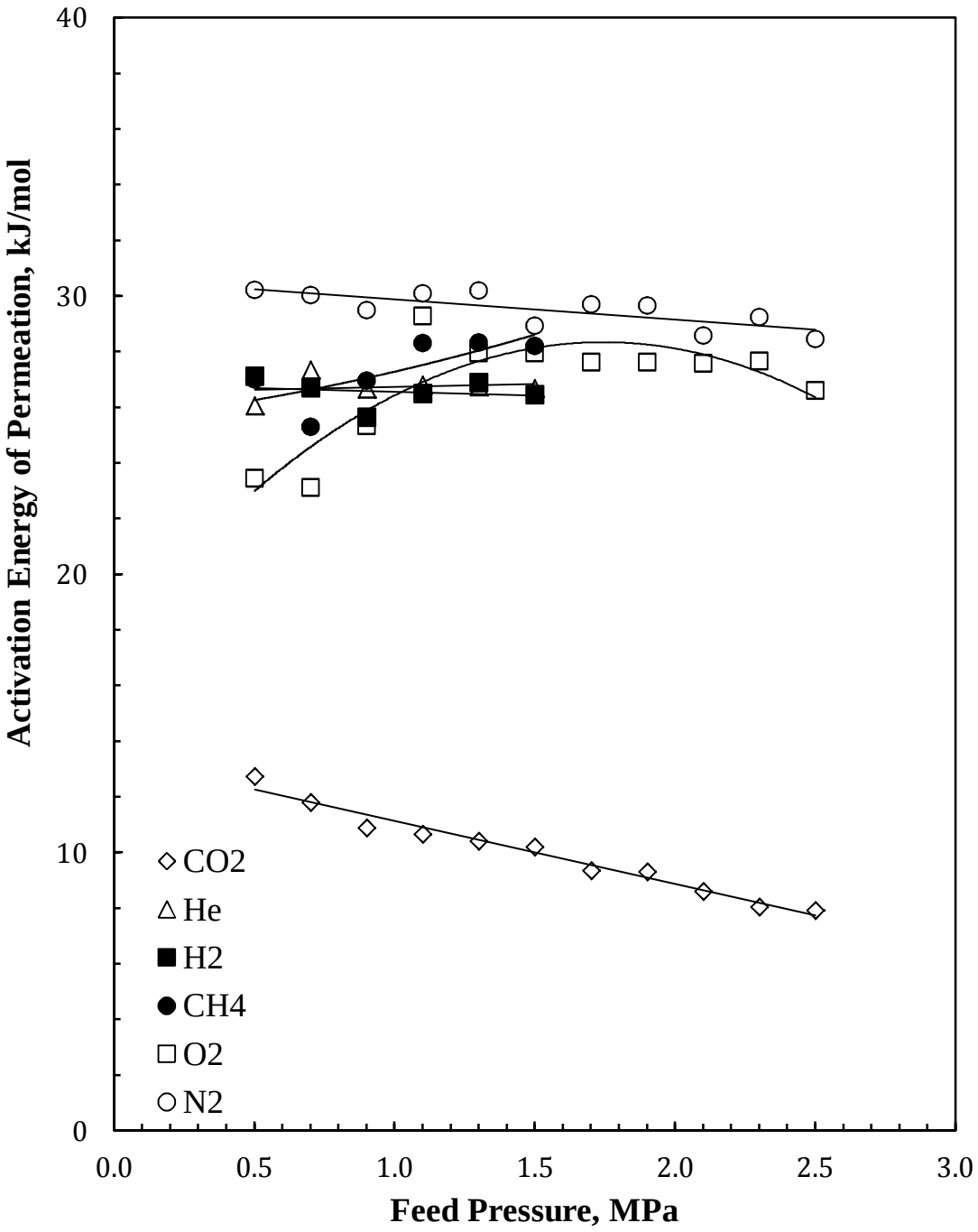

Figure 3.9 Gas permeation activation energies

3.3.3 Effect of Solvents Used in Membrane Preparation

The solvent-polymer interaction is unique during the dissolution process; hence, the solvents may play an important role in membrane formation and morphology. Two solvents, NMP and 1-butanol, were studied to determine whether the solvent used to prepare the membrane would influence the membrane permeability and selectivity. Polymer solutions containing 6 wt% Pebax®1074 in each solvent were cast to prepare membranes. The physical properties of the two solvents are shown in Table 3.1 and their chemical structures are shown Figure 3.10. The effect of different solvents on the permeation flux, permeability and selectivity of the resulting membranes are shown in Figure 3.11 to Figure 3.13, respectively.

Table 3.1 Physical properties of 1-butanol and NMP

Property	1-Butanol	NMP
Molecular weight (g mol^{-1})	74.12	99.13
Density (g cm^{-3})	0.81	1.028
Boiling point (°C)	118	202

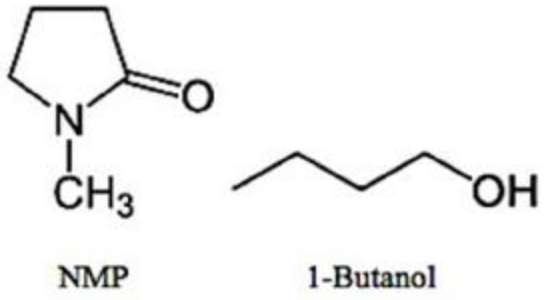

Figure 3.10 Chemical structures of NMP and 1-butanol

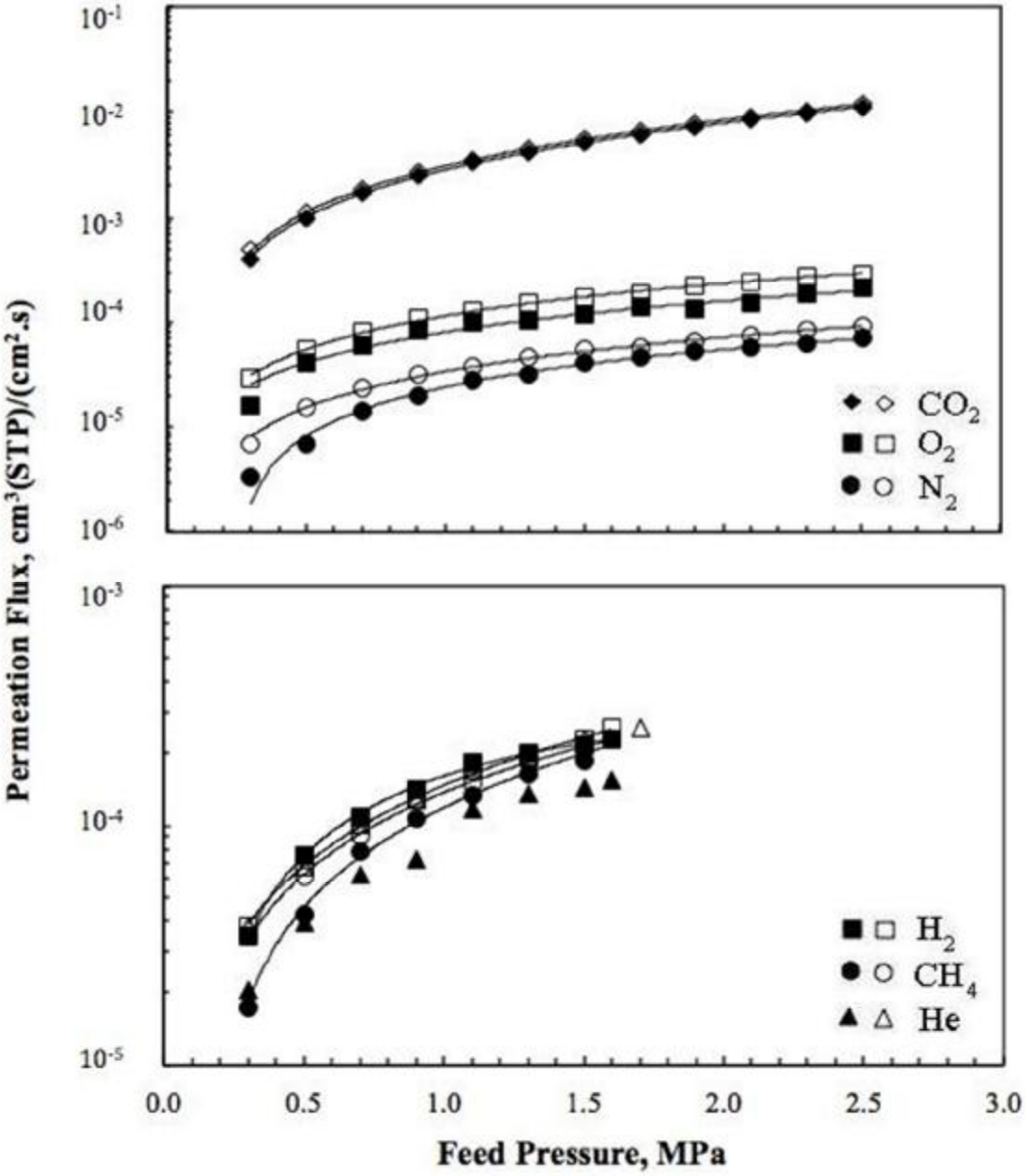

Figure 3.11 Effect of solvents used in membrane preparation on gas permeation flux
Note: open markers indicate NMP and closed markers indicate 1-butanol

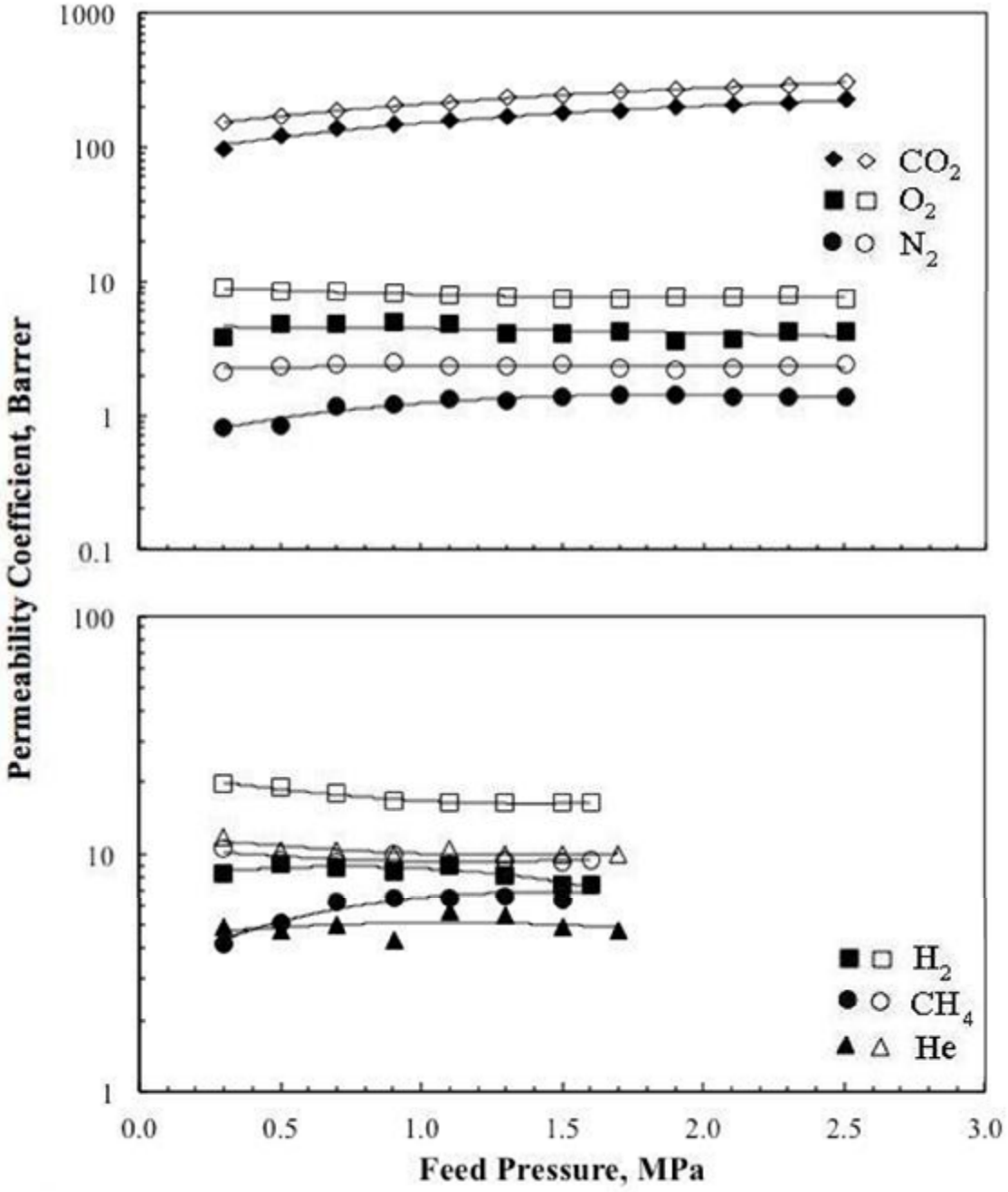

Figure 3.12 Effect of solvents used in membrane preparation on gas permeability coefficients
Note: open markers indicate NMP and closed markers indicate 1-butanol

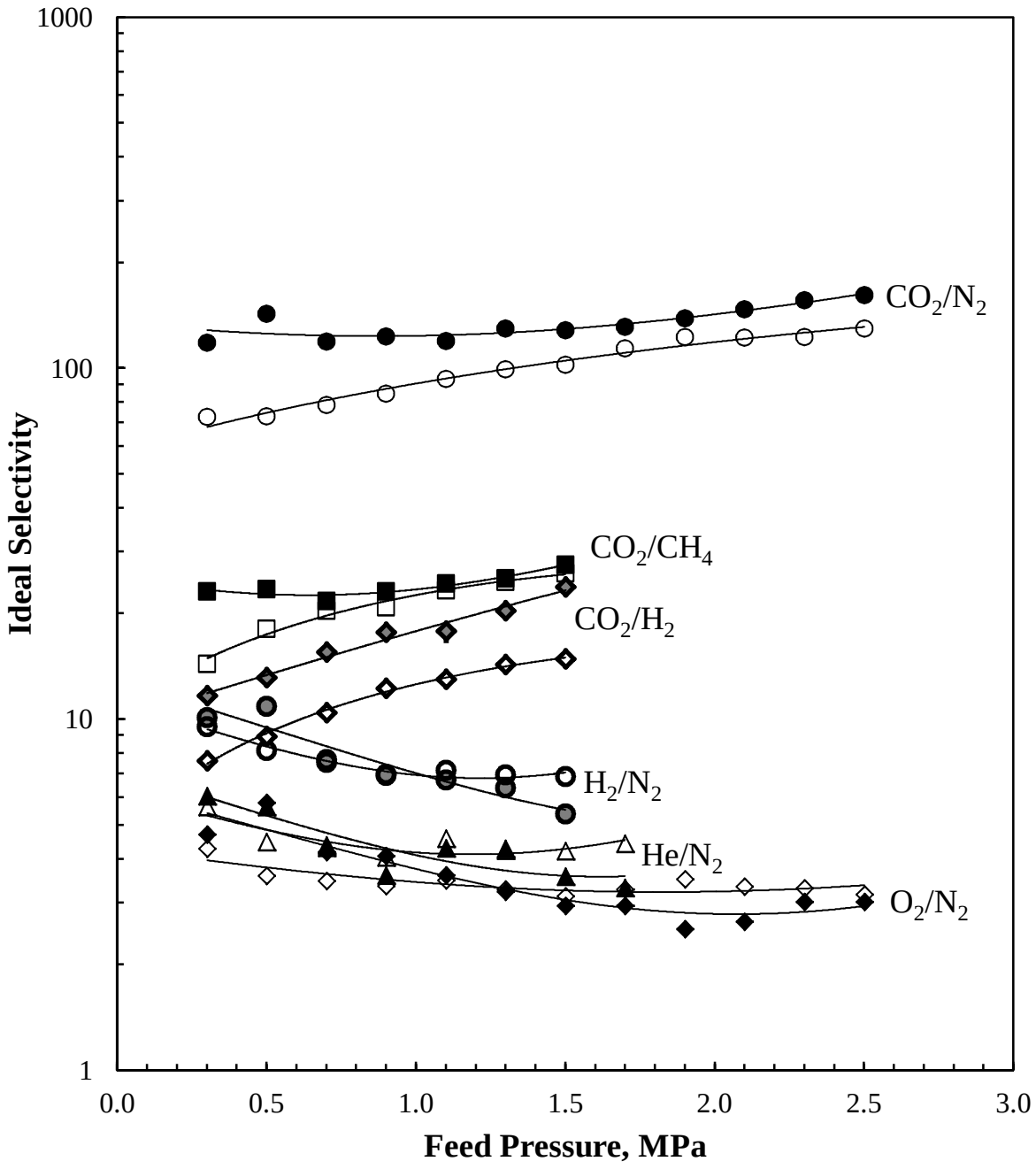

Figure 3.13 Effect of solvent used in membrane preparation on ideal selectivity
Note: open markers indicate NMP and closed markers indicate 1-butanol

As shown in Figure 3.11 and Figure 3.12, membranes prepared using in NMP as solvent appear to have greater gas flux and permeability, and lower selectivity than membranes prepared using 1-butanol as solvent. During the experiment, it was found that the polymer/1-butanol solution required lower temperature and a longer dissolution time than the polymer/NMP solution to achieve homogeneity. Qualitatively, the polymer in NMP solution was observed to be slightly more viscous than the polymer in 1-butanol solution at the same polymer concentration. From their chemical structures, 1-butanol appears to be linear while NMP seems to be larger in size and round in shape. Thus, it may be hypothesized that the "cavities" created by NMP in the membrane matrix will be greater than those created by butanol, leading to a higher permeability and a lower selectivity. The latter observation is shown in Figure 3.13. In addition, if the membrane retained any residual solvent, the solvent molecules become plasticizers and will facilitate gas transport across the membrane. This will result in reduced diffusivity selectivity as well. NMP is less volatile than 1-butanol, as indicated by its higher boiling point, and therefore it is more readily retained in the membrane matrix.

According to Han and Nam (2002), the solvents affect the thermodynamics and rheology of the polymer solution. The polymer-solvent interaction parameter, χ, for this solution system is unavailable; however, the polymer was observed to be miscible in each solvent. In addition, an increased solution viscosity hinders the kinetic phase separation. Conditions of solvent removal are important as well because it controls the rate of outflux of solvent from the membrane due to evaporation during membrane formation (Yeow *et al.*, 2004).

3.3.4 Effect of Membrane Heat-Treatment

Heat-treatment has been observed to noticeably enhance selectivity in polymeric membranes (Zhao *et al.*, 2006). Thus, a batch of membranes cast from 15 wt% solution in NMP was heat-treated in the oven at 100 °C for 80 mins to determine the effects of heat-treatment. Initially a heat-treatment condition of 200 °C and 2 hours was used, but the resulting membrane was found to be very brittle, presumably due to degradation at high temperatures. Figure 3.14 and Figure 3.15 demonstrate the differences in flux and permeability coefficients between heat-treated and non heat-treated membranes.

As observed in Figure 3.14 and Figure 3.15, the heat-treated membrane permeates slightly slower than the non heat-treated membrane. However, both follow a similar trend as pressure changes. The heat treatment allows the polymer chains to reorient, stretch and rearrange themselves into a more stable formation. After this process, the membrane becomes more compact due to a better ability to "stack" their chains (Ghosal and Freeman, 1994). Hence, the gas permeability through heat-treated membranes is lower than that of non heat-treated membranes. The selectivity of the membrane is shown to increase when the membrane is heat-treated, as illustrated in Figure 3.16. Since heat-treatment also helps remove residual solvent in the membrane, the membrane will be less plasticized after the heat-treatment, which helps increase the selectivity and decrease the permeability as well.

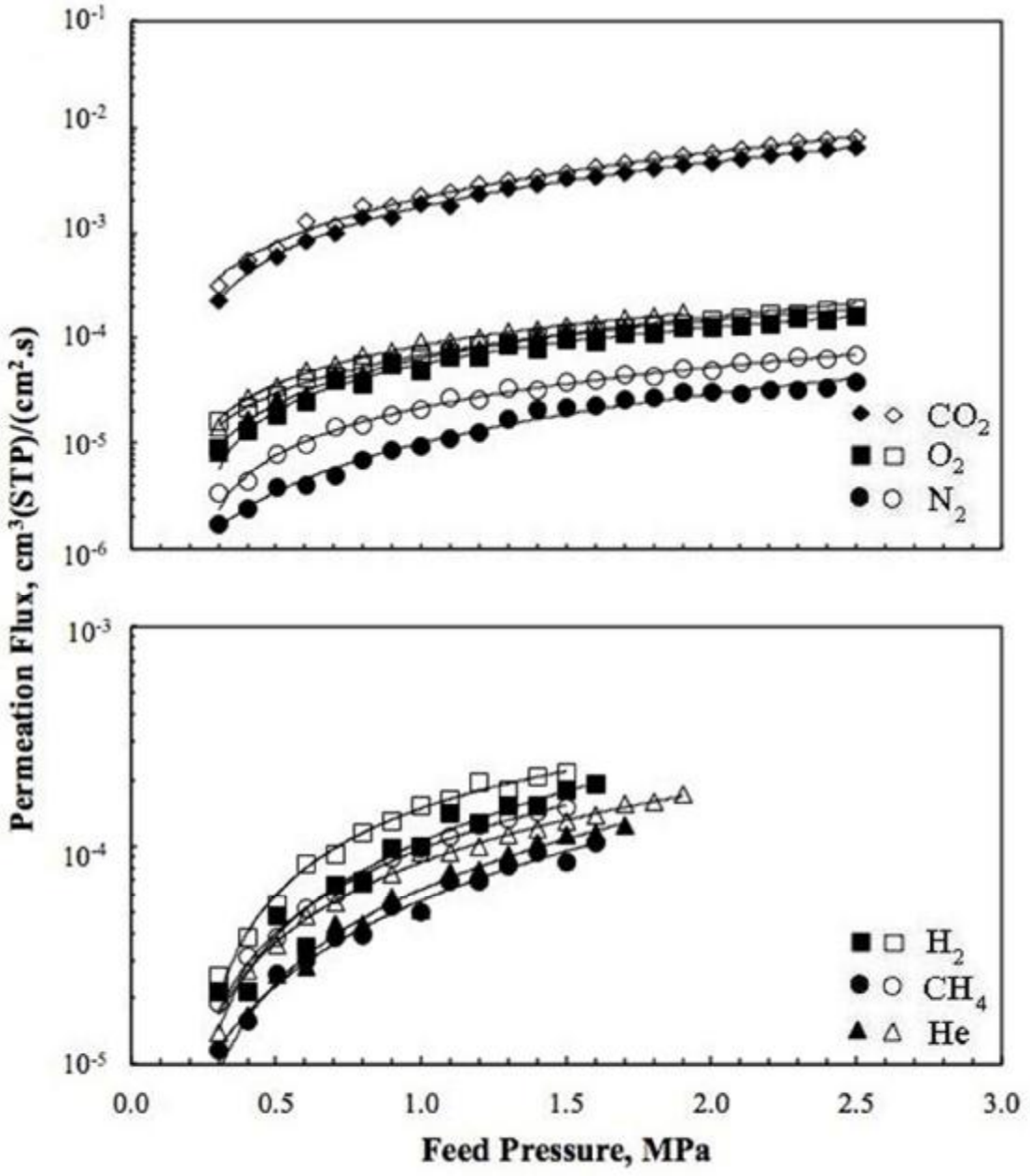

Figure 3.14 Effect of heat-treatment on gas permeation flux
Note: open markers indicate not heat-treated and closed markers indicate heat-treated

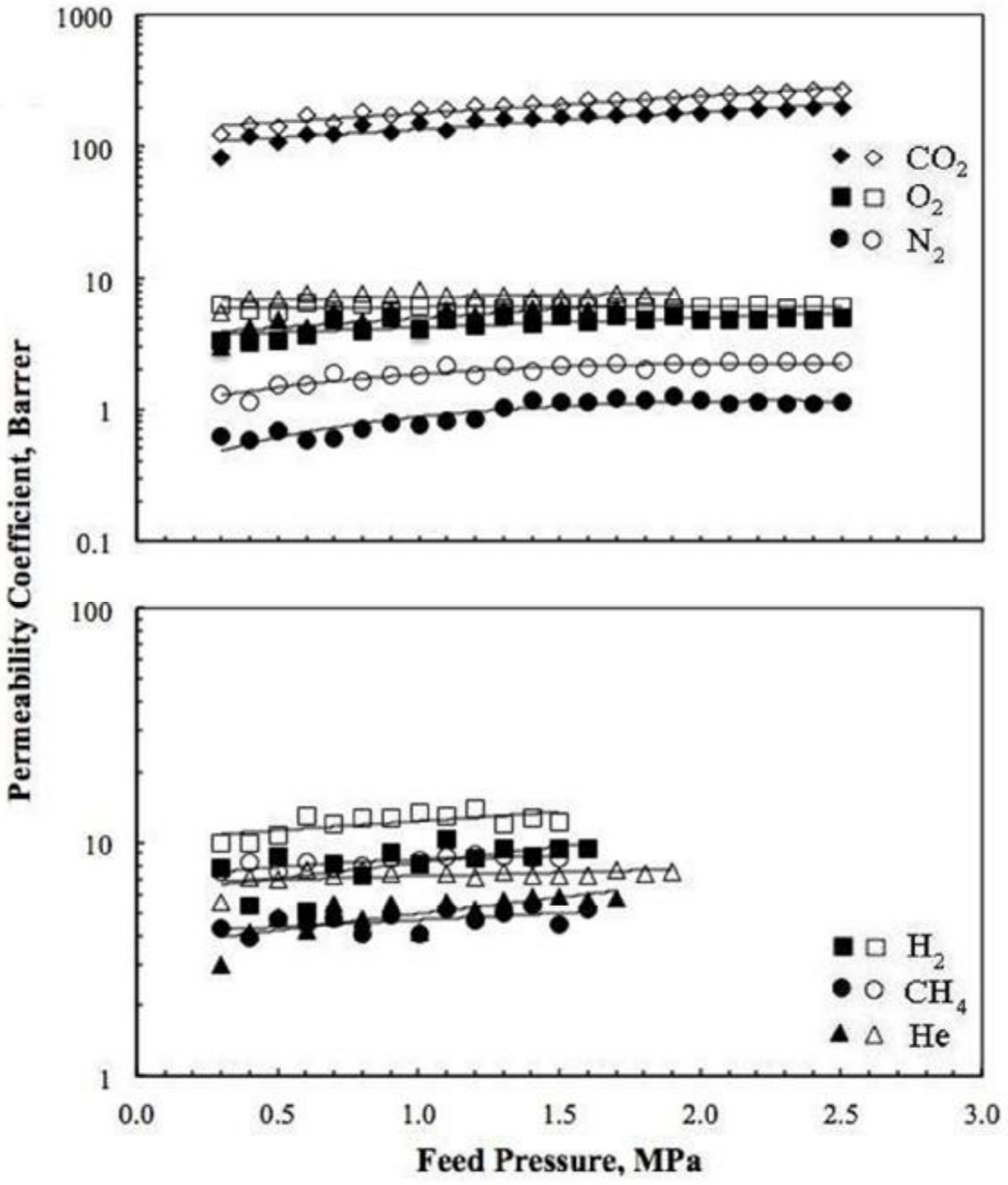

Figure 3.15 Effect of heat-treatment on gas permeability coefficient
Note: open markers indicate not heat-treated and closed markers indicate heat-treated

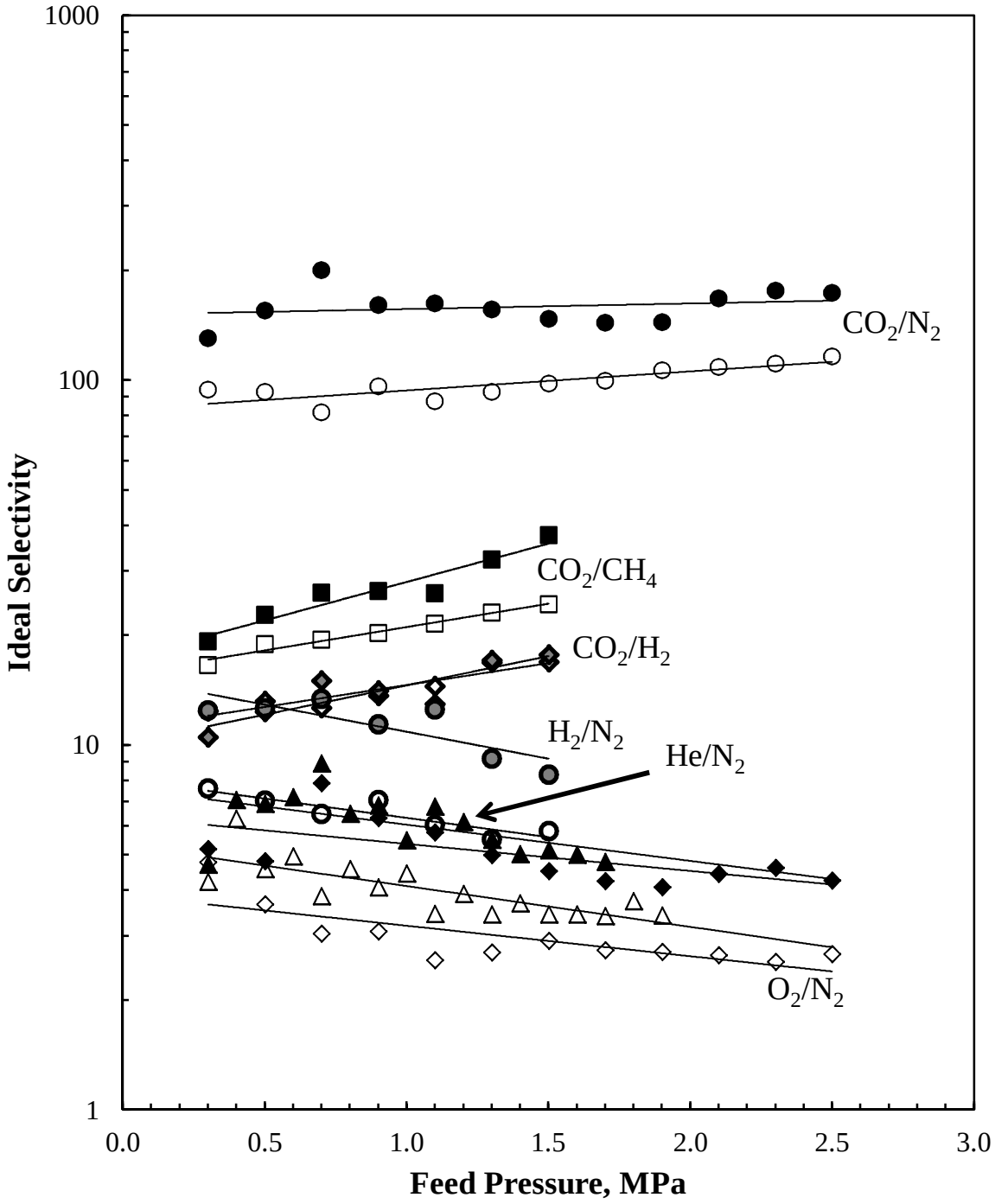

Figure 3.16 Effect of heat-treatment on ideal selectivity
Note: open markers indicate not heat-treated and closed markers indicate heat-treated

3.3.5 Effect of Membrane Thickness and Polymer Concentration

The thickness of the membrane was varied using wires of different diameters when casting 15 wt% NMP polymer solution. The thickness of the membrane was measured at 10 different locations (2 in the center and 2 in each quadrant) using a Mitutoyo micrometer, and then averaged to obtain an accurate estimate of the membrane thickness. The permeation tests were carried out at room temperature.

As observed in Figure 3.17, an increase in membrane thickness correlates to a decrease in permeation flux. This behaviour is consistent for all gases tested (see Appendix C). However, the permeability coefficient of the membranes, which is the permeation flux normalized by the membrane thickness, is almost a constant independent of the membrane thicknesses, as shown in Figure 3.18. This also confirms that the membranes are homogeneous and the permeability coefficient is thus an intrinsic property of Pebax®1074.

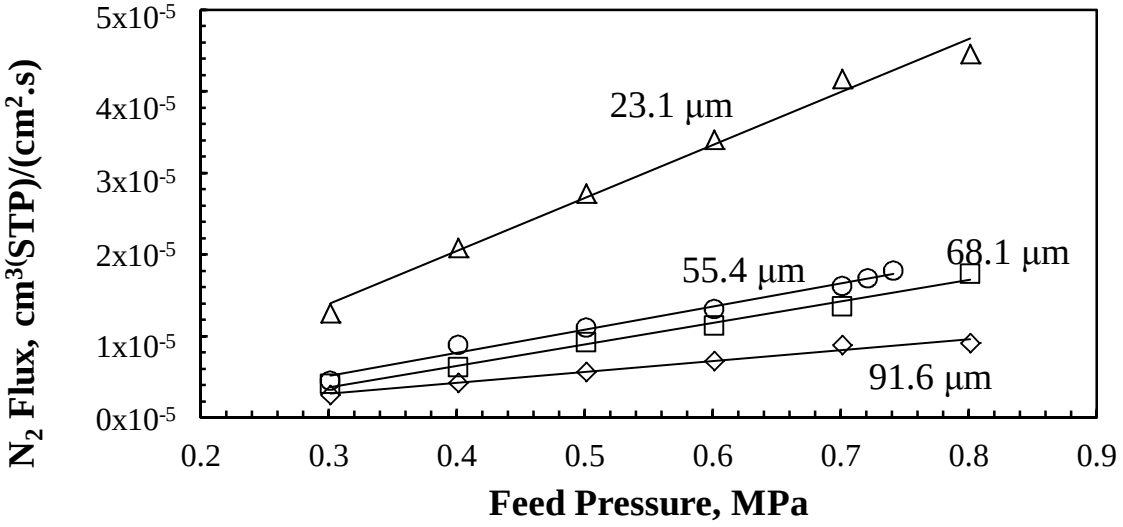

Figure 3.17 Effect of membrane thickness on nitrogen gas permeation flux

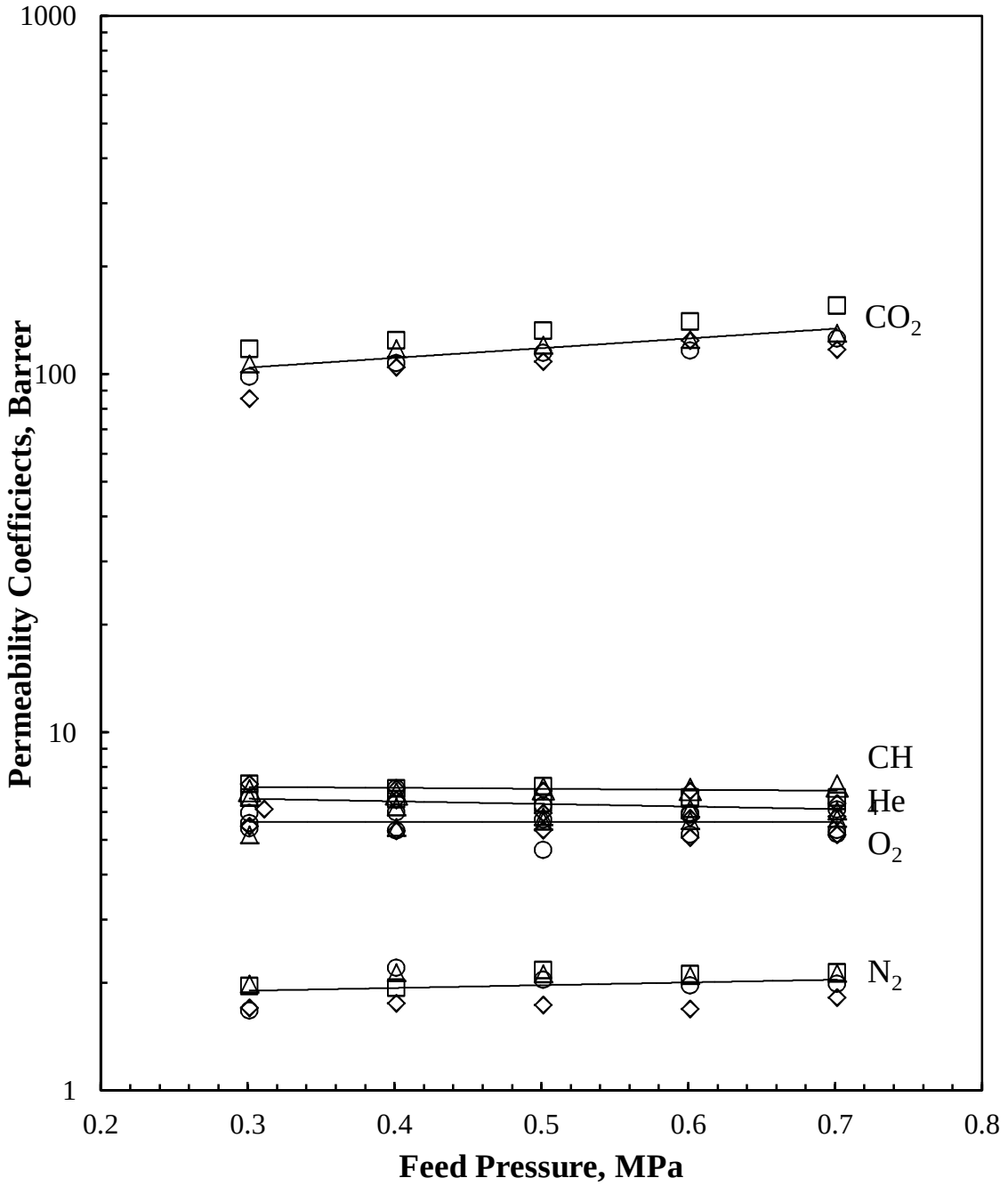

Figure 3.18 The gas permeability coefficient has no distinct relationship with membrane thickness (◇ 0.0916 mm, □ 0.0681 mm, ○ 0.0554 mm, △ 0.0231)

The concentration of polymer in the membrane casting solution may affect the formation and morphology of the membrane. Membranes were prepared from solution containing 15 wt% and 6 wt% polymer in NMP and tested at room temperature. In order to purely study the effect of concentration, the permeability values must be temperature-normalized using a ratio of the activation energies and Arrhenius equation. Permeability is also adjusted for thickness due to inconsistent thickness measurements. A sample calculation is shown in Appendix B.

Figure 3.19 shows that the temperature-normalized permeability values for the 15 wt% and 6 wt% polymer solutions are not significantly different. Figure 3.20 shows the selectivities of membranes prepared from the two concentrations also do not appear to be considerably different. Polymer chains in a less concentrated solution have more space to stretch out than in a more concentrated solution with the same volume. Thus, the polymer chains are more relaxed than those in higher concentration solutions. As a result, there is more free volume in membranes fabricated from the lower concentration solution, resulting in higher penetrant diffusivity. There is also lower concentration of polymer at the penetrant-membrane interface, thus providing lower resistance to sorption.

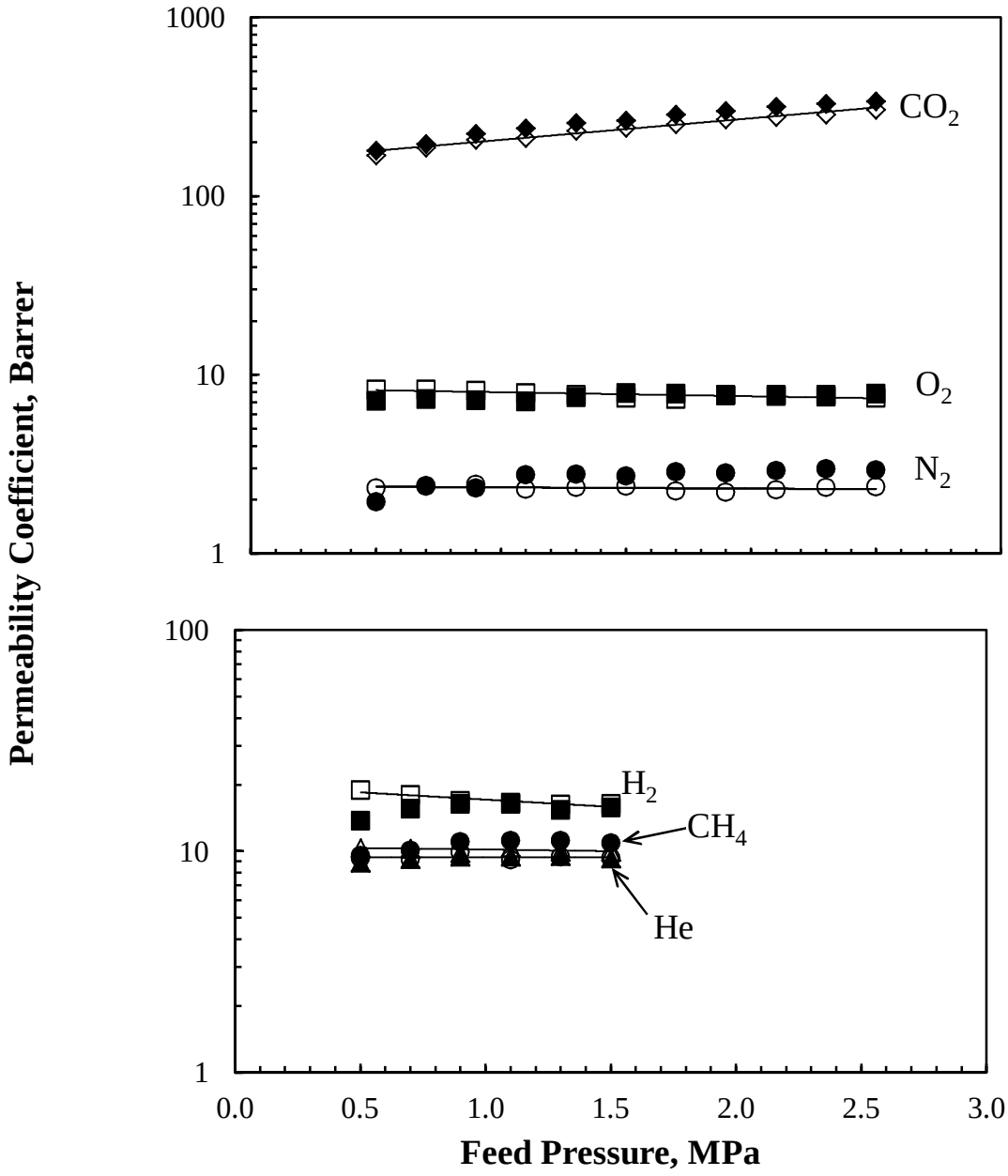

Figure 3.19 Effect of polymer concentration on gas permeability coefficient
Note: open markers indicate 6 wt% and closed markers indicate 15 wt%

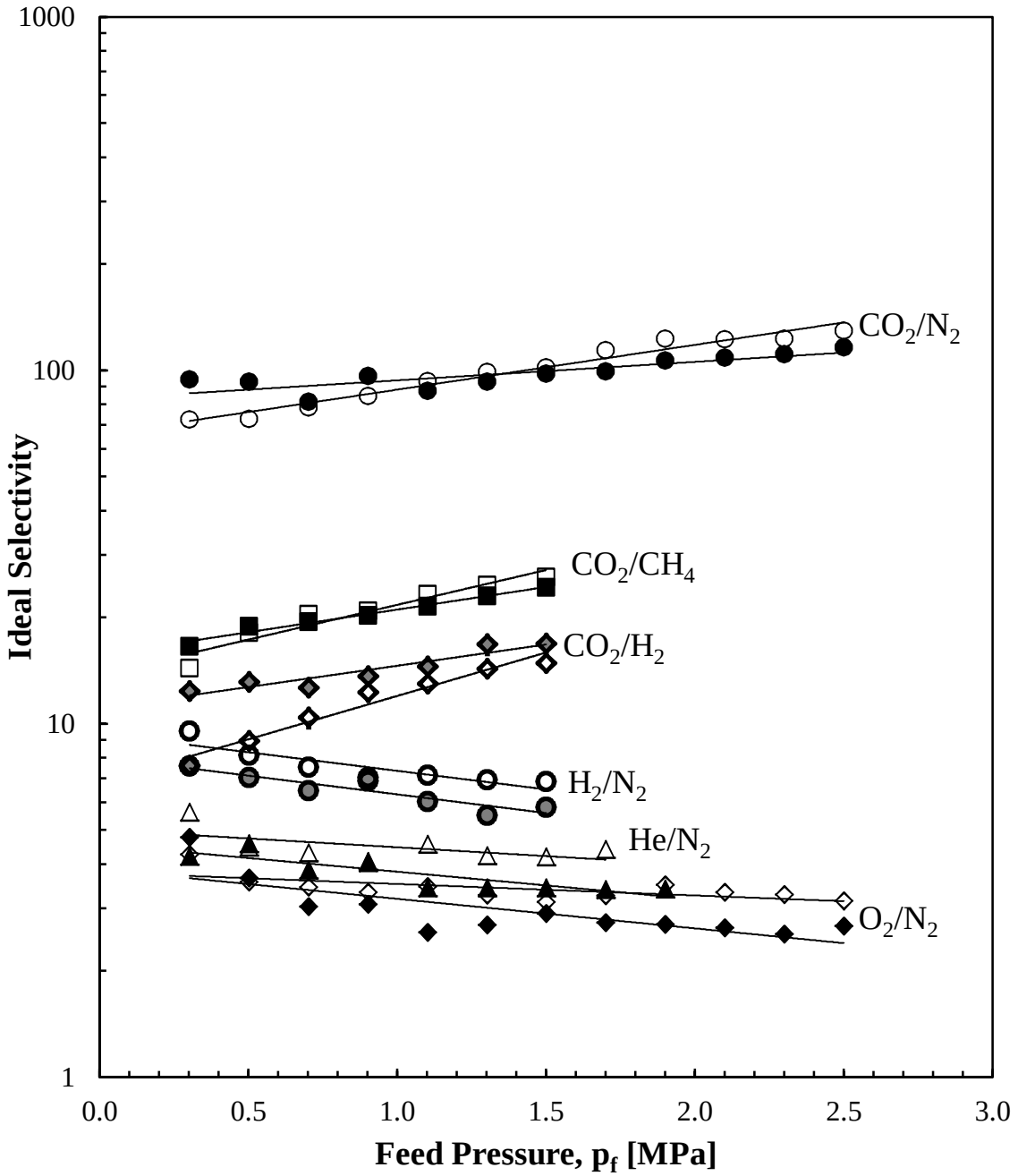

Figure 3.20 Effect of polymer concentration on ideal selectivity
Note: open markers indicate 6 wt% and closed markers indicate 15 wt%

3.4 Conclusions

The pure gas permeability of N_2, O_2, CH_4, He, H_2, and CO_2 in Pebax®1074 was determined. The order of gas permeability was observed to be CO_2> H_2> He > CH_4> O_2> N_2, where CO_2 and N_2 permeability coefficients were determined to be 90±3 and 2.79±0.03 Barrers, respectively, at room temperature and 0.3 MPa feed pressure. Additionally, the gas permeability was not significantly affected by feed pressure. The highest gas pair selectivity was observed to be an average of 70 for CO_2/N_2, followed by CO_2/CH_4 at 17, CO_2/H_2 at 11, H_2/N_2 at 4.8, and O_2/N_2 at 2.2 and He/N_2 at 2.4, over the pressure range tested. Pebax®1074 did not suffer from "memory" or hysteresis of previous permeations. Meanwhile, the temperature dependence of gas permeabilities could be characterized by the Arrhenius equation. With an increase in temperature, the gas permeabilities increased, whereas selectivity decreased. The activation energy of permeation is the lowest for CO_2 and highest for N_2, with values of 30 and 12 kJ/mol, respectively. In addition, out of the two solvents used during membrane fabrication, NMP and 1-butanol, the film prepared using 1-butanol has a slightly better selectivity. Heat-treatment of the membrane lowered the gas permeabilities, however selectivities were raised as high as 60% for CO_2/non-polar gas pairs. Lastly, membrane thickness and polymer concentration used in membrane fabrication did not show a noticeable effect on the performance of the resulting membranes.

CHAPTER 4

Pervaporation of Water and DMMP in Pebax®1074

4.1 Introduction

Pervaporation, as the name suggests, involves both permeation and vaporization of penetrant molecules. During this process, a liquid feed is in contact with the membrane, and transport through the membrane is induced by vapour pressure difference between the feed and permeate sides. The pressure difference can be maintained by using a vacuum pump or sweeping gas, on the permeate side (Baker, 2004). When a vacuum is applied on the permeate side, the penetrant is vapourized and removed from the membrane. The vapourized penetrants are then condensed and collected as a liquid permeate. This technique is especially attractive for separating azeotropic or closely-boiling mixtures that ordinarily are difficult to separate using distillation or other processes. Additionally, Nguyen *et al.* (2001) found that pervaporation is a more reliable testing method than traditional American Society for Testing and Materials (ASTM) standards for testing moisture vapour transmission rate due to minimized mass and heat transfer

resistances. Currently, the main industrial application for pervaporation is dehydration of organic solvents (Baker, 2004).

Similar to gas separation, pervaporation requires nonporous membranes, preferably with asymmetric structure to improve flux (Mulder, 1991). The choice of polymeric material depends strongly on the type of application. For this study, the application is focused on chemical protective clothing due to outstanding water permeation ability of Pebax® polymers (Jonquieres *et al.,* 2002b). Effective chemical protective clothing is essential for military and civilian personnel during chemical warfare attacks. Dimethyl methylphosphonate (DMMP) was selected as the challenge chemical because it is a non-toxic simulant of sarin, a nerve agent.

The objective of this investigation was to use pervaporation technique to measure water and DMMP permeation through Pebax®1074. The water permeation was used to simulate perspiration from people wearing the potential protective materials. The tests would establish the feasibility of using Pebax®1074 in protective textile applications based on percutaneous (i.e. skin) protection. The effects of aging, temperature extremes, laundering and other factors were beyond the scope of this study. Additionally, 4 commonly available glove materials and 3 other experimental candidates were also tested under same conditions for comparison.

Similar to gas separation, mass transport through pervaporation membranes also follow the solution-diffusion mechanism, as described previously. Since the silicone membrane used here was coated onto a substrate and its exact thickness is not known; the permeance was used in this section instead of permeability coefficient to measure the permeation rate.

Since the membrane contacts liquid on one side, membrane swelling may result if the liquid has a good affinity to the membrane (Mulder, 1991). Plasticization results in an increased

permeation rate and drastically reduced selectivity. Thus selection of suitable membrane material is of utmost importance. The polymer should not swell too much otherwise the selectivity would be compromised. Additionally, plasticization effectively reduces the glass transition temperature of polymers (Ghosal and Freeman, 1994), which may cause a glassy polymer to behave as a rubbery one. However, a low sorption or swelling will result in a very low flux. Thus an optimum sorption of 5 – 25 wt% was found to be useful (Mulder, 1991).

The temperature dependence of the permeation flux and permeance was also studied. Temperature is a vital parameter in pervaporation because it significantly affects solubility and diffusivity of penetrant molecules.

4.2 Experimental

4.2.1 Materials

The Pebax®1074 used was the same as the one described in Chapter 3.The glove materials and other experimental candidate materials tested are listed in Table 4.1. The materials were tested in new, as-received condition. Water was deionized and distilled prior to use. Dimethyl methylphosphonate (DMMP) (97%) was purchased from Sigma Aldrich and used without further purification.

Table 4.1 List of membrane materials tested

Material	Manufacture Information	Membrane Thickness (mm)
Pebax®1074	15 wt% in NMP using solution casting	0.0384
Pebax®2533	15 wt% in DMAc using solution casting	0.0419
Nitrile (SemperCare® Nitrile PF)	Sempermed USA Inc. (Clearwater, FL)	0.0941
Natural latex rubber	VWR® (West Chester, PA)	0.1354
Polyvinyl chloride (PVC)	DAK Technical (12" Antistatic)	0.1678
Low density polyethylene (LDPE)	Glad Cling Wrap	0.0116
Silicone	Silicone coated onto porous substrate	0.1785[a]
Silicone polycarbonate copolymer (Si-PC)	Flat nonporous membrane	0.0613

[a] Overall thickness. The silicone skin layer thickness is unknown.

4.2.2 Membrane Preparation

Both Pebax®1074 and 2533 membranes were prepared using the solution-casting method described in Section 3.3.2 at 15 wt% with 1-methyl-2-pyrrolidinone (NMP) as the solvent. Sample swatches of each glove material were cut directly from the palm of a glove. The silicone and silicone-polycarbonate copolymer membranes were provided by Membrane Products, Troy, NY.

4.2.3 Pervaporation Experiments

The membrane cell used in this portion of the experiments was similar to the one described in Figure 3.1, except that the membrane cell was incorporated with a jacketed feed reservoir, as shown in Figure 4.1. A small amount of feed, 10 mL, was loaded into the reservoir to cover the entire membrane area while not exerting a significant pressure onto the membrane by the liquid.

The effective area of the membrane in this cell was 13.85 cm^2. The water jacket was connected to a thermal bath circulator (Haake-Fisons Instruments Inc.), to adjust and maintain the temperature of the feed. The walls of the jacket were covered with polystyrene insulation to minimize heat loss to the surrounding air.

A duo-seal vacuum pump (model no. 1405), Welch Vacuum Technology, Niles, IL, two cold traps, and a vacuum gauge (model CG16K) from Edwards High Vacuum International, West Sussex, England, were connected to the permeate side of the membrane, as shown in Figure 4.1. When vacuum was applied, the liquid feed – either water or DMMP –was drawn through the membrane into the cold trap submerged in liquid nitrogen. The permeant was condensed and collected in one of the cold traps. The vacuum level on the permeate side was maintained at < 2 mmHg throughout the experiments. Before each run, the vacuum valve was opened to air a few times to purge the setup, and the system was operated for at least one hour to ensure steady state prior to data collection. The permeation rate was determined using the weight of the permeant collected over a known period of time.

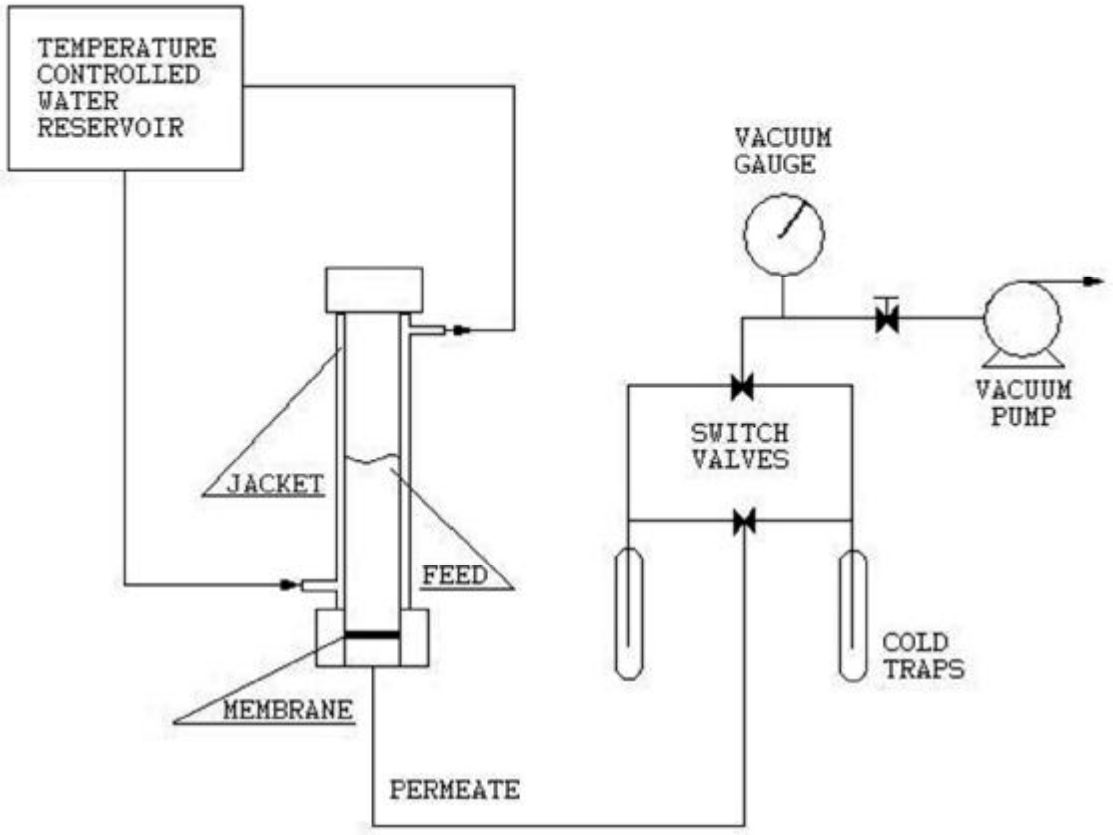

Figure 4.1 Flow diagram of vapour permeation system

4.2.4 Contact Angle

The water and DMMP droplet contact angles were measured for all the materials tested using a Tantec Half Angle Technique contact angle meter. This characterizes interfacial properties of the membranes.

4.3 Results and Discussion

4.3.1 Contact Angle

The average value of the contact angles of water on Pebax®1074 is 70 °C – indicating Pebax®1074 is a slightly hydrophilic polymer. A polymer with a water droplet contact angle lower than 90° is considered hydrophilic. It was noticed that heat-treatment appears not to have significantly affected the contact angle. Table 4.2 summarizes the contact angles of water and DMMP in the membranes tested. The data in Table 4.2 show that the polymers appear to have a better affinity to DMMP than water except for nitrile. This suggests that the diffusivity aspect dominates the permeation, if these materials are to be used as protective wear for DMMP.

Table 4.2 Contact angles of water and DMMP

Polymer	H_2O Contact Angle (°)	DMMP Contact Angle (°)
Nitrile	14	25
PVC	110	44
Latex	1.0×10^2	54
LDPE	98	41
Pebax®2533	95	65
Pebax®1074	7.0×10^2	3.0×10^1
Silicone	110	73
Si-PC	120	62

4.3.2 Pervaporation

The vapour transmission rates (VTR) of water and DMMP in Pebax®1074 at 35 °C were determined to be 57500 g/(m^2.day) and 184 g/(m^2.day), respectively. The water flux in a Pebax®1074 membrane (25 μm thick) was reported by Nguyen *et al.* (2001) to be 85 kg/(m^2.day) at 38 °C. A few recent studies on water and DMMP permeation are summarized in Table 4.3. Comparing water fluxes of the materials studied, Pebax®1074 is proven to be the most permeable

to water, and thus the most breathable material. In contrast, the DMMP flux in Pebax®1074 is not the lowest. However, its H_2O/DMMP selectivity is 84 at 35 °C, which is greater than most of the reported values, meaning it is very resistant to DMMP permeation. Although the selectivity reported by Lu *et al.* (2008) is very high, their cross-linked lyotropic liquid crystal-butyl rubber composite membrane material is very complicated to fabricate and most likely very expensive; therefore, it is a less feasible option for protective textiles compared to Pebax®1074. Other factors should also be considered when selecting polymers for protective clothing such as durability, cost, weight, process ability, and other physical properties.

Table 4.3 Recent investigations of water and DMMP permeation properties

Membrane	Thickness (mm)	Test Method	Water	DMMP	H_2O/DMMP Selectivity[c]	Reference
Silicone (PDMS)	0.033	PV with N_2 sweep gas 25 °C	NA	56800 x 10^9 cm^3(STP) .cm/ (cm^2.s.cmHg)	NA	Almquist and Hwang (1999)
Nafion 117	0.178	vapour permeation cell	790 g/(m^2.day)	599 g/(m^2.day)	0.047 [a]	Rivin *et al.* (2004)
Material C	0.179 –0.187	ASTM E96 35 °C	1.09×10^{-2} g/(mmHg.m. day)	2.13×10^{-3} g/(mmHg.m. day)	5.12	Napadensky and Elabd (2004)
N-methylolated nylon-6/chitosan blend membranes	Not reported	ASTM E96 35 °C	1.92×10^{-3} g/(mmHg.m. day)	1.26×10^{-4} g/(mmHg.m. day)	15.3	Napadensky and Elabd (2006)
LLC-BR composite membrane	Not reported	ASTM E96 25 °C	5900 g.μm/(m^2.day)	3.69 g.μm/(m^2.day)	55.6[a]	Lu *et al.* (2008)
Luminoflon added polyurethane	Not reported	ASTM E96 35 °C	0.864 [b] g/(day.m)	1.464 [b] g/(day.m)	0.59	Levine *et al.* (2010)
PAMPS	0.35	ASTM E96 35 °C	1.5×10^{8} mol/(mmHg. m.s)	0.9×10^{8} mol/(mmHg. m.s)	1.67	Jung *et al.* (2010)

[a] Calculated permeability selectivity from flux with water/DMMP vapour pressure ratio
[b] Calculated from per hour value
[c] Selectivity based on water/DMMP permeability ratio

As mentioned, temperature is a very important factor in pervaporation not only in energy consumption but also the separation performance of the system. Figure 4.2 and Figure 4.3 show the water permeation flux and permeance of the various materials tested. Their temperature dependencies follow an Arrhenius relationship; the same behaviour was observed for DMMP permeation flux and permeance, as shown in Figure 4.4 and Figure 4.5, respectively. A common trend among all four figures is that permeation flux increases and permeance decreases when the temperature increases. The increase in permeation flux can be attributed to combined effects from three factors. Firstly according to classic Eyring theory of diffusion, an increase in temperature makes the penetrant molecules more energetic, and thus permeation rate is increased due to increased diffusivity (Xu *et al.*, 2010). Secondly, the polymer chain segmental motion is increased in frequency and amplitude at higher temperatures, resulting in the formation of voids or channels, which allow penetrants to diffuse more easily (Xu *et al.*, 2010; Cao *et al.*, 1999). Lastly, an increase in temperature increases the vapour pressures of water and DMMP, thereby increasing the driving force for mass transport across the membrane (Xu *et al.*, 2010). On the other hand, the permeance is shown to decrease with an increase in temperature due to the opposing effects of sorption and diffusion based on the solution-diffusion model. As discussed earlier, the diffusion coefficient increases with increasing temperature. However, since the sorption is an exothermic process, the solubility coefficient decreases with increasing temperature (Reineke *et al.*, 1987). Hence, when the decrease in solubility is greater than the increase in diffusivity, the overall permeance will decrease. Similar behaviour can be observed in other pervaporation systems with hydrophilic membranes (Xu *et al.*, 2010; Du *et al.*, 2010; Mujiburohman and Feng, 2007).

Additionally, it can be observed that the permeation flux of water through all test materials is greater than that of DMMP. This can be attributed to the smaller size of water molecules, its higher volatility, and stronger affinity between water and the polymer materials. A comparison of water and DMMP properties is presented in Table 4.4.

Table 4.4 Comparison of DMMP and water properties

Property	**DMMP**	**Water**[a]
Molecular weight (g/mol)	124.08	18.01
Boiling point (°C)	181	100
Saturated vapour pressure (Pa) @ 25 °C[b]	110.93	3187.7
Liquid density (g/cm^3) @ 25 °C	1.145	1.00
ΔH_{vap} (kJ/mol) @ 25 °C	52.8[c]	1.882

[a] Poling *et al.* (2001)
[b] calculated from Antoine equation
[c] Butrow *et al.* (2009)

On the other hand, the permeances of DMMP through some polymers, such as nitrile, LDPE, latex, silicone and PVC, are higher than that of water. This can be ascribed to the stronger affinity between DMMP and these polymers, as discussed later. However, the water permeance in the two Pebax® copolymers (i.e. 1074 and 2533) remained higher than that of DMMP, presumably due to the hydrophilic polyamide segments present in the copolymers. The selectivity of Pebax®1074 to water/DMMP is especially promising, and this suggests that this material may be a good candidate for protection against chemical agents.

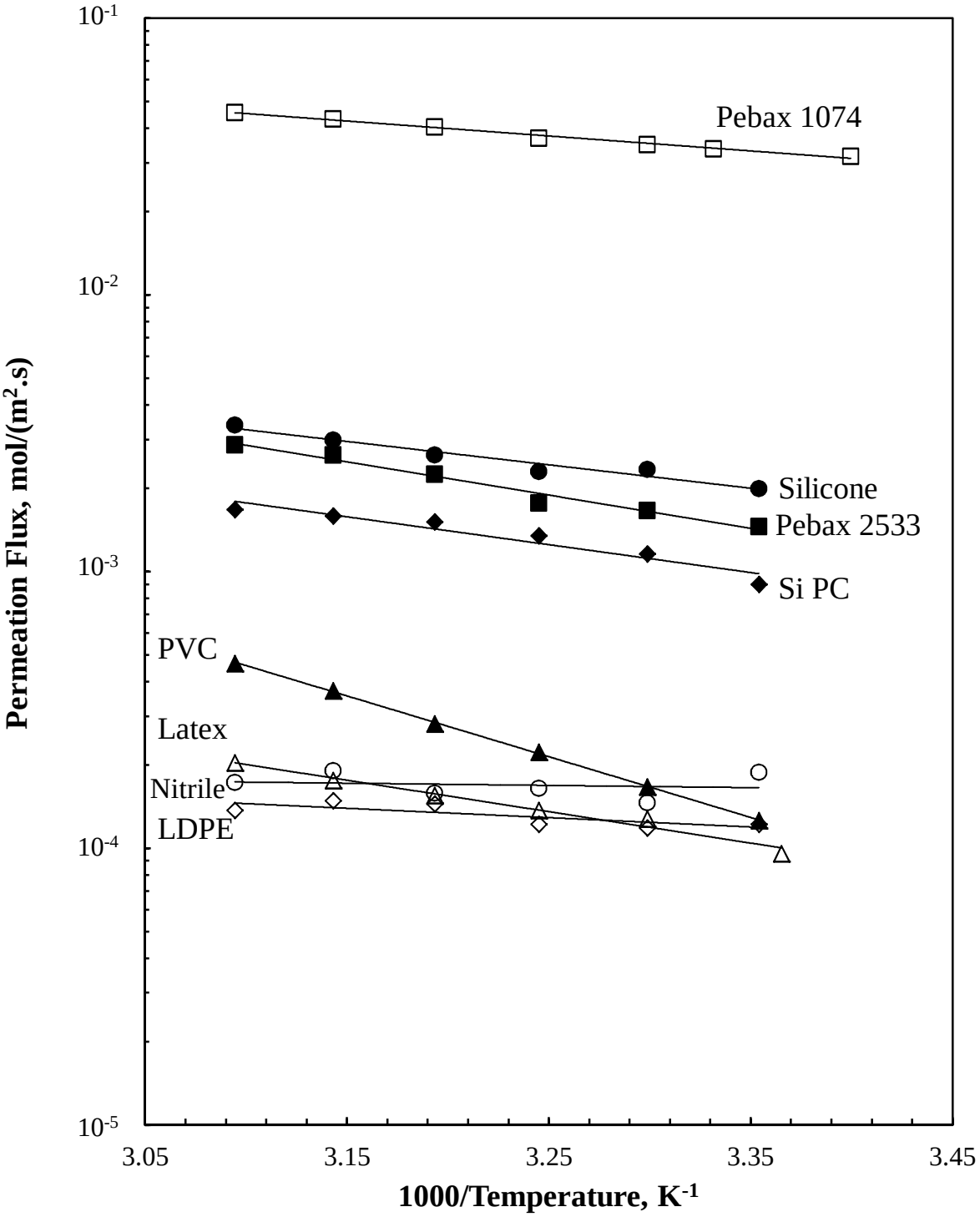

Figure 4.2 Effect of temperature on water permeation flux of tested materials

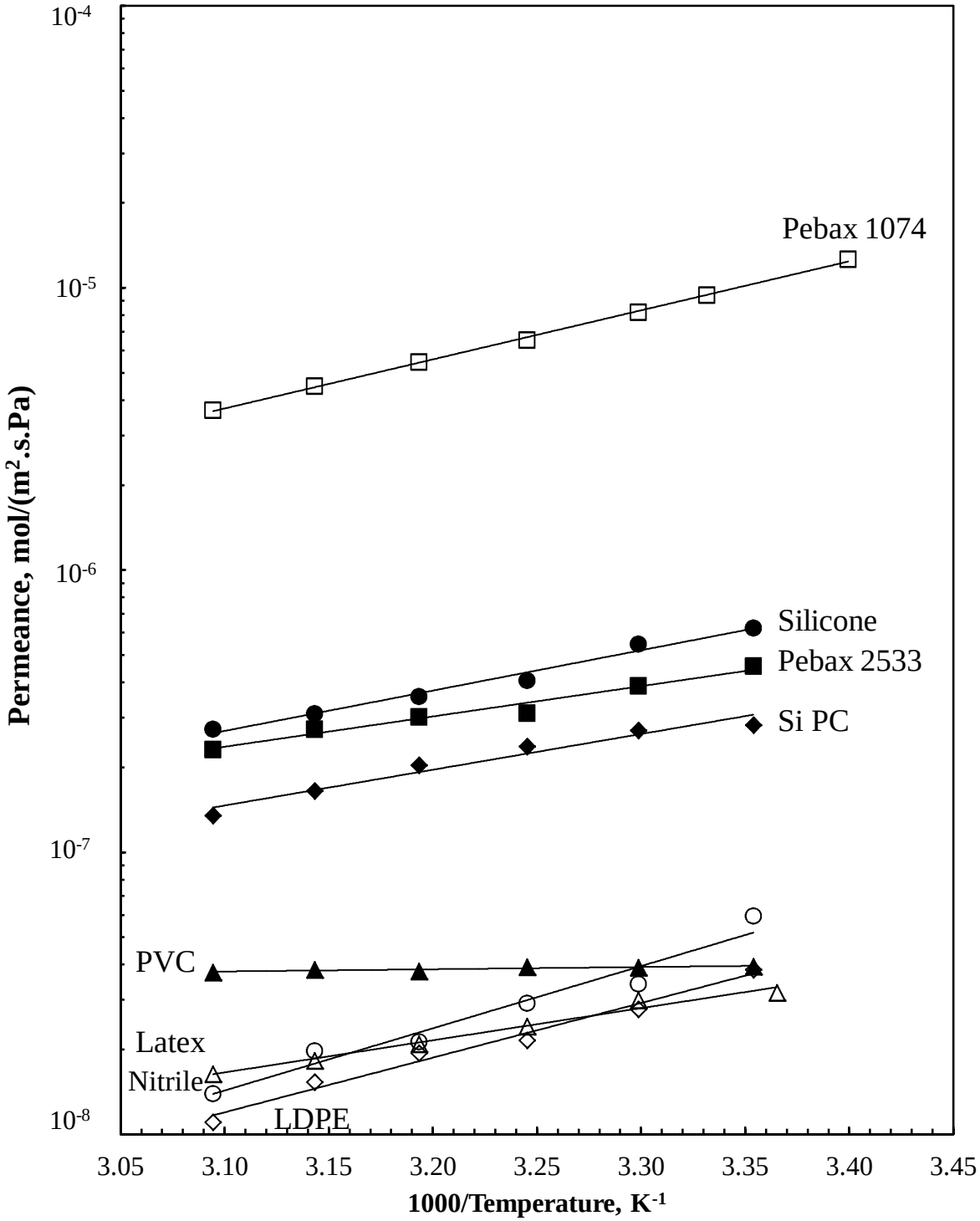

Figure 4.3 Effect of temperature on water permeance of tested materials

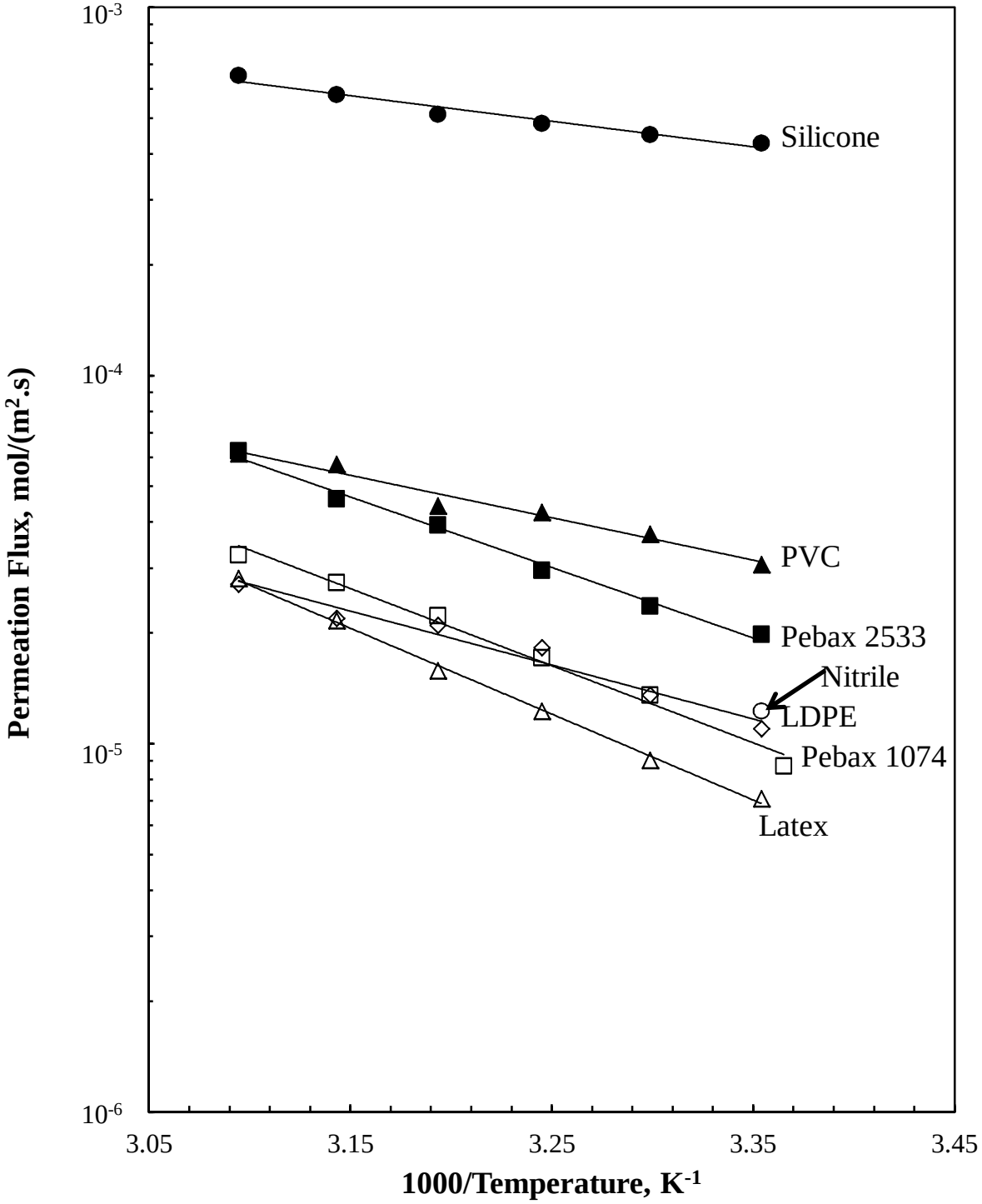

Figure 4.4 Effect of temperature on DMMP permeation flux of tested materials

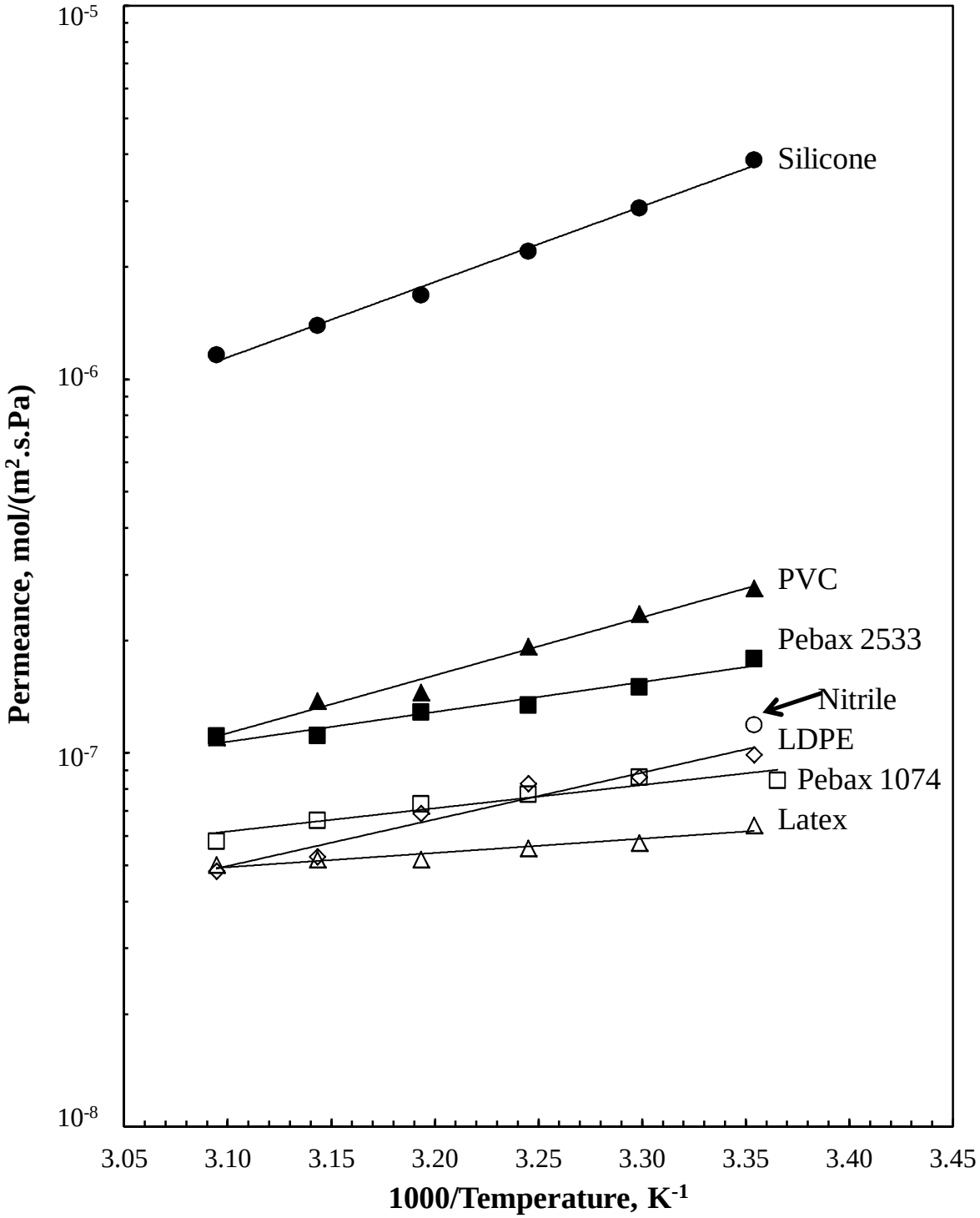

Figure 4.5 Effect of temperature on DMMP permeance of tested materials

The choice of polymers directly impacts the effectiveness of chemical resistance in protective barriers. Hence, the permeability of 4 commonly available glove materials – nitrile, latex, PVC, and LDPE – and 3 other experimental candidates – Pebax®2533, silicone and silicone-polycarbonate copolymer – were tested and compared to Pebax®1074. Silicone-polycarbonate is a copolymer. The silicone is comparable to the soft PEO block in Pebax®1074, whereas the polycarbonate component is analogous to the rigid polyamide 12 block. Qualitatively, it was observed that DMMP attacked nitrile, PVC, and silicone-polycarbonate copolymer. After immersing the polymers in DMMP for pervaporation tests, the membranes gradually became softer, more stretchy, and easily tearable. In particular, DMMP rendered nitrile and silicone-polycarbonate copolymer too unstable to collect permeation data for the entire temperature range tested; the mechanical integrity of these membranes were attacked by DMMP easily.

Pebax®1074 is noted to have the highest water and permeance of all the materials. This can be attributed to its highly hydrophilic poly(ethylene oxide) (PEO) block, resulting in an overall hydrophilicity as suggested by its low contact angle. For DMMP, silicone is observed to have the largest permeance. As Almquist and Hwang (1999) observed, the good condensability and small size of DMMP resulted in relatively good solubility coefficient and high diffusivity coefficient, respectively, compared to other organophosphorus penetrants in silicone membrane.

Hydrophobic Pebax® films show much higher permeation rate for hydrophobic organics than for water (Nguyen *et al.,* 2001). Thus, the reverse also must be true – hydrophilic penetrants permeate hydrophilic membranes faster than hydrophobic ones. This can be ascribed to the popular aphorism: “like dissolves like”, indicating a solute is miscible with a solvent of similar

chemical properties as itself. In this case, the penetrants are analogous to solutes, and the polymer membrane is seen as the solvent. From the contact angles in Table 4.2, Pebax®1074 is a hydrophilic membrane; therefore, it readily permeates water. DMMP is very soluble in water; therefore, it must also be hydrophilic and polar. However, it does not permeate fastest in hydrophilic Pebax®1074, thus chemical interactions, such as hydrogen bonding, between the penetrant and polymer must also play an important role in determining the transmission rate. As observed from the chemical structures of polymer materials tested, polyethylene is a non-polar polymer, resulting in a low permeability to water. Additionally, hydrogen bonds may form between oxygen in the polymer backbone of Pebax®, and silicone-polycarbonate copolymer membranes, resulting in their relatively high water flux and permeance.

Figure 4.6 shows the H_2O/DMMP permeance ratio of the different materials tested. As Wijmans and Baker (1993) approximated, the total pervaporation separation is a combination of liquid evaporation and vapour permeation steps based on relative volatility and relative permeabilities of the penetrants, respectively. Comparing water and DMMP permeances with the overall selectivity, it is evident that the effect of evaporation is significant, which can be associated with large volatility difference between the two penetrants. Thus, a good selectivity involves combined efforts of penetrant evaporation and permeation.

Pebax®1074 is observed to be the most selective over the temperature range tested, and is 30 times more selective than the next most selective material – Pebax®2533. All other materials have a H_2O/DMMP selectivity smaller than one, meaning DMMP permeated faster than water, which is undesirable, because in counter-current flow, water (simulating perspiration) should permeate faster than DMMP in order to provide breathability and effective protection. The high

selectivity of Pebax®1074 originates mainly from two effects: the greater interaction between water and the polymer relative to DMMP, and the small size of the water molecule, which increases the entropy of mixing and diffusivity (Rivin *et al.*, 2004). Due to large differences between the components with respect to size and chemical properties such as polarity and hydrogen bonding ability, the separation of water from organic solvents is relatively easy to achieve. As the components become more similar, separation becomes more difficult. Pebax®2533 did not perform as well as Pebax®1074 due to its less hydrophilic poly(tetramethylene oxide) (PTMO) block compared to PEO in Pebax®1074 (Jonquieres *et al.*, 2002a), which reduced permeation of water in the 2533 copolymer.

Additionally, it is noted that the selectivity for all materials except PVC and silicone decreased with an increase in temperature, due to negative contributions to diffusivity selectivity from plasticization effects. The selectivity in PVC and silicone increased with increasing temperature, because the permeance of DMMP decreased faster than permeance of water with increasing temperature. This may be attributed to different interactions between the penetrants and the polymers.

Figure 4.7 shows the far superior water/DMMP ideal selectivity of Pebax®1074 to Pebax®2533 and Material C from Napadensky and Elabd (2004) (the most selective material they tested)

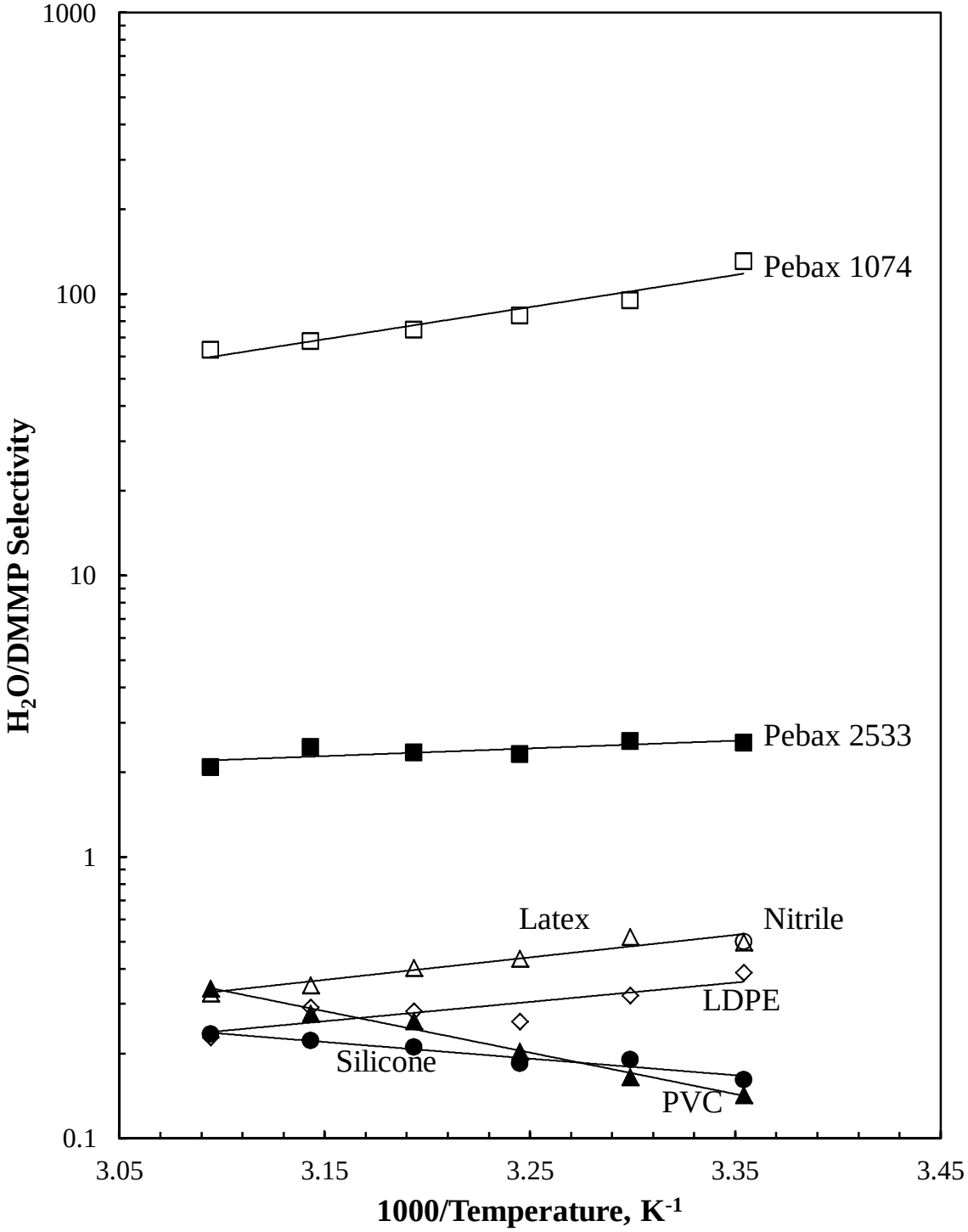

Figure 4.6 Effect of temperature on H_2O/DMMP selectivity of tested materials

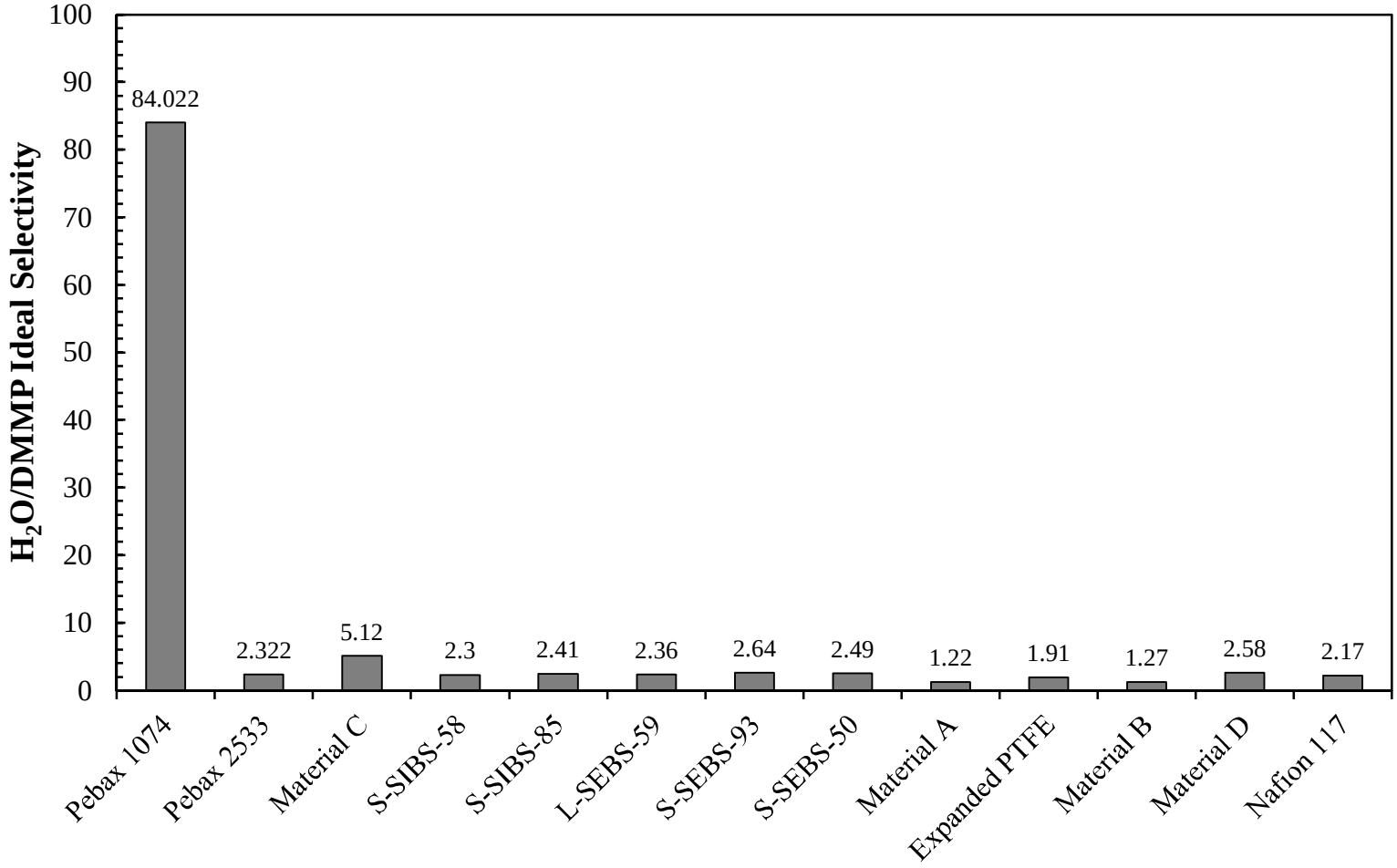

Figure 4.7 Comparison of water/DMMP selectivity of few select materials

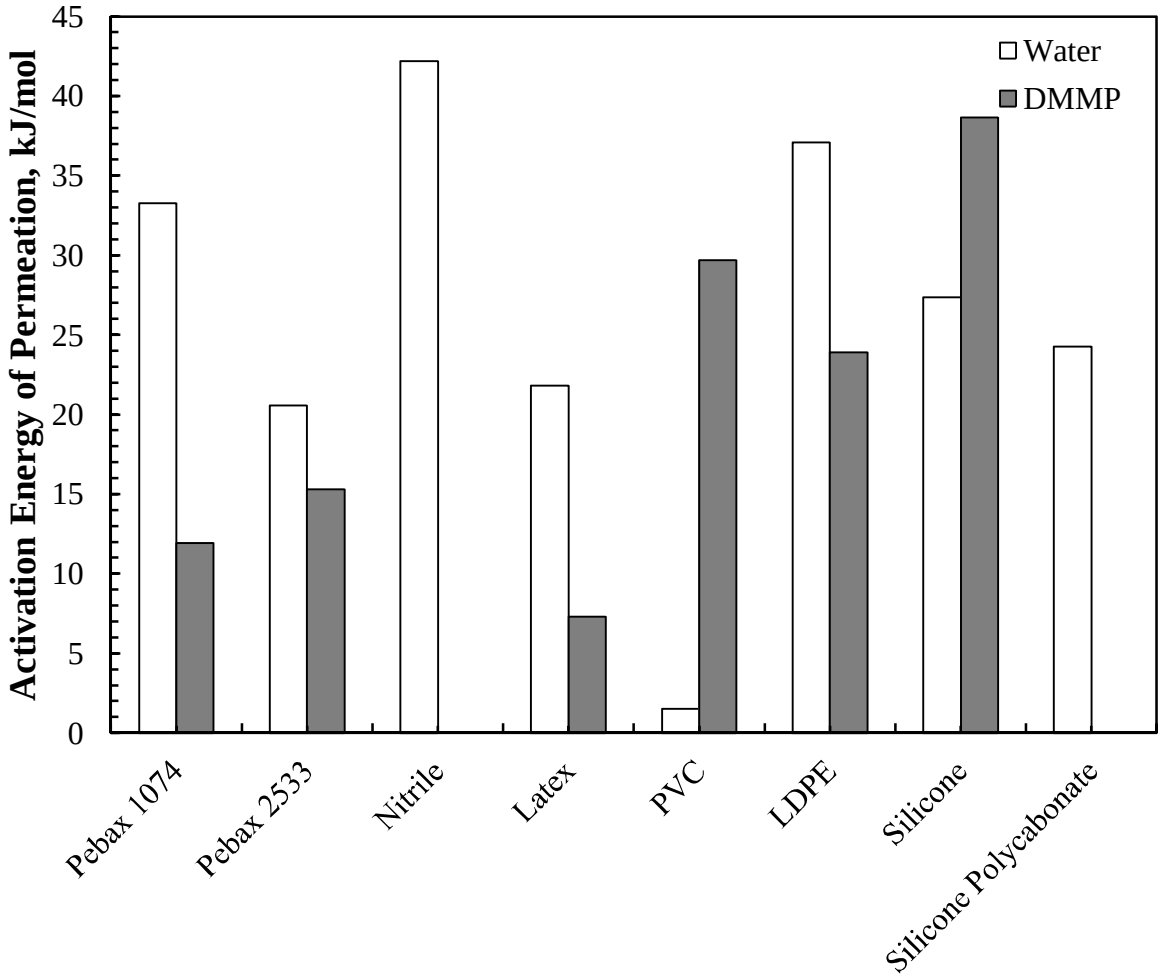

Figure 4.8 Comparison of water and DMMP activation energy of permeation for tested materials

The activation energy can be evaluated from the temperature dependence of permeance (i.e., slopes of the Arrhenius plot, Figure 4.3 and Figure 4.5) and are compared for the different polymers in Figure 4.8. The activation energies for DMMP in nitrile and silicone polycarbonate are not zero, but could not to be measured, because the membranes broke prior to sufficient data collection due to their instability in DMMP. The activation energy represents the temperature dependence of membrane permeability, and is the summation of the enthalpy of penetrant sorption and the activation energy of the penetrant diffusion through the membrane. Since

permeance is used to calculate the activation energy, the temperature dependence is solely based on the effects of temperature on the solubility and diffusivity of the membrane. For most polymers, except for PVC and silicone, the effect of temperature on water permeance is greater than DMMP permeance, as shown by its higher activation energy. This may be due to strong temperature dependence of solubility coefficient of water in those materials, as is observed in polyelectrolyte membranes (Xu *et al.*, 2010; Reineke *et al.*, 1987). Of these polymers, the largest difference in DMMP and water activation energies is in Pebax®1074, which explains its high H_2O/DMMP selectivity.

4.4 Conclusions

Pebax®1074 was found to be highly breathable, and thus its application as protective barrier against harmful chemicals was investigated. The performance of water and DMMP permeation at different temperatures were demonstrated for Pebax®1074, Pebax®2533, nitrile, latex, PVC, LDPE, silicone, and silicone-polycarbonate copolymer.

Pebax®1074 was found to be the most permeable to water, among the polymer materials tested, and thus the most breathable. This can be attributed to the highly favourable interactions between water molecules and hydrophilic PEO block in Pebax®1074. On the other hand, DMMP attacked nitrile and silicone-polycarbonate copolymer easily, making them unsuitable for the targeted application.

Additionally, temperature had a significant influence on membrane performance. An increase in temperature resulted in an increased flux due to more energized penetrant molecules,

plasticization effects, and increased vapour pressure driving force across the membrane. However, the permeance decreased with an increase in temperature because the decrease in solubility outweighed the increase in diffusivity, resulting in an overall reduced permeability.

Pebax®1074 displayed the highest H_2O/DMMP selectivity. Water is both more volatile and more soluble in Pebax®1074 than DMMP, resulting in its high selectivity. The selectivity was found to decrease with an increase in temperature. The activation energy of permeation is a measure of temperature dependency of membrane permeability. The activation energy for water in most polymers was larger than that of DMMP. This is attributed to its higher heat of vaporization and greater saturated vapour pressure dependency on temperature.

Overall, Pebax®1074 is a promising material as a breathable barrier in protective clothing. Further research should be conducted to investigate its other characteristics, such as durability, process ability, and other physical properties.

CHAPTER 5

Conclusions and Recommendations

5.1 Conclusions

The gas permeation properties of poly(ether-*b*-amide) Pebax®1074 segmented block copolymers were determined. This polymer exhibited high selectivities to polar/non-polar gas (e.g., CO_2/N_2). The highest gas pair selectivity was observed to be an average of 70 for CO_2/N_2 over the pressure range tested. The order of gas permeability was observed to be $CO_2 > H_2 > He > CH_4 > O_2 > N_2$. Additionally feed pressure was shown to have little effect on the gas permeability, whereas the temperature influenced gas permeability significantly. The temperature dependence of gas permeabilities followed the Arrhenius relationship. The activation energy for permeation for CO_2 was the lowest and activation energy for N_2 is the highest. In addition, solvents used during membrane fabrication was shown to affect the membrane performance; membranes prepared using 1-butanol as the solvent has slightly better selectivity than those prepared with NMP. Heat-treatment of the membranes improved selectivities for CO_2/non-polar gas-pair. The membrane thickness and polymer concentration used in membrane preparation had no noticeable

effect on membrane performance. Lastly, as seen from the standard deviation values in Appendix D, the experiments are fairly repeatable.

The permeabilities of water and dimethyl methylphosphonate (DMMP) were measured at different temperatures under pervaporation mode to determine Pebax®1074's performance as a chemical resistant barrier in protective clothing applications. Pebax®2533, latex, nitrile, PVC, LDPE, silicone, and silicone-polycarbonate copolymer were also tested for comparisons. Pebax®1074 was found to be the most permeable to water among all the materials tested, and thus the most breathable. Additionally, it showed the highest H_2O/DMMP selectivity. Similar to gas separation, the temperature dependence of liquid pervaporation through all the materials also followed an Arrhenius relationship.

5.2 Recommendations

The gas permeation portion of this investigation provided a more comprehensive understanding of Pebax®1074. Based on this work, a few recommendations can be made to gain further insight into the gas permeation process in Pebax®1074. First, the diffusion of gases through the membrane can be determined using the time-lag method described by Favre *et al.* (2002). When this is combined with gas sorption characterization conducted by Bondar *et al.* (1999), the individual contributions of the solution and diffusion steps can be evaluated for a more in-depth understanding of the process. Additionally, the permeation of gas mixtures should be tested using, because the penetrant-penetrant and penetrant-polymer interactions may occur and alter the gas permeation properties. Generally, there exists a tradeoff between permeability

and selectivity, and chemical modifications of the membranes to further improve permeability and selectivity of Pebax®1074 could be explored. Lastly, the Pebax® polymer has a degree of crystallinity for the PA phase. For such a polymer presumably the degree of crystallization would vary depending on conditions of deposition; therefore, it is worth studying this variable in the future as well.

The pervaporation section of this work confirmed the high breathability of Pebax®1074. In fact, it was the most breathable material tested, and it also had the highest H_2O/DMMP selectivity, making it a promising material for chemically protective wear applications. Further research must be conducted to investigate its other characteristics, such as durability, weight, processing ability, and other physical properties. Additionally, Pebax®1074 may be constructed into anisotropic membranes to improve flux without compromising selectivity. Moreover, the permeation of water and DMMP mixtures should be studied because as Rivin *et al.* (2004) pointed out, there exist penetrant-penetrant interactions that may change their permeation properties. Lastly, the effects of membrane plasticization in the system should be studied in detail through gravimetric sorption tests, similar to the experiments conducted by Almquist and Hwang (1999). If excessive swelling is found, then crosslinking should be considered to improve membrane performance.

Bibliography

Abetz, V., T. Brinkmann, M. Dijkstra, K. Ebert, D. Fritsch, K. Ohlrogge, D. Paul, K. Peinemann, S.P. Nunes, N. Scharnagl, and M. Schossig, "Developments in Membrane Research: from Material via Process Design to Industrial Application", *Adv. Eng. Mater.*, 8 (2006)328 – 358.

Albuqerque, E.X., S.S. Deshpande, M. Kawabuchi, Y. Aracava, M. Idriss, D.L. Rickett, and A.F. Boyne, "Multiple actions of anticholinesterase agents on chemosensitive synapses: molecular bases for prophylaxis and treatment of organophosphate poisoning", *Fundam. Appl. Toxicol.*, 5 (1985) S182 – S203.

Almquist, C.B., and S.T. Hwang, "The permeation of organophosphorus compounds in silicone rubber membranes", *J. Membr. Sci.*, 153 (1999) 57 – 69.

Andrews, R.J., and E.A. Grulke, "Glass transition temperatures of polymers", in "Polymer Handbook", (4th Ed.), J. Brandrup, E.H. Immergut, E.A. Grulke, A. Abe, and D.R. Blotch (Ed.), John Wiley & Sons, New York (1999), pp. 149 – 253.

Antonson, C.R., R.J. Gardner, C.R. King and D.Y. Ko, "Analysis of gas separation by permeation in hollow fibres", *Ind. Eng. Chem. Proc. Des. Dev*, 16 (1977) 463 – 469.

Aungsupravate, O., D. Lucas, N.A. Hassan, M.P. Tonge, G. Warrender, P. Castigolles, M. Gaborieau, and R.G. Gilbert, "Water vapour transmission in butadiene – MMA – methacrylic acid latex films", *Eur. Polym. J.*, 44 (2008) 342 – 356.

Baker, R., "Future directions of membrane gas separation technology", *Ind. Eng. Chem. Res.*, 41 (2002) 1391 – 1411.

Baker, R., "Membrane Technology and Applications", John Wiley & Sons, Ltd., West Sussex, England (2004), pp. 301 – 389.

Barney, R.J., "Synthesis and biological evaluation of novel phosphonates", University of Iowa PhD. Dissertation, (2010).

Berens, A.R., and H.B. Hopfenberg, "Diffusion of organic vapors at low concentrations in glassy PVC, polystyrene, and PMMA", *J. Membr. Sci.,* 10 (1982) 283 – 303.

Bernardo, P., E. Drioli, and G. Golemme, "Membrane gas separation: a review/state of the art", *Ind. Eng. Chem. Res.,* 48 (2009) 4638 – 4663.

Black, R.M., and J.M. Harrison, "The chemistry of organophosphorus chemical warfare agents", in "Patai's Chemistry of Functional Groups: Organophosphorus Compounds", S. Patai (Ed.), Wiley, New York (1996) pp. 3 – 55.

Bodzek, M., "Membrane techniques in air cleaning", *Pol. J. Environ. Stud.,* 9 (2000) 1 –12.

Bondar, V.I., B.D. Freeman, and I. Pinnau, "Gas sorption and characterization of poly(ether-b-amide) segmented block copolymers", *J. Polym. Sci.: Polym. Phys.,* 37 (1999)2463 – 2475.

Bondar, V.I., B.D. Freeman, and I. Pinnau, "Gas transport properties of poly(ether-b-amide) segmented block copolymers", *J. Polym. Sci.: Polym. Phys.,* 38 (2000) 2051-2062.

Bowen, T.C., R.D. Noble, and J.L. Falconer, "Fundamentals and applications of pervaporation through zeolite membranes", *J. Membr. Sci.,* 245 (2004) 1 – 33.

Breck, D.W., "Zeolite Molecular Sieves—Structure, Chemistry, and Use", John Wiley & Sons, New York (1974), pp. 636.

Brun, J.P., C. Larchet, R. Melet, G. Bulvestre, "Modeling of the pervaporation of binary mixtures through moderate swelling, non-reacting membranes", *J. Membr. Sci.,* 23, 257, (1985).

Butrow, A.B., J.H. Buchanan, and D.E. Tevault, "Vapour pressure of organophosphorus nerve agent simulant compounds", *J. Chem. Eng. Data,* 54 (2009) 1876 – 1883.

"Chemical Resistance Guide: Permeation & Degradation Data", (7th Ed.), Ansell Occupational Healthcare, Coshocton, OH (2003).

Chen, J., "Evaluation of polymeric membranes for separation processes: poly(ether-b-amide) (Pebax 2533®) block copolymer", University of Waterloo Masters thesis, (2002).

Costello, L.M., and W.J. Koros, "Effect of structure on the temperature dependence of gas transport and sorption in a series of polycarbonates", *J. Polym. Sci.: Polym. Phys.,* 32 (1994) 701 –713.

Daugherty, M.L., A.P. Watson and T. Vo-Dinh, "Currently available permeability and breakthrough data characterizing chemical warfare agents and their simulants in civilian protective clothing materials", *J. Hazardous Mater.,* 20 (1992) 243 – 267.

Delfino, R.T., T.S. Ribeiro, and J.D. Figueroa-Villar, "Organophosphorus compounds as chemical warfare agents: a review*", J. Braz. Chem. Soc.,* 20 (2009) 407 – 428.

Du, R., X. Feng, A. Chakma, "Poly(N,N-dimethylaminoethyl methacrylate)/polysulfone composite membranes for gas separations", *J. Membr. Sci*., 279 (2006) 76 – 85.

Du. R., L. Liu, A. Chakma, and X. Feng, "Using poly(N,N-dimethylaminoethyl methacrylate)/polyacrylonitrile composite membranes for gas dehydration and humification", *Chem. Eng. Sci.,* 65 (2010) 4672 – 4681.

Favre, E., N. Morliere, D. Roizard, "Experimental evidence and implication of an imperfect upstream pressure step for the time-lag technique", *J. Membr. Sci.,* 207 (2002) 59 –72.

Feng, X., and R.Y.M. Huang, "Estimation of activation energy for permeation in pervaporation processes", *J. Membr. Sci.,* 118 (1996) 127 – 131.

Feng, X., and R.Y.M. Huang, "Liquid separation by membrane pervaporation: a review", *Ind. Eng. Chem. Res.,* 36 (1997) 1048 – 1066.

Freeman, B., "Basis of permeability/selectivity tradeoff relations in polymeric gas separation membranes", *Macromol.,* 32 (1999) 375 – 380.

Fried, J.R., "Molecular simulation of gas and vapour transport in highly permeable polymers", in "Materials Science of Membranes for Gas and Vapour Separation", Y. Yampolskii, I. Pinnau, and B.D. Freeman, (Ed.), John Wiley & Sons Ltd., West Sussex, England (2006), pp. 95 – 136.

George, S.C., and S. Thomas, "Transport phenomena through polymeric systems", *Prog. Polym. Sci.,* 26 (2001) 985 – 1017.

Ghosal, K., and B.D. Freeman, "Gas separation using polymer membranes: an overview", *Polym. Adv. Technol.,* 5(1994) 673 – 697.

Han, M.J., and S.T. Nam, "Thermodynamic and rheological variation in polysulfone solution by PVP and its effect in the preparation of phase inversion membrane", *J. Membr. Sci.,* 202 (2002) 55 – 61.

Hanft, S., "Membrane Technology for Liquid and Gas Separations", Report Code MST041E [Online], BCC Research, Wellsley, MA, (2010), http://www.bccresearch.com/report/MST041E.html, (accessed on January 24, 2011).

Henis, J.M.S., and M.K. Tripodi, "Composite hollow fibre membranes for gas separations: The resistance model approach", *J. Membr. Sci.,* 8 (1981) 233 – 246.

Hoang, D., and J. Kim, "Synthesis and applications of biscyclic phosphorus flame retardants", *Polym. Degrad. Stab.,* 93 (2008) 36 – 42.

Hwang, S.T., "Fundamentals of membrane transport", *Korean J. Chem. Eng.,* 28 (2011) 1 –15.

Huang, R.Y.M., P. Shao, X. Feng, and W.A. Anderson, "Separation of ethylene glycol-water mixtures using sulfonated poly(ether ether ketone) pervaporation membranes: membrane relaxation and separation performance analysis", *Ind. Eng. Chem. Res.,* 41 (2002) 2957 – 2965.

Ismail, A.F., and W. Lorna, "Penetrant-induced plasticization phenonmenon in glassy polymers for gas separation membrane", *Sep. Purif. Technol.,* 27 (2002) 173 – 194.

Iwami, S., "Multi-piece solid golf ball", US Patent No. 7,901,300, (2011).

Jansen, J., "Gas and water vapour permeation through highly hydrophilic membranes", University of Twente, Bachelor thesis, (2007).

Jansen, J.C., M. Macchione, and E. Drioli, "On the unusual solvent retention and the effect on the gas transport in perfluorinated Hyflon AD® membranes", *J. Membr. Sci.,*287 (2007) 132 – 137.

Jonquieres, A., R. Clement, and P. Lochon, "Permeability of block copolymers to vapors and liquids", *Prog. Polym. Sci.,* 27 (2002a) 1803 – 1877.

Jonquieres, A., R. Clement, P. Lochon, J. Neel, M. Dresch, and B. Chretien, "Industrial state-of-the-art of pervaporation and vapour permeation in the western countries", *J. Membr. Sci.,* 206 (2002b) 87 – 117.

Jung, K.H., L. Ji, B. Pourdeyhimi, and X. Zhang, "Structure-property relationships of polymer-filled nonwoven membranes for chemical protection applications", *J. Membr. Sci.,* 361 (2010) 63 – 70.

Kim, J.H.K., S.Y. Ha, and Y.M. Lee, "Gas permeation of poly(amide-6-ethylene oxide) copolymer", *J. Membr. Sci.*, 190 (2001) 179 – 193.

Koros, W.J., and G.K. Fleming, "Membrane-based gas separation", *J. Membr. Sci.*, 83 (1993) 1 – 80.

Koros, W.J., and R. Mahajan, "Pushing the limits on possibilities for large scale gas separation: which strategies?", *J. Membr. Sci.*, 175 (2000) 181 – 196.

Levine, F., J.L. Scala, and W. Kosik, "Properties of clear polyurethane films modified with fluoropolymer emulsion", *Prog. Org. Coat.*, 69 (2010) 63 – 72.

Loeb, S., "The Loeb-Sourirajan Membrane: How It Came About", in "Synthetic Membranes", A. Tubak, (Ed.), ACS Symp. Ser. 153: ACS, Washington DC (1981), pp. 1 – 9.

Lindsay, R., "Swatch test results of commercial chemical protective gloves to challenge by chemical warfare agents", Edgewood Chemical Biological Center, Aberdeen Proving Ground, MD (2001).

Lu, X., V. Nguyen, X. Zeng, B.J. Elliott, and D.L. Gin, "Selective rejection of a water-soluble nerve agent stimulant using a nanoporous lyotropic liquid crystal-butyl rubber vapour barrier material: evidence for a molecular size-discrimination mechanism", *J. Membr. Sci.*, 318 (2008) 397 – 404.

Marcq, J., Q. Nguyen, D. Langevin, and B. Brule, "Abatement of CO_2 emissions by means of membranes – characterization of industrial PEBAX^{TM} films," *Environ. Protect Eng.*, 31(2005) 13 – 22.

Massey, L., "Permeability Properties of Plastics and Elastomers: A Guide to Packaging and Barrier Materials", Plastics Design Library, Norwich, New York (2003), pp. 427 – 430, Appendix II.

Mauviel, G., J. Berthiaud, C. Vallieres, D. Roizard, and E. Favre, "Dense membrane permeation: From the limitations of the permeability concept back to the solution-diffusion model", *J. Membr. Sci.*, 266 (2005) 62 – 67.

Metz, S.J., W.J.C. van de Ven, J. Potreck, M.H.V. Mulder, and M. Wessling, "Transport of water vapour and inert gas mixtures through highly selective and highly permeable polymer membranes", *J. Membr. Sci.*, 251 (2005) 29 – 41.

Mohtadi, H., and A.P. Murshid, "A global chronology of incidents of chemical, biological, radioactive and nuclear attacks: 1950 – 2005", National Center of Food Protection Defense, working paper (2006).

Mujiburohman, M., and X. Feng, "Permselectivity, solubility and diffusivity of propyl propionate/water mixtures in poly(ether block amide) membranes", *J. Membr. Sci.*, 300 (2007) 95 – 103.

Mulder, M., "Basic Principles of Membrane Technology", Kluwer Academic Publishers, Dordrecht, The Netherlands (1991), pp. 17 – 280.

Nakai, Y., "Conjugate fibres excellent in antistatic property, water absorption and cool feeling by contact", US Patent No. 7,892,640, (2011).

Napadensky, E., and Y.A. Elabd, "Breathability and selectivity of selected materials for protective clothing", Army Research Laboratory, AR-TR-3235 (2004).

Napadensky, E., and Y.A. Elabd, "Transport properties of n-methylolated nylon-6:chitosan blend membranes", Army Research Laboratory, AR-TR-3917 (2006).

Neel, J., "Pervaporation", in "Membrane Separations Technology: Principles and Applications", Noble, R., and S. Stern (Ed.), Elsevier Science B. V., Amsterdam, The Netherlands (1995), pp. 143 – 211.

Nguyen, Q.T., Y. Germain, R. Clement, and Y. Hirata, "Pervaporation, a novel technique for the measurement of vapour transmission rate of highly permeable films", *Polym. Test.*, 20 (2001) 901 – 911.

Ockwig, N.W., and T.M. Nenoff, "Membranes for hydrogen separation", *Chem. Rev.*, 107, (2007) 4078 – 4110.

Paul, D.R., and Y.P. Yampolskii, "Introduction and Perspective", in "Polymeric Gas Separation Membranes", D. R. Paul and Y. P. Yampol'skii (Ed.), CRC Press Inc., Boca Raton, Florida (1994), pp. 1 -- 17.

Pauly, S., "Permeability and Diffusion Data" in "Polymer Handbook", (4th Ed.), J. Brandrup, E.H. Immergut, E.A. Grulke, A. Abe, and D.R. Blotch (Ed.), John Wiley & Sons, New York (1999), pp. 543 –568.

"Pebax® Breathable Films", Literature Request [Online], Arkema Inc., Philadelphia, PA, (2002), http://www.arkema-inc.com/literature/pdf/26.pdf (accessed November 2, 2009).

"Pebax® MV 1074 SA 01", Technical Data Sheets [Online], Arkema Inc., Philadelphia, PA, (2009), http://www.pebax.com/pdf/pebax/en/tds_pebax_mv1074sa01_2009.pdf (accessed February 16, 2010).

Pinnau, I., and B.D. Freeman, "Formation and Modification of Polymeric Membranes: Overview", in "Membrane Formation and Modification", Pinnau, I., and B. D. Freeman (Ed.), ACS Symp. Ser. 744: ACS, Washington, DC (2000), pp. 1 – 22.

Pfromm, P.H., "The impact of physical aging of amorphous glassy polymers on gas separation membranes", in "Materials Science of Membranes for Gas and Vapour Separation", Y. Yampolskii, I. Pinnau, and B. D. Freeman, (Ed.), John Wiley & Sons Ltd., West Sussex, England (2006), pp. 293 – 304.

Poling, B.E., J. M.Prausnitz, and J.P. O'Connell, "The Properties of Gases and Liquids", (5^{th} Ed.), McGraw-Hill, New York (2001), Appendix A.

Potreck, J., K. Nijmeijer, T. Kosinski, and M. Wessling, "Mixed water vapour/gas transport through the rubbery polymer PEBAX® 1074", *J. Membr. Sci.,* 338(2009) 11 – 16.

Prasad, R., R.L. Shaner, and K.J. Doshi, "Comparison of membranes with other gas separation technologies", in "Polymeric Gas Separation Membranes", D. R. Paul and Y. P. Yampol'skii (Ed.), CRC Press Inc., Boca Raton, Florida (1994), pp. 531 – 614.

Reesor, J.B., B.J. Perry, and E. Sherlock, "The synthesis of highly radioactive isopropyl methylphosphonofluoridate (sarin) containing P^{32} as tracer element", *Can. J. Chem.,* 38 (1960) 1416 – 1427.

Reineke, C.E., J.A. Jagodzinski, K.R. Denslow, "Highly water selective cellulosic polyelectrolyte membranes for the pervaporation of alcohol-water mixtures", *J. Membr. Sci.,* 32 (1987) 207 – 221.

Reinsch, V.E., A.R. Greenberg, S.S. Kelley, R. Peterson, and L.J. Bond, "A new technique for the simultaneous, real-time measurement of membrane compaction, and performance during exposure to high-pressure gas", *J. Membr. Sci.,* 171 (2000) 217 – 228.

Rezac, M.E., T. John, and P.H. Pfromm. "Effect of copolymer composition on the solubility and diffusivity of water and methanol in a series of polyether amides", *J. App. Polym. Sci.,* 65 (1997) 1983 – 1993.

Rich, J.D., P.J. McDermott, G.C. Davis, P.P. Policastro, K.A. Regh, P.K. Hernandez, and T.L. Guggenheim, "Silicone-polycarbonate block copolymers", US Patent No. 4,945,148, (1990).

Rivin, D., G. Meermeier, N.S. Schneider, A. Vishnyakov, and A.V. Neimark, "Simultaneous transport of water and organic molecules through polyelectrolyte membranes", *J. Phys. Chem. B*, 108 (2004) 8900 – 8909.

Salemme, R.M., "Preparation of microporous polycarbonate resin membranes", US Patent No. 4,032,309, (1977).

Sato, Y., M. Yurugi, K. Fujiwara, S. Takishima, H. Masuoka, "Solubilities of carbon dioxide and nitrogen in polystyrene under high temperature and pressure", *Fluid Phase Equilib.*, 125 (1996) 129 – 138.

Schaetzel, P., C. Vauclair, Q. T. Nguyen, and R. Bouzerar, "A simplified solution-diffusion theory in pervaporation: the total solvent volume fraction model", *J. Membr. Sci.*, 244 (2004) 117 – 127.

Schucker, R.C., "Highly aromatic polyurea/urethane membranes and their use for the separation of aromatics from non-aromatics", US Patent No. 5,055,632, (1991).

Schuld, N., and B.A. Wolf, "Polymer-solvent interaction parameter",in "Polymer Handbook", (4^{th} Ed.), J. Brandrup, E.H. Immergut, E.A. Grulke, A. Abe, and D.R. Blotch (Ed.), John Wiley & Sons, New York (1999), pp. 247 – 262.

Scott, K., "Handbook of Industrial Membranes", (2^{nd} Ed.), Elsevier Advanced Technology, Oxford, UK (1998).

Semenova, S.I., H. Ohya, and K. Soontarapa, "Hydrophilic membranes for pervaporation: An analytical review", *Desalination*, 110 (1997) 251 – 286.

Shao, P., and R.Y.M. Huang, "Review: Polymeric membrane pervaporation", *J. Membr. Sci.*, 287 (2007) 162 – 179.

Sijbesma, H., K. Nymeijer, R. Marwijk, R. Heijboer, J. Potreck, and M. Wessling, "Flue gas dehydration using polymer membranes", *J. Membr. Sci.*, 313(2008) 263 – 276.

Smith, J.M., H.C. Van Ness, and M.M. Abbott, "Introduction to Chemical Engineering Thermodynamics", (7^{th} Ed.), McGraw-Hill, Boston (2005), pp. 682.

"Stainless steel filter holders", Product specifications [Online], Millipore, Billerica, MA (2010), http://www.millipore.com/catalogue/module/C263#Specifications, (accessed January 17, 2011).

"Standard Test Methods for Water Vapour Transmission of Materials", ASTM Standard E96/E96M-10, ASTM International, West Conshohocken, PA, (2010).

"Standard Test Methods for Permeation of Liquids and Gases through Protective Clothing Materials under Conditions of Continuous Contact", ASTM Standard F739-07, ASTM International, West Conshohocken, PA, (2007).

Stern, A., "Polymers for gas separations: the next decade", *J. Membr. Sci.,* 94 (1994) 1 – 65.

Strathmann, H., "Synthetic membranes and their preparation", in "Handbook of Industrial Membrane Technology", Porter, M. (Ed.), Noyes Publications, Park Ridge, NJ (1990), pp. 1 – 56.

Szinicz, L., "History of chemical and biological warfare agents", *Toxicol*., 214 (2005) 167 – 181.

Tevault, D.E., J. Keller, and J. Parsons, "Vapour pressure of dimethyl methylphosphonate", Proceedings of the 1998 ERDEC Scientific Conference on Chemical and Biological Defense Research, ECBC-SP-004 (1999), pp. 815-822. Unclassified Special Report.

Ulrich, S., "Solvent cast technology – a versatile tool for thin film production", *Progr. Colloid Polym. Sci.,* 130 (2005) 1 –14.

White, L.S., R.F. Wormsbecher, and M. Lesmann, "Membrane separation for sulfur reduction", US Patent No. 7,048,846, (2006).

Wilson, B.M., J.P. Durcan, and J.A. Simpson, "Method of making a balloon catheter shaft having high strength and flexibility", US Patent No. 7,906,066, (2011).

Wijmans, J.G., and R.W. Baker, "A simple predictive treatment of the permeation process in pervaporation", *J. Membr. Sci.,* 79 (1993) 101 – 113.

Wijmans, J.G., and R.W. Baker, "The solution-diffusion model: a review", *J. Membr. Sci.* 107 (1995) 1 – 21.

Wijmans, J.G., and R.W. Baker, "The Solution-Diffusion Model: A Unified Approach to Membrane Permeation", in "Materials Science of Membranes for Gas and Vapour Separation", Y. Yampolskii, I. Pinnau, and B. D. Freeman, (Ed.), John Wiley & Sons Ltd., West Sussex, England (2006), pp. 159 – 188.

Xu, J., C. Gao, and X. Feng, "Thin-film-composite membranes comprising of self-assembled polyelectrolytes for separation of water from ethylene glycol by pervaporation", *J. Membr. Sci.*, 352 (2010) 197 – 204.

Yarborough, P.D., "Overview", in "Performance of protective clothing", P. D. Yarborough, and C.N. Nelson (Ed.), ASTM International, Wes Conshohocken, PA (2005), pp. vii –viii.

Yeow, M.L., Y.T. Liu, and K. Li, "Morphological study of poly(vinylidene fluoride) asymmetric membranes: effects of the solvent, additive, and dope temperature", *J. App. Polym. Sci.,* 92 (2004), 1782 – 1789.

Yoshikawa, M., H. Yokoi, N. Ogata, and T. Shimidzu, "Effect of membrane environment on permselectivity for water-ethanol binary mixtures", *Polym. J.*, 16 (1984) 653 – 656.

Zhao, J., Z. Wang, J. Wang, and S. Wang, "Influence of heat-treatment on CO2 separation performance of novel fixed carrier composite membranes prepared by interfacial polymerization", *J. Membr. Sci.*, 283 (2006) 346 – 356.

Zheng, Q., Y. Fu, and J. Xu, "Advances in the chemical sensors for the detection of DMMP – a simulant for nerve agent sarin", *Procedia Engineering*, 7 (2010) 179 – 184.

Appendix A

Available Gas Separation Pebax®1074 Research

Table A.1 Summary of membrane preparation methods and testing conditions in existing gas separation research of Pebax®1074

Literature	Membrane Preparation	Membrane Testing
Sijbesma*et al.* (2008)	- 2 wt% solution in 1-butanol at 60 °C - soln poured in Petri dish, dried at room temperature under N_2 for 12 h - thickness: 78 ± 4 μm flat film	Feed: H_2O/N_2 at 2.5 bar Sweep: He at 1.0 bar Permeability (P): N_2 = 2.45, He = 8.3, CO_2 = 122; mixed feed: N_2 = 1.92, H_2O = $2x10^5$ Barrer at 30 °C
Bondar *et al.* (2000)	- 2 wt% solution in n-butanol on Teflon coated glass plate, - air dry at room temp. for 1 week, vacuum dry at 80 °C for 3 days - thickness: 95 μm	T = 35 °C, Pressure up to 15 atm P: CO_2 = 120 Barrer Selectivity, α: (CO_2/N_2) = 51.4, α(CO_2/H_2) = 9.8
Marcq *et al.* (2005)	Extruded films	Pressure = 3 bar, T = 25 °C P(CO_2) = 25, P(N_2) = 0.58 Barrer α (CO_2/N_2) = 43.8
Potreck *et al.* (2009)	- 7 wt% dissolved at 100 °C in NMP - cast on glass plate (80 °C) with casting knife - solvent evaporated in N_2 oven at 80 °C for 1 week, removed and washed for 3 days with water, stored in vacuum oven at 30 °C, no further change in mass (~14 days) - thickness: 0.47 mm casting knife	Mixed water vapour/N_2 permeation Feed T = 30, 50, 70 °C Dry P(N_2) = 2.2, 6, 12 Barrer α (H_2O/N_2 @ 50 °C) = 50

Appendix B

Sample Calculations

B.1 Gas Permeation Calculations

Sample calculations are performed for feed pressure of 2.4 MPa (179.43 cmHg), measured the bubble flowing 120 s over 0.1 mL, through a membrane of thickness 0.025 mm.

Calculate ΔP

$$p_{permeate} = 1 \text{ atm} = 76 \text{ cmHg}$$

$$\Delta p = p_{feed} - p_{permeate} = 179.43\ cmHg - 76\ cmHg = 103.43\ cmHg$$

Calculate Volumetric Flow rate:

$$\dot{V} = \frac{V}{t} = \frac{0.1\ mL}{120\ s} = 8.33 \times 10^{-4} \frac{mL}{s}\left(\frac{1\ cm^3}{1\ mL}\right) = 8.33 \times 10^{-4} \frac{cm^3}{s}$$

Calculate Flux:

$$\text{Flux (J)} = \frac{\dot{V}_{STP}}{A} = \dot{V}\left(\frac{273.15\ K}{T}\right)\left(\frac{P_{baro}}{101.325\ kPa}\right)\left(\frac{D^2\pi}{4}\right)^{-1}$$

$$\text{J} = \left(8.33 \times 10^4\ \frac{mL}{s}\right)\left(\frac{273.15\ K}{296.15\ K}\right)\left(\frac{102.3\ kPa}{101.325\ kPa}\right)\left(\frac{(4\ cm)^2\pi}{4}\right)^{-1}\left(\frac{1\ cm^3}{1\ mL}\right)$$

$$= 6.17 \times 10^{-5}\ \frac{cm^3(STP)}{cm^2\ \cdot\ s}$$

V = volume (mL)

t = time (s)

T = room temperature (K)

P_{baro} = barometric pressure (kPa) from UW weather station

D = membrane diameter (cm)

J = flux [cm^3(STP)/(cm^2.s)]

Calculate Gas Permeance (Q)

$$Permeance(Q) = \frac{J}{\Delta p} = \frac{\left(6.17 \times 10^{-5}\ \frac{cm^3(STP)}{cm^2 \cdot s}\right)}{103.4\ cmHg} = 5.97 \times 10^{-7}\ \frac{cm^3(STP)}{cm^2\ \cdot\ s \cdot cmHg}$$

$$1\ GPU = 1\ \times\ 10^{-6}\ \frac{cm^3(STP)}{cm^2\ \cdot\ s \cdot cmHg}$$

$$Q = \left(5.97 \times 10^{-7}\ \frac{cm^3(STP)}{cm^2\ \cdot\ s \cdot cmHg}\right)\left(\frac{1\ GPU}{1\ \times\ 10^{-6}\ \frac{cm^3(STP)}{cm^2 \cdot s \cdot cmHg}}\right) = 0.597\ GPU$$

Q = Permeance [cm^3(STP)/(cm^2.s.cmHg)]

Calculate Gas Permeability

$$Permeability(P) = \frac{J \cdot l}{\Delta p} = \frac{\left(6.17 \times 10^{-5} \frac{cm^3(STP)}{cm^2 \cdot s}\right)(0.025\ mm)\left(\frac{1\ cm}{10\ mm}\right)}{103.4\ cmHg}$$

$$= 1.49 \times 10^{-9} \frac{cm^3(STP) \cdot cm}{cmHg\ \cdot cm^2 \cdot s}$$

P = Permeability [cm^3 (STP).cm/(cm^2.s.cmHg)]

l = membrane thickness (cm)

Calculate Permeability Coefficient

$$1\ Barrer = 1 \times 10^{-10} \frac{cm^3(STP) \cdot cm}{cmHg \cdot cm^2 \cdot s}$$

$$\left(1.49 \times 10^{-9} \frac{cm^3(STP) \cdot cm}{cmHg \cdot cm^2 \cdot s}\right)\left(\frac{1\ Barrer}{1 \times 10^{-10} \frac{cm^3(STP) \cdot cm}{cmHg \cdot cm^2 \cdot s}}\right) = 14.9\ Barrer$$

Calculate Ideal Selectivity

$$\alpha_{CO_2/N_2} = \frac{P_{CO_2}}{P_{N_2}} = \frac{131.5\ Barrer}{2.01\ Barrer} = 65.4$$

Calculate Activation Energy

$$P = P_0 exp\left(\frac{-E_p}{RT}\right)$$

$$\ln P = \left(\frac{-E_P}{R}\right)\left(\frac{1000}{T}\right) + \ln(P_0)$$

P_0 = pre-exponential factor

E_p = activation energy of permeation

R = 8.314 J/(mol.K)

1000/T is used to simplify the unit conversion to kJ.

Plot Permeability vs. 1000/T for CO_2 at 0.7 MPa, resulting slope (m) and intercept (b) are:

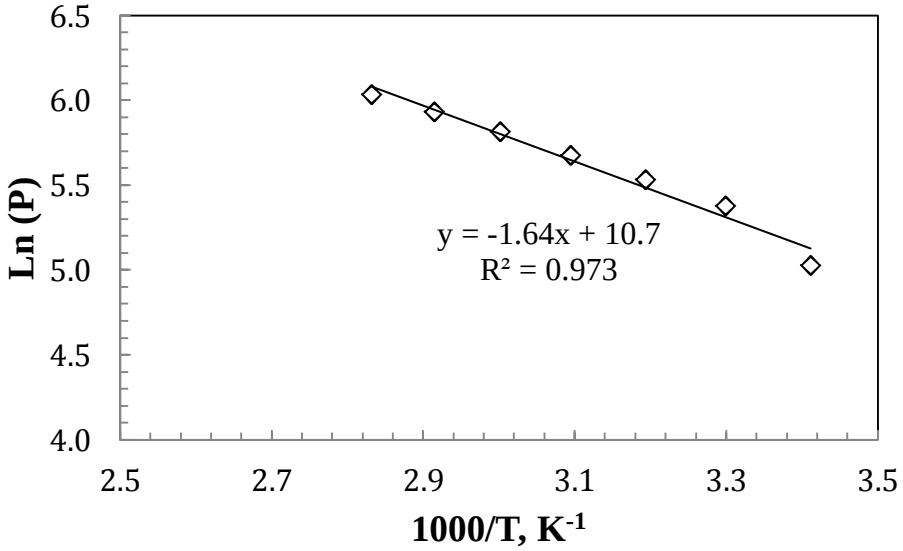

m = -1.64

b = 10.7

$$E_P = -m \times R = -(-1.64)\left(8.314\frac{kJ}{mol \cdot K}\right) = 13.7\ \frac{kJ}{mol}$$

$$P_0 = \exp(b) = \exp(10.7) = 46546\ Barrer$$

Permeability Adjustment

Permeability values were temperature and thickness adjusted for effect of polymer solution concentration on permeability (see Figure 3.19).

Sample calculate for O_2 permeation at the following conditions:

Conditions	15 wt%	6 wt%
T (K)	295.15	299.15
P (MPa)	0.501	0.501
Thickness (mm)	0.059	0.046
Un-adjusted Permeability (Barrer)	5.55	8.31
Calculated N_2 activation energy (kJ/mol)	23.4	

Thickness ratio:

$$\frac{x}{0.0591} = \frac{1}{0.046}$$

$$x = 1.28$$

Permeability correction:

$$\ln\left(\frac{P_2}{P_1}\right) = \frac{E_p}{R}\left(\frac{1}{T_2} - \frac{1}{T_1}\right)$$

$$P_2 = \exp\left[\frac{E_p}{R}\left(\frac{1}{T_2} - \frac{1}{T_1}\right)\right] \cdot P_1 \cdot x$$

$$P_2 = \exp\left[\frac{23.4\,\frac{kJ}{mol}}{8.314\,\frac{kJ}{mol\cdot K}}\left(\frac{1}{298.15} - \frac{1}{295.15}\right)\right](5.56)(1.28)$$

$$P_2 = 7.14$$

B.2 Pervaporation Calculations

Pressure Differential Across Membrane

Table B.1 Antoine equation constants for water and DMMP

	Water[a]	**DMMP**[b]
A	16.3872	22.319
B	3885.7	4340
C	230.17	-51.7
Units	P (kPa), T (°C)	P (Pa), T (K)

[a] Smith *et al.*,2005
[b]Butrow *et al.*, 2009

Sample calculations for water at 30 °C, collected 1.580 g of permeate over 30 mins for membrane of 0.0384 mm thickness.

Antoine Equation

$$\ln p = A - \frac{B}{C + T}$$

$$p^*_{sat} = \exp\left(A - \frac{B}{C + T}\right) = \exp\left(16.3872 - \frac{3885.7}{230.17 + 30\ ℃}\right) = 4.27\ kPa$$

$$\Delta p = p_{feed} - p_{permeate} = p^*_{sat} - 0\ Pa = p^*_{sat} = 4.27\ kPa = 4271\ Pa$$

$p_{permeate}$ is estimated as 0 Pa as a result of the vacuum applied to the permeate side of the membrane.

Calculate Flux

$$\text{Flux (J)} = \frac{\Delta m}{A \cdot t} = \frac{1.580\ g\left(\frac{1}{18.01\ g/mol}\right)}{13.8\ cm^2\left(\frac{1^2 m^2}{100^2 cm^2}\right)(1806\ s)} = 0.0351\ \frac{mol}{m^2 \cdot s}$$

Δm = mass difference between empty and collected cold trap (g)

J = Flux [mol/(m^2.s)]

M_W = molar mass of water (18.01 g/mol)

M_{DMMP} = molar mass of DMMP (124.08 g/mol)

Calculate Permeance

$$Q = \frac{J}{\Delta p} = \frac{0.03506 \frac{mol}{m^2 \cdot s}}{4271\ Pa} = 8.21 \times 10^{-6} \frac{mol}{m^2 \cdot s \cdot Pa}$$

Calculate Permeability

$$P = \frac{J \cdot l}{\Delta p} = 8.21 \times 10^{-6} \frac{mol}{m^2 \cdot s \cdot Pa} \times 0.0000384\ m = 3.15 \times 10^{-10} \frac{mol \cdot m}{m^2 \cdot s \cdot Pa}$$

Selectivity and activity energy are calculated similar to the gas permeation methods.

Appendix C

Supporting Figures

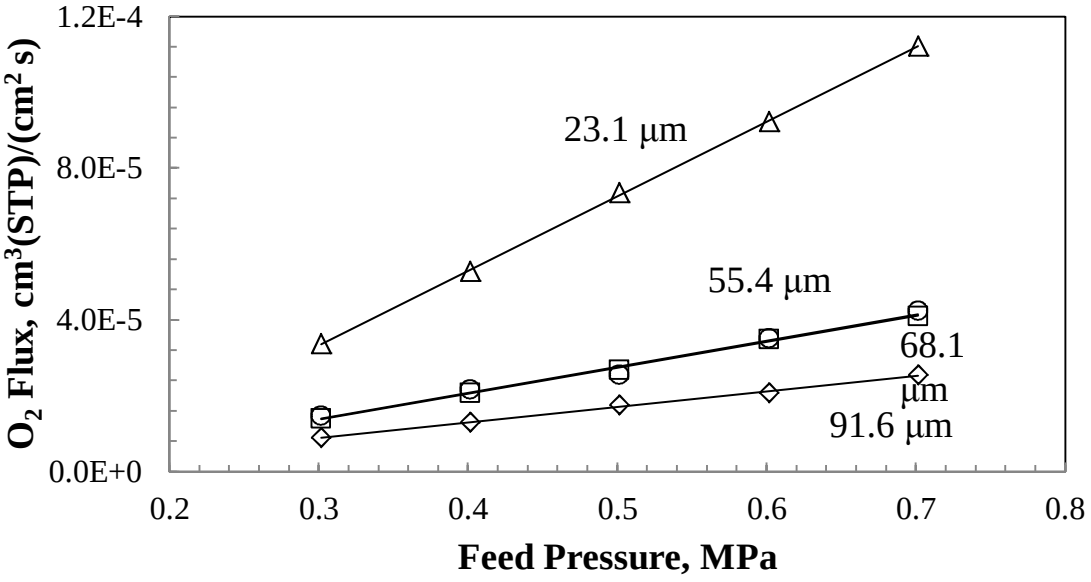

Figure C.1 Effect of membrane thickness on oxygen gas permeability coefficient

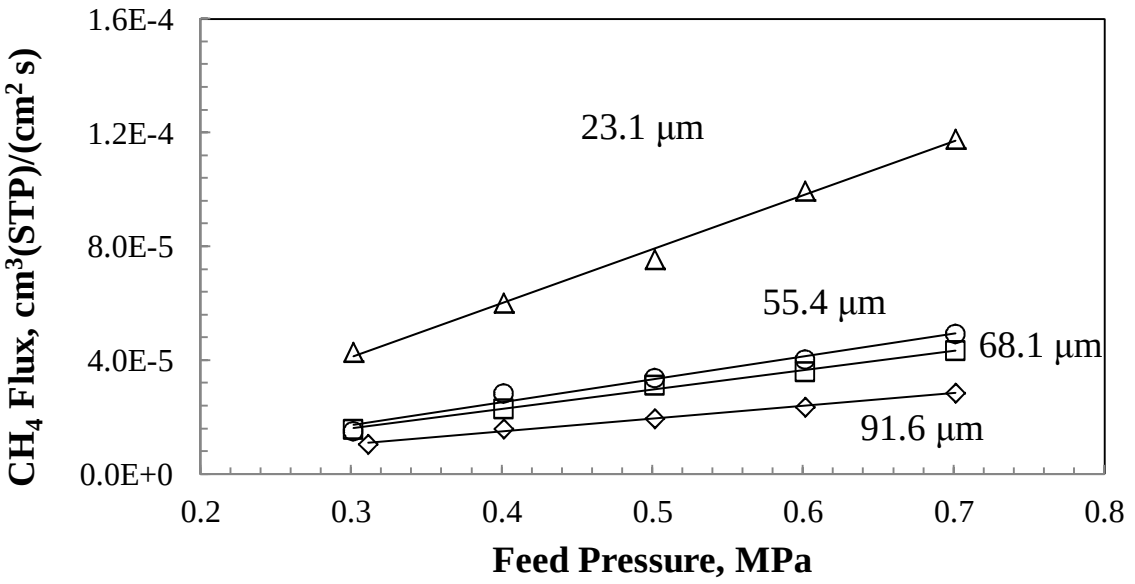

Figure C.2 Effect of membrane thickness on methane gas permeability coefficient

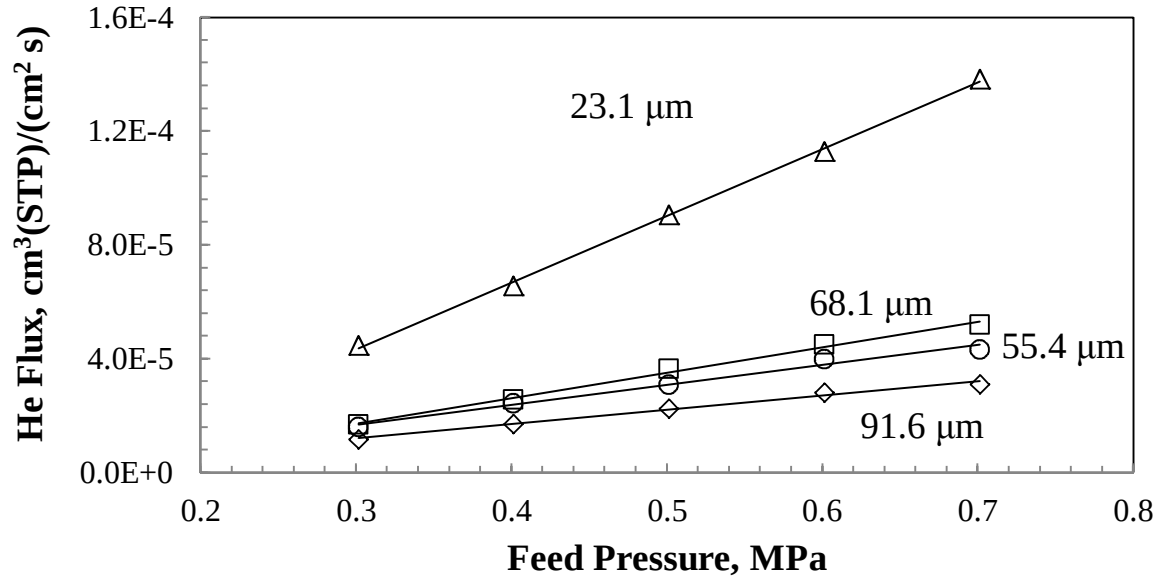

Figure C.3 Effect of membrane thickness on helium gas permeability coefficient

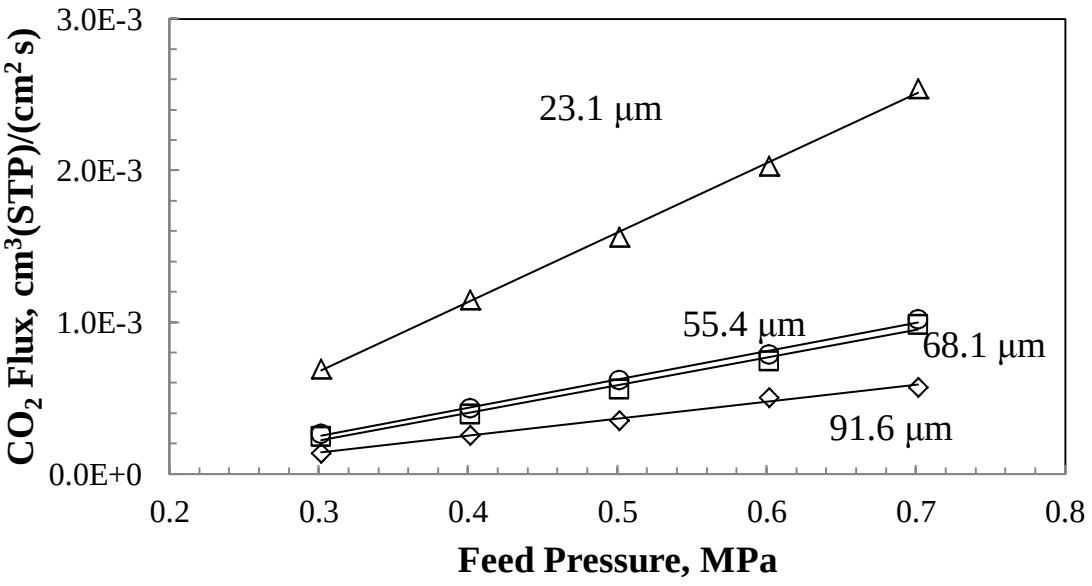

Figure C.4 Effect of membrane thickness on carbon dioxide gas permeability coefficient

Appendix D

Raw Data

D.1 Gas Permeation

D.1.1 Effect of Pressure

Membrane conditions:

thickness: 0.0356 mm

preparation: 15 wt% in NMP

Permeation flux and permeability coefficients

N_2						
Pressure [MPa]	**Temp. [K]**	**Baro. P [kPa]**	**Time [s]**	**Volume [mL]**	**Avg. Flux 10^{-5}[cm^3/(cm^2.s)]**	**Permeability Coefficient [Barrer]**
	297.15	101.7	123.18	0.02		
	297.15	101.7	126.16	0.02		
0.301	297.15	101.7	124.9	0.02	1.18±0.01	2.79±0.03
	297.15	101.7	63.78	0.02		
	297.15	101.7	64.13	0.02		
0.501	297.15	101.7	63.51	0.02	2.30±0.01	2.73±0.01
	297.15	101.6	55.56	0.02		
	297.15	101.6	54.71	0.02		
0.701	297.15	101.6	55.5	0.02	2.65±0.02	2.10±0.02
	297.15	101.6	42.53	0.02		
	297.15	101.6	41.97	0.02		
0.901	297.15	101.6	42.21	0.02	3.47±0.02	2.06±0.02
	297.15	101.6	34.56	0.02		
	297.15	101.6	35.09	0.02		
1.101	297.15	101.6	34.74	0.02	4.22±0.03	2.00±0.01
	297.15	101.6	32.04	0.02		
	297.15	101.6	31.78	0.02		
1.301	297.15	101.6	31.59	0.02	4.61±0.03	1.82±0.01
	297.15	101.6	27.28	0.02		
	297.15	101.6	27.5	0.02		
1.501	297.15	101.6	27.48	0.02	5.35±0.02	1.81±0.01
	297.15	101.6	23.75	0.02		
	297.15	101.6	23.88	0.02		
1.701	297.15	101.6	23.5	0.02	6.19±0.05	1.83±0.01
	297.15	101.6	21.04	0.02		
	297.15	101.6	21.18	0.02		
1.901	297.15	101.6	21.12	0.02	6.95±0.02	1.83±0.01
	297.15	101.6	18.84	0.02		
	297.15	101.6	18.91	0.02		
2.101	297.15	101.6	18.73	0.02	7.79±0.03	1.85±0.01
	297.15	101.6	17.96	0.02		
	297.15	101.6	17.75	0.02		
2.301	297.15	101.6	18	0.02	8.19±0.06	1.77±0.01
	297.15	101.6	16.81	0.02		
	297.15	101.6	16.9	0.02		
2.501	297.15	101.6	16.78	0.02	8.72±0.03	1.72±0.01

O_2						
Pressure [MPa]	**Temp. [K]**	**Baro. P [kPa]**	**Time [s]**	**Volume [mL]**	**Avg. Flux [$cm^3/(cm^2.s)$]**	**Permeability Coefficient [Barrer]**
	297.65	102.4	65.77	0.02		
	297.65	102.4	67.8	0.02		
0.301	297.65	102.4	66.27	0.02	$2.22\pm0.03\times10^{-5}$	5.26±0.08
	297.65	102.3	35.33	0.02		
	297.65	102.3	36.36	0.02		
0.501	297.65	102.3	35.24	0.02	$4.14\pm0.07\times10^{-5}$	4.91±0.08
	297.65	102.3	26.86	0.02		
	297.65	102.3	27.11	0.02		
0.701	297.65	102.3	26.77	0.02	$5.48\pm0.04\times10^{-5}$	4.33±0.03
	297.65	102.3	19.34	0.02		
	297.65	102.3	19.25	0.02		
0.901	297.65	102.3	19.12	0.02	$7.67\pm0.04\times10^{-5}$	4.55±0.03
	297.15	102.2	15.5	0.02		
	297.15	102.2	15.12	0.02		
1.101	297.15	102.2	15.25	0.02	$9.65\pm0.12\times10^{-5}$	4.58±0.06
	297.15	102.2	12.87	0.02		
	297.15	102.2	13.12	0.02		
1.301	297.15	102.2	12.97	0.02	$1.14\pm0.01\times10^{-4}$	4.49±0.04
	297.15	102.2	11.13	0.02		
	297.15	102.2	11.22	0.02		
1.501	297.15	102.2	11.19	0.02	$1.32\pm0.01\times10^{-4}$	4.47±0.02
	297.15	102.2	9.56	0.02		
	297.15	102.2	9.94	0.02		
1.701	297.15	102.2	9.78	0.02	$1.51\pm0.03\times10^{-4}$	4.49±0.09
	297.15	102.2	8.69	0.02		
	297.15	102.2	8.88	0.02		
1.901	297.15	102.2	8.44	0.02	$1.70\pm0.04\times10^{-4}$	4.49±0.11
	297.15	102.2	8.16	0.02		
	297.15	102.2	8	0.02		
2.101	297.15	102.2	8.02	0.02	$1.83\pm0.02\times10^{-4}$	4.34±0.05
	297.15	102.2	38.31	0.1		
	297.15	102.2	37.62	0.1		
2.301	297.15	102.2	38.26	0.1	$1.94\pm0.02\times10^{-4}$	4.18±0.04
	297.15	102.2	34.56	0.1		
	297.15	102.2	34.88	0.1		
2.501	297.15	102.2	34.61	0.1	$2.13\pm0.01\times10^{-4}$	4.21±0.02

CH_4						
Pressure [MPa]	**Temp. [K]**	**Baro. P [kPa]**	**Time [s]**	**Volume [mL]**	**Avg. Flux [$cm^3/(cm^2.s)$]**	**Permeability Coefficient [Barrer]**
	296.15	101.8	71.69	0.02		
	296.15	101.8	69.78	0.02		
0.301	296.15	101.8	70.6	0.02	$2.92\pm0.01\times10^{-5}$	6.94±0.02
	296.15	101.8	32.59	0.02		
	296.15	101.8	32.78	0.02		
0.501	296.15	101.8	32.53	0.02	$5.65\pm0.07\times10^{-5}$	6.70±0.08
	296.15	101.8	23.22	0.02		
	296.15	101.8	20.97	0.02		
0.701	296.15	101.8	22.75	0.02	$8.52\pm0.20\times10^{-5}$	6.74±0.16
	295.15	101.7	17.22	0.02		
	295.15	101.7	17.15	0.02		
0.901	295.15	101.7	17.53	0.02	$1.16\pm0.01\times10^{-4}$	6.86±0.07
	295.15	101.7	13	0.02		
	295.15	101.7	13.19	0.02		
1.101	295.15	101.7	13.43	0.02	$1.36\pm0.01\times10^{-4}$	6.45±0.04
	296.15	101.7	11.16	0.02		
	296.15	101.7	11.4	0.02		
1.301	296.15	101.7	11.07	0.02	$1.62\pm0.07\times10^{-4}$	6.39±0.31
	296.15	101.7	9.71	0.02		
	296.15	101.7	9.65	0.02		
1.501	296.15	101.7	9.86	0.02	$1.90\pm0.05\times10^{-4}$	6.44±0.17

He						
Pressure [MPa]	**Temp. [K]**	**Baro. P [kPa]**	**Time [s]**	**Volume [mL]**	**Avg. Flux [$cm^3/(cm^2.s)$]**	**Permeability Coefficient [Barrer]**
	297.15	102.2	32.03	0.02		
	297.15	102.2	30.41	0.02		
0.301	297.15	102.2	31.35	0.02	$2.09\pm0.03\times10^{-5}$	4.95±0.07
	297.15	102.2	15.88	0.02		
	297.15	102.2	15.94	0.02		
0.501	297.15	102.2	15.74	0.02	$4.52\pm0.02\times10^{-5}$	5.36±0.02
	297.15	102.2	11.47	0.02		
	297.15	102.2	10.95	0.02		
0.701	297.15	102.2	11.13	0.02	$6.62\pm0.36\times10^{-5}$	5.24±0.29
	297.15	102.2	8.28	0.02		
	297.15	102.2	8.43	0.02		
0.901	297.15	102.2	8.34	0.02	$8.54\pm0.09\times10^{-5}$	5.07±0.06
	297.15	102.2	7	0.02		
	297.15	102.2	7.16	0.02		
1.101	297.15	102.2	7.25	0.02	$1.12\pm0.02\times10^{-4}$	5.31±0.09
	297.15	102.2	29.56	0.1		
	297.15	102.2	30.41	0.1		
1.301	297.15	102.2	30.88	0.1	$1.31\pm0.02\times10^{-4}$	5.20±0.08
	297.15	102.2	25.28	0.1		
	297.15	102.2	26.03	0.1		
1.501	297.15	102.2	25.82	0.1	$1.51\pm0.02\times10^{-4}$	5.13±0.06
	297.15	102.2	24.75	0.1		
	297.15	102.2	24.44	0.1		
1.601	297.15	102.2	24.78	0.1	$1.68\pm0.04\times10^{-4}$	5.30±0.11

H_2						
Pressure [MPa]	**Temp. [K]**	**Baro. P [kPa]**	**Time [s]**	**Volume [mL]**	**Avg. Flux [$cm^3/(cm^2.s)$]**	**Permeability Coefficient [Barrer]**
	297.15	102.2	32.03	0.02		
	297.15	102.2	30.41	0.02		
0.301	297.15	102.2	31.35	0.02	$4.72\pm0.12\times10^{-5}$	11.2±0.3
	297.15	102.2	15.88	0.02		
	297.15	102.2	15.94	0.02		
0.501	297.15	102.2	15.74	0.02	$9.31\pm0.06\times10^{-5}$	11.0±0.1
	297.15	102.2	11.47	0.02		
	297.15	102.2	10.95	0.02		
0.701	297.15	102.2	11.13	0.02	$1.32\pm0.03\times10^{-4}$	10.4±0.2
	297.15	102.2	8.28	0.02		
	297.15	102.2	8.43	0.02		
0.901	297.15	102.2	8.34	0.02	$1.76\pm0.02\times10^{-4}$	10.5±0.1
	297.15	102.2	7	0.02		
	297.15	102.2	7.16	0.02		
1.101	297.15	102.2	7.25	0.02	$2.07\pm0.04\times10^{-4}$	9.81±0.17
	297.15	102.2	29.56	0.1		
	297.15	102.2	30.41	0.1		
1.301	297.15	102.2	30.88	0.1	$2.44\pm0.05\times10^{-4}$	9.64±0.21
	297.15	102.2	25.28	0.1		
	297.15	102.2	26.03	0.1		
1.501	297.15	102.2	25.82	0.1	$2.87\pm0.04\times10^{-4}$	9.73±0.15
	297.15	102.2	24.75	0.1		
	297.15	102.2	24.44	0.1		
1.601	297.15	102.2	24.78	0.1	$2.99\pm0.02\times10^{-4}$	9.47±0.07

CO_2						
Pressure [MPa]	**Temp. [K]**	**Baro. P [kPa]**	**Time [s]**	**Volume [mL]**	**Avg. Flux [$cm^3/(cm^2.s)$]**	**Permeability Coefficient [Barrer]**
	297.15	101.4	18.78	0.1		
	297.15	101.4	20.28	0.1		
0.301	297.15	101.4	19.57	0.1	$3.75\pm0.14\times10^{-4}$	89.0±3.4
	297.15	101.4	9.06	0.1		
	297.15	101.4	9.07	0.1		
0.501	297.15	101.4	9.07	0.1	$8.07\pm0.01\times10^{-4}$	95.8±0.1
	297.15	101.4	59.97	1		
	297.15	101.4	60.02	1		
0.701	297.15	101.4	59.39	1	$1.22\pm0.01\times10^{-3}$	96.8±0.6
	297.15	101.4	37.06	1		
	297.15	101.4	37.03	1		
0.901	297.15	101.4	37.13	1	$1.97\pm0.01\times10^{-3}$	117±1
	297.15	101.4	27.12	1		
	297.15	101.4	26.85	1		
1.101	297.15	101.4	26.98	1	$2.71\pm\times10^{-3}$	129±1
	297.15	101.4	21.25	1		
	297.15	101.4	20.81	1		
1.301	297.15	101.4	21.48	1	$3.46\pm0.01\times10^{-3}$	137±2
	297.15	101.4	17.38	1		
	297.15	101.4	17.58	1		
1.501	297.15	101.4	17.35	1	$4.20\pm0.06\times10^{-3}$	142±1
	297.15	101.4	14.63	1		
	297.15	101.4	14.46	1		
1.701	297.15	101.4	14.39	1	$5.05\pm0.03\times10^{-3}$	149±1
	297.15	101.4	11.85	1		
	297.15	101.4	12.13	1		
1.901	297.15	101.4	11.91	1	$6.12\pm0.04\times10^{-3}$	161±2
	297.15	101.4	10.5	1		
	297.15	101.4	10.31	1		
2.101	297.15	101.4	10.35	1	$7.05\pm0.07\times10^{-3}$	167±2
	297.15	101.4	8.97	1		
	297.15	101.4	8.82	1		
2.301	297.15	101.4	9.06	1	$8.18\pm0.11\times10^{-3}$	176±2
	297.15	101.4	8.03	1		
	297.15	101.4	8.08	1		
2.501	297.15	101.4	7.96	1	$9.12\pm0.07\times10^{-3}$	180±1

Ideal selectivity

Pressure [MPa]	CO_2/N_2	CO_2/CH_4	O_2/N_2	He/N_2	H_2/N_2	CO_2/H_2
0.301	31.8±0.8	12.8±0.5	1.88±0.01	1.77±0.05	4.01±0.15	7.94±0.51
0.501	35.1±0.2	14.3±0.2	1.80±0.02	1.96±0.01	4.04±0.01	8.67±0.06
0.701	46.1±0.6	14.4±0.3	2.06±0.03	2.49±0.11	4.97±0.09	9.27±0.22
0.901	56.8±0.4	17.1±0.1	2.21±0.01	2.46±0.03	5.09±0.08	11.2±0.1
1.101	64.3±0.8	20.0±0.2	2.29±0.05	2.65±0.04	4.90±0.08	13.1±0.3
1.301	74.9±1.4	21.4±1.1	2.46±0.04	2.85±0.04	5.28±0.15	14.2±0.4
1.501	78.5±0.5	22.1±0.7	2.47±0.01	2.83±0.03	5.36±0.06	14.6±0.2
1.701	81.6±0.7					
1.901	88.1±0.8					
2.101	90.4±1.0					
2.301	99.8±0.6					
2.501	105±0.4					

"Memory" of Pebax®1074

Membrane conditions:

thickness: 0.059 mm

preparation: 15 wt% in NMP

Pressure [MPa]	CO_2 Permeability Coefficient [Barrer]	CH_4 Permeability Coefficient [Barrer]	O_2 Permeability Coefficient [Barrer]	N_2 Permeability Coefficient [Barrer]	He Permeability Coefficient [Barrer]	H_2 Permeability Coefficient [Barrer]
0.301	123	7.44	6.25	1.31	5.52	9.94
0.501	140	7.45	5.56	1.52	6.95	10.7
0.701	153	7.87	5.70	1.88	7.24	12.1
0.901	174	8.61	5.59	1.81	7.39	12.8
1.101	187	8.73	5.53	2.14	7.39	12.9
1.301	201	8.72	5.84	2.16	7.44	11.9
1.501	207	8.51	6.14	2.11	7.25	12.2
1.701	222		6.13	2.24	7.61	
1.901	234		5.96	2.20	7.51	
2.101	246		6.00	2.26	7.40	
2.301	257		5.89	2.32	7.19	
2.501	265		6.11	2.28	7.20	
2.401	264		6.22	2.18	7.11	
2.201	248		6.18	2.19	8.16	
2.001	237		6.14	2.06	7.59	
1.801	228		6.08	1.98	7.59	
1.601	223		6.09	2.09	7.04	
1.401	210	8.64	6.18	1.95	5.52	12.6
1.201	201	8.89	6.04	1.81	6.95	14.0
1.001	192	8.48	6.07	1.83	7.24	13.4
0.801	187	7.91	6.22	1.66	7.39	12.8
0.601	174	8.19	6.44	1.53	7.39	13.1
0.401	146	8.18	5.66	1.12	7.44	9.99

D.1.2 Effect of Temperature
Membrane conditions:
thickness: 0.059 mm
preparation: 15 wt% in NMP

Permeability coefficient

1000/T [K^{-1}]	CO_2 [Barrer]	He [Barrer]	H_2 [Barrer]	CH_4 [Barrer]	O_2 [Barrer]	N_2 [Barrer]
3.30	217	12.2	22.1	15.5	13.4	4.38
3.19	254	17.3	31.8	22.8	16.4	6.64
3.09	293	24.7	44.7	29.0	21.8	9.39
3.00	337	32.1	58.7	39.8	29.4	13.6
2.91	378	42.5	73.2	52.0	37.5	18.6
2.83	418	58.2	94.5	64.8	47.4	23.1

Ideal selectivity

T [°C]	1000/T [K^{-1}]	CO_2/N_2	CO_2/CH_4	H_2/N_2	He/N_2	O_2/N_2	CO_2/H_2
30	3.30	49.4	14.0	5.03	2.79	3.06	9.82
40	3.19	38.2	11.1	4.78	2.61	2.46	7.98
50	3.09	31.2	10.1	4.76	2.63	2.32	6.54
60	3.00	24.8	8.46	4.33	2.37	2.16	5.73
70	2.91	20.3	7.28	3.93	2.28	2.01	5.17
80	2.83	18.1	6.45	4.09	2.52	2.05	4.43

Activation energy

Feed Pressure [MPa]	CO_2 E_p[kJ/mol]	He E_p[kJ/mol]	H_2 E_p[kJ/mol]	CH_4 E_p[kJ/mol]	O_2 E_p[kJ/mol]	N_2 E_p[kJ/mol]
0.501	12.7	26.1	27.1	27.0	23.4	30.2
0.701	11.8	27.3	26.7	25.3	23.1	30.0
0.901	10.9	26.7	25.6	26.9	25.3	29.5
1.101	10.6	26.8	26.5	28.3	29.3	30.1
1.301	10.4	26.7	26.9	28.3	28.0	30.2
1.501	10.2	26.7	26.4	28.2	28.0	28.9
1.701	9.36				27.6	29.7
1.901	9.32				27.6	29.7
2.101	8.61				27.6	28.6
2.301	8.05				27.7	29.2
2.501	7.93				26.6	28.5

D.1.3 Effect of Solvents

Permeability coefficients

Membrane conditions:

thickness: 0.0361 mm

preparation: 6 wt% in butanol

Feed Pressure, P [MPa]	CO_2 [Barrer]	He [Barrer]	H_2 [Barrer]	CH_4 [Barrer]	O_2 [Barrer]	N_2 [Barrer]
0.301	96.9	4.96	8.29	4.19	3.85	0.820
0.501	120	4.73	9.13	5.11	4.85	0.839
0.701	137	5.01	8.81	6.31	4.80	1.15
0.901	150	4.36	8.46	6.47	4.96	1.21
1.101	158	5.69	8.88	6.50	4.77	1.33
1.301	166	5.46	8.12	6.58	4.12	1.28
1.501	177	4.94	7.43	6.43	4.06	1.38
1.701	186				4.18	1.42
1.901	196				3.56	1.41
2.101	203				3.66	1.38
2.301	215				4.17	1.38
2.501	225				4.20	1.39

Membrane conditions:

thickness: 0.046 mm

preparation: 6 wt% in NMP

Feed Pressure, P [MPa]	CO_2 [Barrer]	He [Barrer]	H_2 [Barrer]	CH_4 [Barrer]	O_2 [Barrer]	N_2 [Barrer]
0.301	151	11.7	19.8	10.5	8.88	2.08
0.501	169	10.4	18.9	9.35	8.31	2.32
0.701	188	10.3	18.0	9.20	8.27	2.39
0.901	207	9.89	16.8	9.91	8.17	2.44
1.101	213	10.4	16.4	9.15	7.94	2.29
1.301	233	9.97	16.3	9.46	7.72	2.35
1.501	243	10.0	16.3	9.32	7.45	2.38
1.701	254				7.31	2.24
1.901	270				7.72	2.20
2.101	278				7.59	2.27
2.301	288				7.73	2.34
2.501	306				7.46	2.36

Ideal selectivity

Butanol

Pressure [MPa]	CO_2/N_2	CO_2/CH_4	O_2/N_2	He/N_2	H_2/N_2	CO_2/H_2
0.301	118	23.1	4.69	6.04	10.1	11.7
0.501	143	23.5	5.78	5.64	10.9	13.1
0.701	119	21.7	4.18	4.37	7.68	15.5
0.901	123	23.1	4.08	3.59	6.96	17.7
1.101	119	24.4	3.60	4.29	6.70	17.8
1.301	129	25.2	3.22	4.27	6.36	20.4
1.501	128	27.5	2.94	3.57		23.8
1.701	131		2.94			
1.901	139		2.52			
2.101	147		2.65			
2.301	156		3.02			
2.501	162		3.02			

NMP

Pressure [MPa]	CO_2/N_2	CO_2/CH_4	O_2/N_2	He/N_2	H_2/N_2	CO_2/H_2
0.301	72.5	14.3	4.27	5.62	9.53	7.61
0.501	72.8	18.1	3.57	4.48	8.15	8.93
0.701	78.4	20.4	3.46	4.32	7.53	10.4
0.901	84.6	20.9	3.34	4.05	6.90	12.3
1.101	93.0	23.2	3.47	4.57	7.15	13.0
1.301	99.0	24.7	3.28	4.23	6.93	14.3
1.501	102	26.0	3.13	4.21	6.87	14.8
1.701	114		3.27			
1.901	123		3.50			
2.101	122		3.34			
2.301	123		3.29			
2.501	129		3.16			

D.1.4 Effect of Heat-Treatment

Permeability coefficients

Membrane conditions:

thickness: 0.0553 mm

preparation: 15 wt% in NMP heat treated at 100 °C for 80 mins

Feed Pressure, P [MPa]	CO_2 [Barrer]	He [Barrer]	H_2 [Barrer]	CH_4 [Barrer]	O_2 [Barrer]	N_2 [Barrer]
0.301	96.9	4.96	8.29	4.19	3.85	0.820
0.501	120	4.73	9.13	5.11	4.85	0.839
0.701	137	5.01	8.81	6.30	4.80	1.15
0.901	150	4.36	8.46	6.47	4.96	1.21
1.101	158	5.69	8.88	6.50	4.77	1.33
1.301	166	5.46	8.12	6.58	4.12	1.28
1.501	177	4.94	7.43	6.43	4.06	1.38
1.701	186				4.18	1.42
1.901	196				3.56	1.41
2.101	203				3.66	1.38
2.301	215				4.17	1.38
2.501	225				4.20	1.39

Membrane conditions:

thickness: 0.059 mm

preparation: 15 wt% in NMP

Feed Pressure, P [MPa]	CO_2 [Barrer]	He [Barrer]	H_2 [Barrer]	CH_4 [Barrer]	O_2 [Barrer]	N_2 [Barrer]
0.301	151	11.7	19.8	10.5	8.88	2.08
0.501	169	10.4	18.9	9.35	8.31	2.32
0.701	188	10.3	18.0	9.20	8.27	2.39
0.901	207	9.89	16.8	9.91	8.17	2.44
1.101	213	10.4	16.4	9.15	7.94	2.29
1.301	233	9.97	16.3	9.46	7.72	2.35
1.501	243	10.0	16.3	9.32	7.45	2.38
1.701	254				7.31	2.24
1.901	270				7.72	2.20
2.101	278				7.59	2.27
2.301	288				7.73	2.34
2.501	306				7.46	2.36

Ideal selectivity

Heat-treated

Pressure [MPa]	CO_2/N_2	CO_2/CH_4	O_2/N_2	He/N_2	H_2/N_2	CO_2/H_2
0.301	118	23.1	4.69	6.04	10.1	10.5
0.501	143	23. 5	5.78	5.64	10.9	12.3
0.701	119	21.7	4.18	4.37	7.67	15.0
0.901	123	23.1	4.08	3.59	6.96	14.1
1.101	119	24.4	3.60	4.29	6.70	13.0
1.301	130	25.2	3.223	4.27	6.35	17.0
1.501	128	27.5	2.94	3.57		17.7
1.701	131		2.94			
1.901	139		2.52			
2.101	147		2.65			
2.301	156		3.02			
2.501	162		3.02			

Not heat-treated

Pressure [MPa]	CO_2/N_2	CO_2/CH_4	O_2/N_2	He/N_2	H_2/N_2	CO_2/H_2
0.301	72.5	14.3	4.27	5.62	9.53	12.4
0.501	72.8	18.1	3.57	4.48	8.15	13.2
0.701	78.4	20.4	3.46	4.32	7.53	12.6
0.901	84.6	20.9	3.34	4.05	6.90	13.6
1.101	93.0	23.2	3.47	4.57	7.15	14.5
1.301	99.0	24.7	3.28	4.23	6.93	16.8
1.501	102	26.0	3.13	4.21	6.87	16.9
1.701	114		3.27			
1.901	123		3.50			
2.101	122		3.34			
2.301	123		3.29			
2.501	129		3.16			

D.1.5 Effect of Thickness

Permeation flux

Membrane conditions:

thickness: 0.0916 mm

preparation: 15 wt% in NMP

Feed Pressure, P [MPa]	CO_2 10^{-5} [$cm^3/(cm^2.s)$]	He 10^{-5} [$cm^3/(cm^2.s)$]	CH_4 10^{-5} [$cm^3/(cm^2.s)$]	O_2 10^{-5} [$cm^3/(cm^2.s)$]	N_2 10^{-5} [$cm^3/(cm^2.s)$]
0.301	14.0	1.17	1.05	0.279	0.279
0.401	25.7	1.71	1.59	0.431	0.431
0.501	35.5	2.25	1.95	0.568	0.568
0.601	509	2.81	2.36	0.694	0.694
0.701	57.5	3.11	2.86	0.896	0.895

Membrane conditions:

thickness: 0.0681 mm
preparation: 15 wt% in NMP

Feed Pressure, P [MPa]	CO_2 10^{-5} [$cm^3/(cm^2.s)$]	He 10^{-5} [$cm^3/(cm^2.s)$]	CH_4 10^{-5} [$cm^3/(cm^2.s)$]	O_2 10^{-5} [$cm^3/(cm^2.s)$]	N_2 10^{-5} [$cm^3/(cm^2.s)$]
0.301	24.9	1.69	1.58	1.40	0.417
0.401	39.5	2.58	2.31	2.07	0.617
0.501	56.1	3.65	3.12	2.69	0.923
0.601	74.6	4.51	3.60	3.50	1.12
0.701	98.9	5.19	4.34	4.10	1.37

Membrane conditions:
thickness: 0.0554 mm
preparation: 15 wt% in NMP

Feed Pressure, P [MPa]	CO_2 10^{-5} [$cm^3/(cm^2.s)$]	He 10^{-5} [$cm^3/(cm^2.s)$]	CH_4 10^{-5} [$cm^3/(cm^2.s)$]	O_2 10^{-5} [$cm^3/(cm^2.s)$]	N_2 10^{-5} [$cm^3/(cm^2.s)$]
0.301	26.6	1.61	1.51	1.46	0.454
0.401	43.5	2.43	2.83	2.16	0.896
0.501	62.0	3.09	3.39	2.54	1.11
0.601	78.7	4.00	4.03	3.51	1.33
0.701	102	4.33	4.94	4.23	1.61

Membrane conditions:
thickness: 0.0231 mm
preparation: 15 wt% in NMP

Feed Pressure, P [MPa]	CO_2 10^{-5} [$cm^3/(cm^2.s)$]	He 10^{-5} [$cm^3/(cm^2.s)$]	CH_4 10^{-5} [$cm^3/(cm^2.s)$]	O_2 10^{-5} [$cm^3/(cm^2.s)$]	N_2 10^{-5} [$cm^3/(cm^2.s)$]
0.301	69.5	4.48	4.29	3.37	1.29
0.401	115	6.57	6.04	5.29	2.08
0.501	156	9.07	7.57	7.36	2.75
0.601	203	11.2	9.97	9.22	3.41
0.701	254	13.8	11.7	11.2	4.15

D.1.6 Effect of Solution Concentration

Permeability Coefficient

Membrane conditions:

thickness: 0.046 mm

preparation: 6 wt% in NMP

Feed Pressure, P [MPa]	CO_2 [$cm^3/(cm^2.s)$]	He [$cm^3/(cm^2.s)$]	CH_4 [$cm^3/(cm^2.s)$]	O_2 [$cm^3/(cm^2.s)$]	N_2 [$cm^3/(cm^2.s)$]	H_2 [$cm^3/(cm^2.s)$]
0.301	151	11.7	10.5	8.88	2.08	19.8
0.501	169	10.4	9.35	8.31	2.32	18.9
0.701	188	10.3	9.20	8.27	2.39	18.0
0.901	207	9.89	9.91	8.17	2.44	16.8
1.101	213	10.4	9.15	7.94	2.29	16.4
1.301	233	9.97	9.46	7.72	2.35	16.3
1.501	243	10.0	9.32	7.45	2.38	16.3
1.701	254	9.89	9.44	7.31	2.24	16.4
1.901	270			7.72	2.20	
2.101	278			7.59	2.27	
2.301	288			7.73	2.34	
2.501	306			7.46	2.36	

Membrane conditions:

thickness: 0.059 mm

preparation: 15 wt% in NMP

Feed Pressure, P [MPa]	CO_2 [$cm^3/(cm^2.s)$]	He [$cm^3/(cm^2.s)$]	CH_4 [$cm^3/(cm^2.s)$]	O_2 [$cm^3/(cm^2.s)$]	N_2 [$cm^3/(cm^2.s)$]	H_2 [$cm^3/(cm^2.s)$]
0.301	123	5.52	7.44	6.25	1.31	9.94
0.501	140	6.95	7.45	5.56	1.52	10.7
0.701	153	7.24	7.87	5.70	1.88	12.1
0.901	174	7.39	8.61	5.59	1.81	12.8
1.101	188	7.38	8.73	5.53	2.14	12.9
1.301	201	7.44	8.72	5.84	2.16	11.9
1.501	207	7.25	8.51	6.14	2.11	12.2
1.701	222	7.61		6.13	2.24	
1.901	234	7.51		5.95	2.20	
2.101	246			6.00	2.26	
2.301	257			5.89	2.32	
2.501	265			6.11	2.28	

D.2 Pervaporation

D.2.1 Pebax®1074

Membrane conditions:

thickness: 0.0384 mm

preparation: 15 wt% in NMP

Water flux and permeance

T [K]	P_{Baro} [kPa]	m1 [g]	m2 [g]	Δm [g]	t [s]	P_{sat} [kPa]	Avg. Flux [mol/(m^2.s)]	Avg. Permeance 10^{-6} [mol/(m^2.s.Pa)]
294.15	100.2	72.11	73.556	1.446	1807	2.501		
294.15	100.1	68.434	69.851	1.417	1809	2.501		
294.15	100.2	73.134	74.644	1.51	1919	2.501	0.0317±0.0003	12.7±0.1
300.15	100.3	68.429	69.919	1.49	1806	3.588		
300.15	100.3	73.136	74.64	1.504	1806	3.588		
300.15	100.4	68.428	70	1.572	1806	3.588	0.0338±0.0012	9.41±0.35
303.15	100.6	72.112	73.667	1.555	1805	4.271		
303.15	100.5	73.125	74.705	1.58	1806	4.271		
303.15	102.2	73.128	74.82	1.692	1920	4.271	0.0350±0.0015	8.19±0.35
308.15	102.1	68.423	70.103	1.68	1806	5.660		
308.15	102.1	73.121	74.773	1.652	1808	5.660		
308.15	102.1	72.104	73.765	1.661	1802	5.660	0.0369±0.0007	6.53±0.14
313.15	102.1	68.411	70.243	1.832	1802	7.424		
313.15	102.1	73.113	74.934	1.821	1802	7.424		
313.15	102	72.1	73.919	1.819	1807	7.424	0.0405±0.0002	5.46±0.02
318.15	101.6	68.42	70.284	1.864	1805	9.641		
318.15	101.5	72.104	74.114	2.01	1808	9.641		
318.15	101.4	73.125	75.098	1.973	1804	9.641	0.0433±0.0006	4.49±0.06
323.15	101.4	68.411	70.465	2.054	1805	12.405		
323.15	101.5	73.122	75.183	2.061	1805	12.405		
323.15	101.5	72.101	74.154	2.053	1804	12.405	0.0457±0.0008	3.68±0.01

DMMP flux and permeance

T [K]	Flux 10^{-5} [mol/(m^2.s)]	Permeance 10^{-8} [mol/(m^2.s.Pa)]
297.15	0.872	8.44
303.15	1.36	8.62
308.15	1.71	7.77
313.15	2.23	7.32
318.15	2.75	6.60
323.15	3.26	5.81

D.2.2 Nitrile Glove

thickness: 0.0941 mm

Water flux and permeance

T [K]	Flux 10^{-4} [mol/(m^2 s)]	Permeance 10^{-8}[mol/(m^2 s Pa)]
298.15	1.88	5.94
303.15	1.46	3.42
308.15	1.65	2.91
313.15	1.58	2.13
318.15	1.91	1.98
323.15	1.73	1.39

DMMP flux and permeance

T [K]	Flux 10^{-5}[mol/(m^2 s)]	Permeance 10^{-7}[mol/(m^2 s Pa)]
298.15	1.23	1.19

D.2.3 Latex Glove

thickness: 0.1354 mm

Water flux and permeance

T [K]	Flux 10^{-4} [mol/(m^2 s)]	Permeance 10^{-8}[mol/(m^2 s Pa)]
297.15	0.956	3.18
303.15	1.28	2.99
308.15	1.37	2.42
313.15	1.56	2.10
318.15	1.76	1.83
323.15	2.04	1.64

DMMP flux and permeance

T [K]	Flux 10^{-5} [mol/(m^2 s)]	Permeance 10^{-8} [mol/(m^2 s Pa)]
298.15	0.485	6.41
303.15	0.743	5.75
308.15	1.10	5.57
313.15	1.55	5.20
318.15	2.16	5.20
323.15	2.85	5.02

D.2.4 Polyvinyl Chloride (PVC) Glove

thickness: 0.1678 mm

Water flux and permeance

T [K]	Flux 10^{-4} [mol/(m^2 s)]	Permeance 10^{-8} [mol/(m^2 s Pa)]
298.15	1.26	3.95
303.15	1.67	3.91
308.15	2.23	3.93
313.15	2.82	3.79
318.15	3.71	3.85
297.15	4.67	3.76

DMMP flux and permeance

T [K]	Flux 10^{-5} [mol/(m^2 s)]	Permeance 10^{-7} [mol/(m^2 s Pa)]
298.15	3.07	2.76
303.15	3.71	2.36
308.15	4.26	1.93
313.15	4.43	1.45
318.15	5.75	1.38
297.15	6.14	1.10

D.2.5 Low Density polyethylene (LDPE)

thickness: 0.0116 mm

Water flux and permeance

T [K]	Flux 10^{-4} [mol/(m^2 s)]	Permeance 10^{-8} [mol/(m^2 s Pa)]
298.15	1.22	3.84
303.15	1.19	2.78
308.15	1.22	2.16
313.15	1.45	1.95
318.15	1.48	1.54
297.15	1.37	1.11

DMMP flux and permeance

T [K]	Flux 10^{-5} [mol/(m^2 s)]	Permeance 10^{-8} [mol/(m^2 s Pa)]
298.15	1.10	9.90
303.15	1.36	8.62
308.15	1.83	8.29
313.15	2.10	6.89
318.15	2.20	5.28
297.15	2.71	4.83

D.2.6 Silicone

thickness: unknown, casted on substrate

Water flux and permeance

T [K]	Flux 10^{-3}[mol/(m^2 s)]	Permeance 10^{-7}[mol/(m^2 s Pa)]
298.15	1.99	6.25
303.15	2.34	5.47
308.15	2.30	4.06
313.15	2.64	3.56
318.15	2.99	3.10
297.15	3.39	2.73

DMMP flux and permeance

T [K]	Flux 10^{-4} [mol/(m^2 s)]	Permeance 10^{-6} [mol/(m^2 s Pa)]
298.15	4.29	3.86
303.15	4.52	2.87
308.15	4.85	2.20
313.15	5.13	1.68
318.15	5.80	1.39
297.15	6.54	1.16

D.2.7 Pebax®2533

thickness: 0.0419 mm

Water flux and permeance

T [K]	Flux 10^{-3} [mol/(m^2 s)]	Permeance 10^{-7} [mol/(m^2 s Pa)]
298.15	1.46	4.57
303.15	1.66	3.89
308.15	1.77	3.12
313.15	2.25	3.03
318.15	2.64	2.73
297.15	2.88	2.32

DMMP flux and permeance

T [K]	Flux 10^{-5} [mol/(m^2 s)]	Permeance 10^{-7} [mol/(m^2 s Pa)]
298.15	1.99	1.79
303.15	2.36	1.50
308.15	2.96	1.34
313.15	3.93	1.29
318.15	4.63	1.11
297.15	6.25	1.11

D.2.8 Silicone-polycarbonate copolymer

thickness: 0.0613 mm

Water flux and permeance

T [K]	Flux 10^{-3} [mol/(m^2 s)]	Permeance 10^{-7} [mol/(m^2 s Pa)]
298.15	0.901	2.83
303.15	1.16	2.71
308.15	1.35	2.38
313.15	1.51	2.04
318.15	1.59	1.65
297.15	1.68	1.35

H_2O/DMMP Selectivity

T [K]	Pebax 1074	Nitrile	Latex	PVC	LDPE	Silicone	Pebax 2533
298.15	131	0.499	0.497	0.142	0.387	0.161	2.55
303.15	95.0		0.521	0.165	0.322	0.190	2.58
308.15	84.0		0.435	0.203	0.260	0.184	2.32
313.15	74.6		0.403	0.261	0.282	0.211	2.34
318.15	68.0		0.351	0.278	0.291	0.222	2.45
297.15	63.3		0.327	0.340	0.228	0.234	2.08

Activation Energy

Polymer	E_p (H_2O) [kJ/mol]	E_p (DMMP) [kJ/mol]
Pebax 1074	33.3	11.9
Pebax 2533	20.5	15.3
Nitrile	42.2	N/A
Latex	21.8	7.31
PVC	1.50	29.7
LDPE	37.1	23.9
Silicone	27.3	38.7
Silicone polycabonate	24.2	N/A